LUIS FELIPE LATA TENESACA

PHYSIOLOGICAL, BIOCHEMICAL AND MOLECULAR ASPECTS OF INDUCED RESISTANCE IN MAIZE AGAINST *Bipolaris maydis* INFECTION USING A ZINC-POLYPHENOLIC COMPOUND AND SILICON

Thesis submitted to the Plant Physiology Graduate Program of the Universidade Federal de Viçosa in partial fulfillment of the requirements for the degree of *Doctor Scientiae*.

Adviser: Fabrício Ávila Rodrigues

VIÇOSA - MINAS GERAIS
2023

Ficha catalográfica elaborada pela Biblioteca Central da Universidade Federal de Viçosa - Campus Viçosa

T
L351p
2023

Lata Tenesaca, Luis Felipe, 1993-
Physiological, biochemical and molecular aspects of induced resistance in maize against *Bipolaris maydis* infection using a zinc-polyphenolic compound and silicon / Luis Felipe Lata Tenesaca. – Viçosa, MG, 2023.
1 tese eletrônica (98 f.): il. (algumas color.).

Texto em inglês.
Orientador: Fabrício Ávila Rodrigues.
Tese (doutorado) - Universidade Federal de Viçosa, Departamento de Fitopatologia, 2023.
Inclui bibliografia.
DOI: https://doi.org/10.47328/ufvbbt.2023.758
Modo de acesso: World Wide Web.

1. Milho - Resistência a doenças e pragas. 2. Silício. 3. Zinco. 4. Bipolaris. I. Rodrigues, Fabrício Ávila, 1974-. II. Universidade Federal de Viçosa. Departamento de Fitopatologia. Programa de Pós-Graduação em Fisiologia Vegetal. III. Título.

CDD 22. ed. 571.96

Bibliotecário(a) responsável: Euzébio Luiz Pinto CRB-6/3317

LUIS FELIPE LATA TENESACA

PHYSIOLOGICAL, BIOCHEMICAL AND MOLECULAR ASPECTS OF INDUCED RESISTANCE IN MAIZE AGAINST *Bipolaris maydis* INFECTION USING A ZINC-POLYPHENOLIC COMPOUND AND SILICON

Thesis submitted to the Plant Physiology Graduate Program of the Universidade Federal de Viçosa in partial fulfillment of the requirements for the degree of *Doctor Scientiae*.

APPROVED: November 24, 2023.

Assent:

Luis Felipe Lata Tenesaca
Author

Fabrício Ávila Rodrigues
Adviser

ACKNOWLEDGEMENTS

First of all, I thank God for all the blessings and opportunities

Thanks are due to the Universidade Federal de Viçosa (UFV), Department of Plant Biology, Department of Plant Pathology, the Plant-Pathogen Interaction Laboratory and the Postgraduate Program in Plant Physiology for providing conditions for this work.

This study was financed in part by the Coordenação de Aperfeiçoamento de Pessoal de Nível Superior - Brasil (CAPES) - Finance Code 001.

I want to express my sincere thanks to:

Professor Fabricio Ávila Rodrigues for his guidance, teachings and advice to improve my academic and professional skills.

My colleagues at the Laboratory of Host-Pathogen Interaction for all their learning and help Marcos, Leonardo, Aline, Bárbara, and Bruno for their friendship and help while conducting the experiments.

My son Heitor and my wife Gabriela who accompanied me in this long stay in Brazil making my days more pleasant and comfortable.

My mother Anabel, my grandfather Luis, my aunt Rosa and my heavenly angels John, Luis, Maria and Amada who are my daily inspiration and gave me their support in difficult times.

My foreign friends in Viçosa Andrés, Milena, Tatiana, Edison, Javier and Shirley, who have made my days in Brazil so much easier.

UFV employees Bruno, Delfim, Daniel, Mário, and Luciene.

Thanks to all colleagues who contributed, directly or indirectly, to this work.

BIOGRAPHY

LUIS FELIPE LATA TENESACA was born on March 7, 1993 in the city of Guayaquil, Ecuador. In 2015, he obtained the title of Agronomist from the Universidad Técnica de Machala. In March 2016, he started a job at Ecuador's Ministry of Agriculture and Livestock, participating in extension projects for the productive development of banana producers. In March 2019, started the Master's degree program in the Postgraduate Program in Agronomy (Plant Production) at the Universidade Estadual Paulista "Júlio de Mesquita Filho" (UNESP), Jaboticabal campus, under the guidance of Professor Renato de Mello Prado defending his dissertation on February 20, 2021. In March 2020, started the specialization course in Soils and Plant Nutrition at the Escola Superior de Agricultura “Luiz de Queiroz” defending his graduation work on March 19, 2022. In March 2021, he started the doctoral degree in the Plant Pathology Program at UFV under the guidance of Professor Fabrício Ávila Rodrigues defending his thesis on November 24, 2023.

.

ABSTRACT

LATA TENESACA, Luis Felipe, D.Sc., Universidade Federal de Viçosa, November 2023. **Physiological, biochemical and molecular aspects of induced resistance in maize against *Bipolaris maydis* infection using a zinc-polyphenolic compound and silicon.** Advisor: Fabrício Ávila Rodrigues.

Maize leaf blight (MLB), caused by the fungus *Bipolaris maydis*, has great potential to cause considerable losses in the growth and yield of maize. Higher foliar concentration of silicon (Si) or the use of resistance inducers may be promising alternatives for boosting maize resistance against MLB. The first study investigated the potential of using Semia® [zinc (20%) complexed with plant-derived pool of polyphenols (10%)] to boost defense reactions on maize leaves infected by *B. maydis*. Mycelial growth and conidia germination were reduced by the IR stimulus *in vitro*. The IR stimulus-sprayed plants showed reduced MLB symptoms due to less production of malondialdehyde (MDA), hydrogen peroxide (H_2O_2), and radical anion superoxide ($O_2^{\bullet-}$) compared to control plants. During the infection by *B. maydis*, IR stimulus-sprayed plants showed increased concentrations of sucrose and starch and greater activities of catalase (CAT), glutathione reductase (GR), and superoxide dismutase (SOD) compared to water-sprayed plants. Less impairment on the photosynthetic apparatus [higher values for leaf gas exchange (rate of net CO_2 assimilation, stomatal conductance to water vapor, and transpiration rate) and chlorophyll a fluorescence (variable-to-maximum Chl *a* fluorescence ratio, photochemical yield, and yield for dissipation by down-regulation) parameters] along with preserved pool of chlorophyll *a+b* and carotenoids were noticed for infected and IR stimulus-sprayed plants compared to infected plants from the control treatment. Defense-related genes (*IGL*, *CHS02*, *PR1*, *PAL3*, *LOX3*, *CHI*, and *GLU*) were up-regulated for IR stimulus-sprayed plants compared to control plants infected by *B. maydis*. These findings highlight the potential of using this IR stimulus for MLB management. In the second study, we investigated whether maize plants with higher foliar silicon (Si) concentration can be more resistant against MLB was investigated in this study. The +Si plants showed reduced MLB symptoms (smaller lesions and lower disease severity) due to higher foliar Si concentration and less production of MDA, H_2O_2, and $O_2^{\bullet-}$ compared to -Si plants. Higher values for leaf gas exchange and chlorophyll *a* fluorescence parameters along with preserved pool of chlorophyll *a+b* and carotenoids were noticed for infected +Si plants compared to infected -Si plants. Activities of

defense (chitinase, β-1,3-glucanase, phenylalanine ammonia-lyase, polyphenoloxidase, peroxidase, and lipoxygenase) and antioxidative (APX, CAT, SOD, and GR) enzymes were higher for infected +Si plants compared to infected -Si plants. Collectively, this study highlights the importance of using Si to boost the resistance of maize plants against MLB considering the more operative defense reactions and the robustness of the antioxidative metabolism along with the preservation of the photosynthetic apparatus.

Keywords: Antioxidative metabolism. Foliar disease. Host defense responses. Induced resistance. Photosynthesis.

RESUMO

LATA TENESACA, Luis Felipe, D.Sc., Universidade Federal de Viçosa, novembro de 2023. **Aspectos fisiológicos, bioquímicos e moleculares da resistência induzida em milho contra a infecção por *Bipolaris maydis* usando um composto polifenólico de zinco e silício**. Orientador: Fabrício Ávila Rodrigues.

A mancha-foliar-de-Bipolaris (MFB), causado pelo fungo *Bipolaris maydis*, tem grande potencial para causar perdas consideráveis no crescimento e produtividade do milho. Uma maior concentração foliar de silício (Si) e o uso de indutores de resistência podem ser alternativas promissoras para aumentar a resistência do milho à MFB. O primeiro estudo investigou o potencial do uso do Semia® [zinco (20%) complexado com um *pool* de polifenóis derivados de plantas (10%)] para aumentar os mecanismos de defesa em folhas de milho infectadas por *B. maydis*. O crescimento micelial e a germinação de conídios foram reduzidos pelo estímulo IR *in vitro*. As plantas pulverizadas com estímulo IR apresentaram sintomas reduzidos de MLB devido à menor produção de malondialdeído (MDA), peróxido de hidrogênio (H_2O_2) e ânion radical superóxido ($O_2^{\bullet-}$) em comparação com as plantas do controle. Durante a infecção de *B. maydis*, as plantas pulverizadas com estímulo IR apresentaram concentrações maiores de sacarose e amido e atividades maiores da catalase (CAT), glutationa redutase (GR) e superóxido dismutase (SOD) em comparação com as plantas pulverizadas com água. Menor comprometimento do aparato fotossintético [valores mais altos para troca gasosas foliares (taxa de assimilação líquida de CO_2, condutância estomática ao vapor de água e taxa de transpiração) e parâmetros de fluorescência da clorofila a (taxa de fluorescência da Chl *a* variável a máxima, rendimento fotoquímico e rendimento da dissipação não-regulada)], juntamente com o *pool* preservado de clorofila *a+b* e carotenoides, foram observados em plantas infectadas e pulverizadas com estímulo IR em comparação com plantas infectadas do tratamento controle. Os genes relacionados à defesa (*IGL*, *CHS02*, *PR1*, *PAL3*, *LOX3*, *CHI* e *GLU*) foram regulados positivamente nas plantas pulverizadas com estímulo IR em comparação com as plantas controle infectadas por *B. maydis*. Essas descobertas destacam o potencial do uso desse estímulo de IR para o manejo da MFB. No segundo estudo, investigamos se as plantas de milho com maior concentração foliar de silício (Si) podem ser mais resistentes à MFB. As plantas +Si apresentaram sintomas reduzidos de MFB (lesões

menores e menor gravidade da doença) devido à maior concentração foliar de Si e à menor produção de MDA, H_2O_2 e $O_2^{\bullet -}$ em comparação com as plantas -Si. Foram observados valores mais altos para os parâmetros de trocas gasosas foliares e fluorescência da clorofila *a*, juntamente com o *pool* preservado de clorofila *a*+*b* e carotenoides para plantas infectadas +Si em comparação com plantas infectadas -Si. As atividades das enzimas de defesa (quitinase, β-1,3-glucanase, fenilalanina amônia-liase, polifenoloxidase, peroxidase e lipoxigenase) e antioxidantes (APX, CAT, SOD e GR) foram maiores nas plantas infectadas +Si em comparação com as plantas infectadas -Si. Em conjunto, este estudo destaca a importância do uso do Si para aumentar a resistência das plantas de milho contra a MFB, considerando as reações de defesa mais operantes e a robustez do metabolismo antioxidante, juntamente com a preservação do aparato fotossintético.

Palavras-chaves: Metabolismo antioxidante. Doença foliar. Fotossíntese. Respostas de defesa do hospedeiro. Resistência induzida.

SUMMARY

Chapter 1

A zinc-polyphenolic compound increases maize resistance against *Bipolaris maydis* infection

ABSTRACT

Maize leaf blight (MLB), caused by the fungus *Bipolaris maydis*, is an important disease affecting maize production. The use of nutrient-based resistance inducers may become a very promising alternative for MLB control to minimizing fungicide sprays. This study investigated the potential of using Semia® [zinc (20%) complexed with plant-derived pool of polyphenols (10%)] to boost defense reactions on maize leaves infected by *B. maydis*. A 2 × 2 factorial experiment was arranged in a completely randomized design with four replications per sampling time. The factors studied were plants sprayed with water (control) or Semia® (referred to as induced resistance (IR) stimulus hereafter) that were non-inoculated or inoculated with *B. maydis*. Mycelial growth and conidia germination were reduced by the IR stimulus in vitro. The IR stimulus-sprayed plants showed reduced MLB symptoms due to less production of malondialdehyde, hydrogen peroxide, and radical anion superoxide compared to control plants. During the infection by *B. maydis*, IR stimulus-sprayed plants showed increased concentrations of sucrose and starch and greater activities of catalase, glutathione reductase, and superoxide dismutase compared to water-sprayed plants. Less impairment on the photosynthetic apparatus [higher values for leaf gas exchange (rate of net CO_2 assimilation, stomatal conductance to water vapor, and transpiration rate) and chlorophyll *a* fluorescence (variable-to-maximum Chl *a* fluorescence ratio, photochemical yield, and yield for dissipation by down-regulation) parameters] along with preserved pool of chlorophyll *a+b* and carotenoids were noticed for infected and IR stimulus-sprayed plants compared to infected plants from the control treatment. Defense-related genes (*IGL*, *CHS02*, *PR1*, *PAL3*, *LOX3*, *CHI*, and *GLU*) were up-regulated for IR stimulus-sprayed plants compared to control plants infected by *B. maydis*. These findings highlight the potential of using this IR stimulus for MLB management.

Keywords: *Bipolaris maydis*. Antioxidative metabolism. Host defense responses. Induced resistance. Photosynthesis.

RESUMO

A mancha-foliar-de-Bipolaris (MFB), causada pelo fungo *Bipolaris maydis*, é uma doença importante que afeta a produção de milho. O uso de indutores de resistência à base de nutrientes pode se tornar uma alternativa muito promissora para o controle da MFB, minimizando as pulverizações de fungicidas. Este estudo investigou o potencial do uso do Semia® [zinco (20%) complexado com um *pool* de polifenóis derivados de plantas (10%)] para aumentar os mecanismos de defesa em folhas de milho infectadas por *B. maydis*. Um experimento fatorial 2 × 2 foi arranjado em um desenho completamente aleatório com quatro repetições por tempo de amostragem. Os fatores estudados foram plantas pulverizadas com água (controle) ou Semia® (denominado como estímulo de resistência induzida (IR)) que foram não-inoculadas ou inoculadas com *B. maydis*. O crescimento micelial e a germinação de conídios foram reduzidos pelo estímulo IR *in vitro*. As plantas pulverizadas com estímulo IR apresentaram sintomas reduzidos de MLB devido à menor produção de malondialdeído, peróxido de hidrogênio e ânion radical superóxido em comparação com as plantas do controle. Durante a infecção de *B. maydis*, as plantas pulverizadas com estímulo IR apresentaram concentrações maiores de sacarose e amido e atividades maiores da catalase, glutationa redutase e superóxido dismutase em comparação com as plantas pulverizadas com água. Menor comprometimento do aparato fotossintético [valores mais altos para troca gasosas foliares (taxa de assimilação líquida de CO_2, condutância estomática ao vapor de água e taxa de transpiração) e parâmetros de fluorescência da clorofila a (taxa de fluorescência da Chl *a* variável a máxima, rendimento fotoquímico e rendimento da dissipação não-regulada)], juntamente com o *pool* preservado de clorofila *a*+*b* e carotenoides, foram observados em plantas infectadas e pulverizadas com estímulo IR em comparação com plantas infectadas do tratamento controle. Os genes relacionados à defesa (*IGL*, *CHS02*, *PR1*, *PAL3*, *LOX3*, *CHI* e *GLU*) foram regulados positivamente nas plantas pulverizadas com estímulo IR em comparação com as plantas controle infectadas por *B. maydis*. Essas descobertas destacam o potencial do uso desse estímulo de IR para o manejo da MFB.

Palavras-chave: *Bipolaris maydis*. Metabolismo antioxidante. Respostas de defesa do hospedeiro. Resistência Induzida. Fotossíntese.

1. Introduction

Maize (*Zea mays* L.) is one of the main staple crops, both agriculturally and economically, which guarantees global food and nutritional security (Ranum *et al*., 2014). Although maize is more adaptable to abiotic stresses than other cereals, infection by pathogens has been the main factor limiting plant growth and productivity (Jaidka *et al*., 2020). The occurrence of maize leaf blight (MLB), caused by the fungus *Bipolaris maydis* (Y. Nisik. & Miyake) Shoemaker, contributes significantly to yield losses due to photosynthetic impairment, reduced plant growth, and less allocation of assimilates from leaves to the developing grains (Meshram *et al*., 2022).

Fungicide spray, use of hybrids with higher levels of basal resistance, plant genome editing using the CRISPR/Cas9 system, protective formulations using nanotechnology, biological control methods (e.g., *Trichoderma atroviride* and *Bacillus cereus*), crop rotation, and balanced plant nutrition (e.g., nitrogen and potassium) are some of the available strategies for MLB management (Dai *et al*., 2018; Kumar *et al*., 2021; Lai, 2016, Paul, 2021; Worrall, 2018). However, other control strategies must be provided to growers, especially those from developing countries, to reduce the cost associated with fungicides and their harmful effects on human health and the environment. Thinking about more sustainable maize production, the use of resistance inducers may become an environmentally friendly alternative for MLB management, especially if combined with fungicides and other biological control options to reduce chemical inputs without losing their efficacy. It is well known that plants exposed to resistance inducers of abiotic and or biotic nature efficiently activate defense reactions that will hinder the infection process of pathogens of different lifestyles (Siah *et al*., 2018; Reglinski *et al*.,2023). During the induced resistance, which can be assigned as systemic acquired resistance (SAR) or induced systemic resistance (ISR), a plethora of signaling pathways mediated by hormones [e.g., salicylic acid (SA), jasmonic acid (JA), and ethylene (ET)], with the co-participation of mobile signals (e.g., glycerol-3-phosphate, azelaic acid, pipecolic acid, and N-hydroxy-pipecolic acid), will take place to coordinate the temporal and spatial action of different defense mechanisms (Kesel *et al*., 2021; Vlot *et al*., 2021; Zeier, 2021). Interestingly, the spray of nutrient-based resistance inducers has been efficient in reducing the intensities of diverse fungal diseases in crops such as soybean, tomato, and potato (Han *et al*., 2021; Silva *et al*., 2022, Torres *et al*., 2023). The zinc (Zn) is involved in the signaling of SAR and ISR that potentiate different defense reactions in the infection sites of pathogens besides improving the integrity and the permeability of membrane cell wall (Cabot *et al*., 2019; Dimkpa and Elmer, 2023). In maize

challenged with *Curvularia lunata* and *Bipolaris sorokiniana*, the application of Zn compounds was able to induce antioxidant and defense system, promote ROS balance, and improve lignin accumulation (Choudhary *et al*., 2019; Tanwar, 2021).

The hypothesis that spraying maize leaves with a zinc-polyphenolic compound could increase their basal level of resistance (e.g., preservation of the photosynthetic apparatus, boosted defense reactions, and a better response of the antioxidant enzymes) against *B. maydis* infection was investigated in this study using different physiological, biochemical, and molecular approaches. In this regard, plants non-sprayed or sprayed with this compound and non-infected or infected by *B. maydis* were analyzed for their photosynthetic performance, carbohydrate and antioxidative metabolisms, and expression of defense-related genes.

2. Material and methods

2.1. *In vitro* assays

Different volumes of a stock solution (40 mL/L) of Semia® [nitrogen (1%) and zinc (20%) complexed with plant-derived pool of polyphenols (10%); FertiGlobal, Larderello, Italy] were mixed with 1 mL of a conidial suspension of *B. maydis* (5×10^4 conidia/mL) to obtain suspensions containing the concentrations of 1, 2.5, 5, 10, and 15 mL of Semia®/L. A total of 100 µL of conidial suspension containing the different concentrations of Semia® was transferred to a glass slide that was covered with a coverslip and also to a Petri dish containing 20 mL of potato-dextrose-agar (PDA) medium. The conidial suspension of *B. maydis* without Semia® corresponded to the control treatment. The conidial suspension was homogeneously distributed over the PDA medium using a Drigalski glass handle. The glass slides and the Petri dishes were transferred to a growth chamber (25°C and 12 h light/12 h dark photoperiod). Each glass slide and Petri dish received 5 µL of lactofuchsin after 12 h to stop conidium germination. One hundred conidia were randomly examined in each glass slide or Petri dish under light microscope (Carl Zeiss AxioImager A1) using bright field at 400 × magnification. Details on conidia germination were acquired digitally (model AxioCam HR, Germany and Axion Vision software v. 4.8.1.). Conidium with germ tube larger than its diameter was considered germinated. The percentage of conidia germination was calculated per replication of each treatment.

2.2. Plant growth

Maize seeds from cultivar Colorado SCS 156 (EPAGRI, Santa Catarina, Brazil), susceptible to *B. maydis*, were sown in plastic pots containing 2 kg of Tropstrato® (mixture of pine bark, peat, and expanded vermiculite; Vida Verde, São Paulo, Brazil) substrate. A total of 1.63 g of calcium phosphate was added to each pot to provide phosphorus to plants before sowing. After seedlings emergence (≈ five days), two plants were kept per pot. Plants were fertilized with nutrient solution (100 mL per pot twice a week) prepared according to Hoagland and Arnon (1950), with a few modifications, as follows: 2.6 mM KCl, 0.6 mM K_2SO_4, 1.2 mM $MgSO_4$, 1.0 mM CH_4N_2O, 1.2 mM NH_4NO_3, 0.0002 mM $(NH_4)_6Mo_7O_{24}$, 0.03 mM H_3BO_4, 0.04 mM $ZnSO_4$, 0.01 mM $CuSO_4$, 0.03 mM $MnCl_2$, 0.015 mM $FeSO_4$, and 0.015 mM ethylenediaminetetraacetic acid disodium (EDTA). Plants were kept in the greenhouse (temperature of 28 ± 5°C, relative humidity of 80 ± 5%, and natural photosynthetically active radiation (PAR) of 900 ± 15 µmol photons m^{-2} s^{-1} measured at midday).

2.3. Foliar spray of plants with Semia®

Maize plants (V6 growth stage, 30 days after seedlings emergence) were sprayed with Semia® solution (5 mL/L; 12.5 mL per plant in each pot) at 48 h before inoculation with *B. maydis* with the aid of a VL Airbrush atomizer (Paasche Airbrush Co., Chicago, IL, USA). This treatment will be referred to induced resistance (IR) stimulus thereafter according to criteria proposed by Kesel *et al*., (2021). Plants sprayed with water served as the control treatment.

2.4. Plant inoculation with *B. maydis*

Pieces of filter paper (≈ 1 mm^2) containing fungal mycelia of the monosporic isolate of *B. maydis* UFV-DPF-*Bm*12 were transferred to Petri dishes containing PDA medium. The dishes were places inside of a growth chamber (25°C and photoperiod of 12 h of light and 12 h of dark) for fungal growth and conidia production during 15 days. Conidia were collected from each dish using sterile water [0.01% Tween 20 and 0.5% gelatin (w/v)] and the conidial suspension was calibrated to 1 × 10^3 conidia/mL using a Neubauer chamber. Plants were inoculated with the conidial suspension of *B. maydis* using a VL Airbrush atomizer and maintained inside a mist growth chamber (25°C and relative humidity of 90 ± 5%) for 24 h. After this period, plants were transferred

to greenhouse (28 ± 2°C, relative humidity of 80 ± 5%, and natural PAR of 900 ± 15 μmol photons m^{-2} s^{-1} measured at midday) until the end of the experiments.

2.5. Evaluation of MLB severity

The fifth expanded leaf, from base to top, of each plant per replication of each treatment was collected at 156 hours after inoculation (hai) and scanned at 600 dpi resolution. The images from all leaves were processed using the QUANT software (Fagundes-Nacarath *et al*., 2018) to obtain the severity values.

2.6. Determining foliar Zn and N concentrations

At the end of the experiment (156 hai), the fifth and sixth leaves, from base to top, of each plant per replication of each treatment were collected, washed in deionized water, dried for 72 h at 65°C, and ground in a ball mill (TECNAL TE 350, Piracicaba, SP, Brazil) for 2 min. Leaf samples were digested with perchloric acid and nitric acid (1:2) solution following the readings in atomic absorption spectrophotometer to determine Zn concentration (Bataglia *et al*., 1983). For N concentration, leaf samples were digested with sulfuric acid and subsequently oxidized with hydrogen peroxide. Aliquots from the extract were reacted with potassium chloride and Nessler reagent with reading at 440nm in spectrophotometer (Lang, 1958).

2.7. Determining leaf gas exchange parameters

The net carbon assimilation rate (A), stomatal conductance to water vapor (g_s), internal CO_2 concentration (C_i), and transpiration rate (E) were measured on the fifth leaf, from base to top, of each plant per replication of each treatment at 12, 60, 108, and 156 hai from 09:00 to 12:00 h using a portable open-system infrared gas analyzer (LI-6400, LI-COR Inc., Lincoln, NE, USA). These parameters were evaluated on the fifth leaves of non-inoculated plants at the same evaluation times mentioned above. All measurements were carried out under the following conditions: leaf temperature of 25°C, chamber CO_2 concentration of 420 ppm, PAR of 1200 μmol m^{-2} s^{-1}, and amount of blue light set with 10% of PAR to optimize stomatal aperture (Marçal *et al*., 2021).

2.8. Imaging and quantification of Chl *a* fluorescence parameters

The Imaging-PAM fluorometer and the Imaging Win software MAXI version (Heinz Walz GmbH) were used to obtain the images for Chl *a* fluorescence parameters (variable-to-maximum chlorophyll *a* fluorescence ratio (F_v/F_m), photochemical yield [Y(II)], yield for dissipation by down-regulation [Y(NPQ)], and yield for non-regulated dissipation [Y(NO)]) on the fifth leaf, from base to top, of each plant non-inoculated or inoculated with *B. maydis* (12, 60, 108, and 156 hai) per replication of each treatment according to the methodology described by Fagundes-Nacarath *et al*., (2018).

2.9. Determining photosynthetic pigments concentration

The concentrations of Chl *a*, Chl *b*, and carotenoids were quantified on the leaves used to obtain the images of Chl *a* fluorescence parameters. Leaf tissue (50 mg) was ground in liquid nitrogen using a vibration ball mill (Retsch, Haan, Germany) and the fine powder was homogenized with 700 µL of methanol. The supernatant was used for quantify concentrations of Chl *a*, Chl *b*, and carotenoids with readings in spectrophotometer at 470, 653, and 666 nm, respectively, using a saturated solution of methanol as a blank (Picanço *et al*., 2022).

2.10. Histochemical detection of lipid peroxidation, membrane damage, hydrogen peroxide (H_2O_2), and superoxide anion radical ($O_2^{\bullet-}$)

The fifth leaf, from base to top, of each plant per replication of each treatment was collected from both non-inoculated and inoculated plants at 156 hai. Lipid peroxidation, membrane damage, H_2O_2, and $O_2^{\bullet-}$ were visualized using Schiff, Evans' blue, 3,3'-diaminobenzidine tetrahydrochloride, and nitro blue tetrazolium solutions, respectively, following the procedures described by Silva *et al*., (2022).

2.11. Biochemical assays and gene expression analysis

The fifth leaf, from base to top, of each plant per replication of each treatment was collected at 12, 60, 108, and 156 hai. Leaves from non-inoculated plants were sampled at these same evaluation times. Leaf samples were kept in liquid nitrogen during samplings and stored in ultrafreezer (-80°C) until further analysis.

2.11.1. Determining sugars and starch concentrations: leaf tissue (50 mg) was ground into a fine powder as described above and mixed with 700 µL of methanol at 80°C for 20 min. Sugars and starch were extracted according to Medeiros *et al*., (2017). Glucose, fructose, and sucrose were determined in the soluble phase of the methanolic solution and the pellet was used for starch quantification following the procedures described by Fernie (2001).

2.11.2. Determining of malondialdehyde (MDA) concentration: leaf tissue (100 mg) was ground as described above and homogenized in 2 mL of trichloroacetic acid solution [0.1% (w/v)] following centrifugation at 12,000 *g* at 4°C for 15 min. A total of 750 µL of thiobarbituric acid solution was added to 250 µL of the supernatant followed homogenization in a thermomixer at 95°C for 30 min. The samples were centrifuged at 9,000 *g* for 10 min and the absorbance readings were taken at 600 and 532 nm (Heath and Packer, 1968).

2.11.3. Determining H_2O_2 and $O_2^{\bullet-}$ concentrations: leaf tissue (100 mg) was ground as described above and homogenized in 1 mL of solution containing potassium phosphate buffer (50 mM, pH 6.5) and hydroxylamine (1 mM). The homogenate was centrifuged at 10,000 *g* at 4°C for 15 min. The supernatant was used to determine H_2O_2 concentration according to Dias *et al*., (2020). Leaf tissue (100 mg) was ground as described above and the fine powder was homogenized in 1 mL of solution containing potassium phosphate buffer (100 mM, pH 7.2) and sodium diethyldithiocarbamate (1 mM). The homogenate was centrifuged at 22,000 *g* at 4°C for 20 min and the supernatant was used to determine $O_2^{\bullet-}$ concentration according to Chaves *et al*., (2021).

2.11.4. Determining antioxidant enzyme activities: leaf tissue (100 mg) was ground as described above and the fine powder was homogenized with 1 mL solution containing 100 mM potassium phosphate buffer (pH 7.8), 0.1 mM EDTA, 1 mM PMSF, and 0.5% (w/v) PVP. The homogenate was centrifuged at 13,000 *g* for 15 min at 4°C and the supernatant was used to determine the activities of ascorbate peroxidase (APX) (EC 1.11.1.11), catalase (CAT) (EC 1.11.1.6), superoxide dismutase (SOD) (EC 1.15.1.1), and glutathione reductase (GR) (EC 1.8.1.7) following the procedure of Debona (2012).

2.11.5. Gene expression using reverse transcription quantitative real-time PCR (RT-PCR): leaf tissue (75 mg) was ground as described above and the fine powder was used to extract the RNA using TRIzol (Invitrogen). Contamination by DNA was eliminated using RQ1 RNase-Free DNase (Promega). The amount of RNA was measured in a Qubit fluorometer using Qubit RNA HS assay kit (Invitrogen) and RNA quality and integrity were verified by 1% agarose gel electrophoresis. Single-stranded cDNAs were synthesized by reverse transcription using 3 µg of total RNA with oligo(dT) primers in a final volume of 20 µL using the SuperScript First Strand Synthesis System for RT-PCR (Invitrogen). The qRT-PCR was performed on a Bio-Rad CFX Real Time Thermal Cycler using SYBR Green PCR Master Mix according to the recommendations of the manufacturer. All reactions were performed in duplicate and the relative expression values for each gene studied were calculated using the $2^{-\Delta\Delta Ct}$ method (Livak and Schmittgen, 2001). Expression analysis of genes encoding for indole-3-glycerol phosphate lyase (*IGL*), chalcone synthase (*CHS02*), pathogenesis-related protein 1 (*PR1*), linoleate 9S-lipoxygenase3 (*LOX3*), phenylalanine ammonia-lyase 3 (*PAL3*), endochitinase (*CHI*), and endo-1,3(4)-*β*-D-glucanase (*GLU*) were performed using specific primer sequences (Table 1). Expression of the nonribosomal peptide synthetase gene from *B. maydis* (*Bm*) was quantified to confirm fungal infection in maize leaf tissues (Kang *et al*., 2018). The gene encoding for cytosolic glyceraldehyde-3-phosphate dehydrogenase (*GAPDH*) was used as a reference for normalization (Silveira *et al*., 2021).

2.12. Experimental design and statistical analysis

For the *in vitro* assays, the experiment was arranged in a completely randomized design (CRD) with six treatments (control and five IR stimulus concentrations). A total of six and ten replications were used for the glass slide and Petri dish assays, respectively. Each replication corresponded to one glass slide or a Petri dish. A 2 × 2 factorial experiment was arranged in a CRD with four replications, per evaluation time, to assess disease severity as well to determine the foliar concentrations of Zn and N. The factors studied were plants sprayed with water (control) or with IR stimulus and non-inoculated or inoculated with *B. maydis*. Another 2 × 2 factorial experiment was arranged in a CRD with six replications, per evaluation time, and the same factors mentioned above, to evaluate the leaf gas exchange and Chl *a* fluorescence parameters as well to quantify the foliar concentration of pigments. Leaf samples for the biochemical assays and gene expression analysis were obtained from another 2 × 2 factorial experiment arranged in a CRD with

five replications, per evaluation time, and the same factors mentioned above. Each experimental unit consisted of one plastic pot with two plants. All experiments were repeated once. Data from variables and parameters were checked for normality and homogeneity of variance and subjected to analysis of variance (ANOVA). The treatment means were compared by Tukey or *F* tests ($P \leq 0.05$). Data from all variables and parameters obtained from the four treatments at 156 hai were used for principal component analysis (PCA). Statistical analysis of all data obtained was carried out using the Minitab Statistical software (Minitab, Inc., 2021).

3. Results

3.1. Analysis of variance

The factor IR stimulus was significant for most of the variables and parameters studied, except for Y(NPQ), glucose, fructose, APX, and GR (Table 2). The factor plant inoculation (PI), sampling time (ST), and the interactions for IR × PI, IR × ST, PI × ST, and IR × PI × ST were significant for most of the variables and parameters evaluated (Table 2).

3.2. *In vitro* assay

The size and appearance of fungal colony were affected as the IR stimulus rates increased from 1 to 15 mL/L (Fig. 1a-f). The EC_{50} obtained was 6.4 mL of IR stimulus/L (Fig. 1g). In comparison to the control treatment (Fig. 2a), germinated conidia of *B. maydis* had thin and shorter germ tubes when exposed to IR stimulus rates ranging from 1 to 15 mL/L (Fig. 2b-f) compared to the absence of IR stimulus (control treatment) (Fig. 2a). Conidia germination significantly decreased by 6, 9, 18, 31, and 46% for 1, 2.5, 5, 10, and 15 mL of IR stimulus/L, respectively, compared to the control treatment (Fig. 3).

3.3. Foliar Zn and N concentrations

Foliar Zn concentration for non-inoculated and IR stimulus-sprayed plants and inoculated and IR stimulus-sprayed plants significantly increased by 93 and 94%, respectively, compared to non-inoculated and inoculated plants from the control treatment (Fig. 4a). For inoculated and IR stimulus-sprayed plants, foliar Zn concentration significantly increased by 27% compared to non-inoculated and IR stimulus-sprayed plants (Fig. 4a). There was no significant difference for foliar

N concentration between IR stimulus and control treatments regardless of plant inoculation with *B. maydis* (Fig. 4b).

3.4. Symptoms of MLB and disease severity

Many necrotic and elliptical lesions developed in the leaves of maize plants from the control treatment (Fig. 5a) while the lesions in the leaves of IR stimulus-sprayed plant were of reduced size and in less number (Fig. 5b). The MLB severity was significantly reduced by 76% for IR stimulus-sprayed plants compared to plants from the control treatment (Fig. 5c).

3.5. Leaf gas exchange parameters

For non-inoculated plants, A, g_s, C_i, and E were not affected by IR stimulus and control treatments regardless of the evaluation time (Fig. 6a, c, e, and g). For inoculated plants from the IR stimulus treatment, A (31, 35, and 56% at 60, 108, and 156 hai, respectively), g_s (26 and 57% at 60 and 156 hai, respectively), and E (30 and 27% at 60 and 156 hai, respectively) were significantly higher while C_i (19, 34, and 26% at 60, 108, and 156 hai, respectively) was significantly lower compared to inoculated plants from the control treatment (Fig. 6b, d, f, and h). For control treatment, A (38-73% from 60 to 156 hai), g_s (34-75% from 60 to 156 hai), and E (41-48% from 60 to 156 hai) were significantly lower while C_i (17 and 19% at 108 and 156 hai, respectively) was significantly higher for inoculated compared to non-inoculated plants (Fig. 6a-h and e-f). The A (38 and 43%), g_s (32 and 46%), C_i (21 and 16%), and E (35 and 25%) were significantly lower at 108 and 156 hai for inoculated plants from the IR stimulus treatment compared to their non-inoculated counterparts (Fig. 6a-h).

3.6. Imaging and quantification of Chl *a* fluorescence parameters

Damage to the photosynthetic apparatus was noticed in the leaves of plants from the control treatment compared to IR stimulus-sprayed plants based on the darker areas in the images for F_v/F_m, Y(II), Y(NPQ), and Y(NO) parameters (Fig. 7). For non-inoculated plants, there was no significant difference between control and IR stimulus treatments regardless of the evaluation time (Fig. 8a, c, e, and g). For inoculated plants, F_v/F_m (12 and 18% at 108 and 156 hai, respectively), Y(II) (24, 29, and 27% at 60, 108, and 156 hai, respectively), Y(NPQ) (11 and 14% at 108 and 156 hai, respectively), and ETR (20, 19, and 21% at 60, 108 and 156 hai, respectively) were

significantly higher while Y(NO) (16-21% from 60 to 156 hai) was significantly lower for IR stimulus-sprayed plants compared to plants from the control treatment (Fig. 8b, d, f, h, and j). For control treatment, F_v/F_m (6-18% from 12 to 156 hai), Y(II) (13-17% from 12 to 156 hai), and ETR (30-38% from 60 to 156 hai) were significantly lower for inoculated compared to non-inoculated plants (Fig. 8a-d and i-j). For IR stimulus treatment, Y(II) (11 and 20% at 108 and 156 hai, respectively) and Y(NPQ) (11-13% from 60-156 hai) were significantly higher while Y(NO) and ETR were significantly lower for inoculated plants compared to non-inoculated plants from 60 to 156 hai (Fig. 8c-j).

3.7. Photosynthetic pigments

Concentrations of Chl *a+b* and carotenoids for non-inoculated plants were not affected by IR stimulus and control treatments regardless of the evaluation time (Fig. 9a and c). For inoculated plants, concentrations of Chl *a+b* (22-30%) and carotenoids (21-38%) were significantly higher for IR stimulus-sprayed plants compared to plants from the control treatment from 60 to 156 hai (Fig. 9b and d). For control treatment, concentrations of Chl *a+b* (24-36%) and carotenoids (21-46%) were significantly lower for inoculated compared to non-inoculated plants (Fig. 9a-d). For IR stimulus treatment, concentration of carotenoids was significantly reduced by 18% for inoculated compared to non-inoculated plants at 156 hai (Fig. 9a-d).

3.8. Carbohydrates

For non-inoculated plants, there was no significant difference between control and IR stimulus treatments regardless of the evaluation time (Fig. 10a, c, e, and g). For inoculated and IR stimulus-sprayed plants, glucose (13% at 108 hai), fructose (15% at 108 hai), sucrose (14 and 22% at 108 and 156 hai, respectively), and starch (34, 31, and 51% at 12, 60, 156 hai, respectively) concentrations were significantly higher compared to inoculated plants from the control treatment (Fig. 10b, d, f, and h). For control treatment, concentrations of glucose (17 and 14% at 12 and 108 hai, respectively), sucrose (15 and 27% at 108 and 156 hai, respectively), and starch (52% at 156 hai) were significantly lower for inoculated compared to non-inoculated plants (Fig. 10a-b and e-h). For IR stimulus treatment, concentration of starch significantly increased by 26% for inoculated compared to non-inoculated plants at 12 hai (Fig. 10g-h).

3.9. Histochemical assay

No sign of cellular perturbation on leaves of non-inoculated and IR stimulus-sprayed plants was noticed based on the absence of staining for lipid peroxidation, membrane damage as well as depositions of H_2O_2 and $O_2^{\bullet-}$ compared to the leaves of non-inoculated plants from the control treatment (Fig. 11a-d). Lipid peroxidation (pink color), membrane damage (blue color), and depositions of H_2O_2, (brown color) and $O_2^{\bullet-}$ (blue color) were less intense in the leaves of inoculated and IR stimulus-sprayed plants than on leaves of inoculated plants from the control treatment at 156 hai (Fig. 11a-d).

3.10. Concentrations of MDA, H_2O_2, and $O_2^{\bullet-}$

Concentrations of MDA, H_2O_2, and $O_2^{\bullet-}$ for non-inoculated plants were not affected by IR stimulus and control treatments regardless of the evaluation time (Fig. 12a, c, and e). For inoculated plants, MDA (10-18% from 60 to 156 hai), H_2O_2 (15 and 16% at 108 and 156 hai, respectively), and $O_2^{\bullet-}$ (20-25% from 60 to 156 hai) were significantly lower for IR stimulus-sprayed plants compared to plants from the control treatment (Fig. 12b, d, and f). For control treatment, MDA (19-34%), H_2O_2 (20-26%), and $O_2^{\bullet-}$ (24-48%) were significantly higher for inoculated plants compared to non-inoculated plants from 60 to 156 hai. For IR stimulus treatment, MDA (10, 22, and 14% at 60, 108, and 156 hai, respectively), H_2O_2 (14 and 15% at 60 and 156 hai, respectively), and $O_2^{\bullet-}$ (16 and 28% at 108 and 156 hai, respectively) were significantly higher for inoculated compared to non-inoculated plants (Fig. 12a-f).

3.11. Antioxidant enzymes

For non-inoculated plants, there was no significant difference between control and IR stimulus treatments regardless of the evaluation time (Fig. 13a, c, e, and g). For inoculated plants, SOD (14, 11, and 19% at 12, 108, and 156 hai, respectively), APX (33% at 156 hai), CAT (14, 50, and 41% at 12, 108, and 156 hai, respectively), and GR (12 and 27% at 12 and 156 hai, respectively) activities were significantly higher for IR stimulus-sprayed plants compared to plants from the control treatment (Fig. 13b, d, f, and h). Activities of APX (10% at 12 hai) and GR (16 and 18% at 60 and 108 hai, respectively) were significantly lower for inoculated and IR stimulus-sprayed plants compared to inoculated plants from the control treatment (Fig. 13d and h). For control treatment, activities of APX (58, 27, and 29% at 12, 60, and 108 hai, respectively) as well as of

CAT and GR (49 and 33% at 12 hai, respectively) were significantly higher for inoculated compared to non-inoculated plants (Fig. 13c-h). For IR stimulus treatment, SOD (14% at 12 hai), APX (53, 29, and 21% at 12, 60, and 108 hai, respectively), CAT (49, 16, and 46% at 12, 108, and 156 hai, respectively), and GR (36 and 21% at 12 and 156 hai, respectively) were significantly higher for inoculated compared to non-inoculated plants (Fig. 13a-h).

3.12. Gene expression

Comparing non-inoculated vs. inoculated plants for control and IR stimulus treatments

For control treatment, expressions of *PR1*, *PAL3*, *LOX3*, *CHI*, and *GLU* at 12 hai, *IGL*, *CHS02*, *PR1*, *LOX3*, *CHI*, and *GLU* at 60 hai, *PR1*, *PAL3*, *LOX3*, *CHI*, and *GLU* at 108 hai, and *IGL*, *PR1*, *PAL3*, *CHI*, and *GLU* at 156 hai were significantly higher for inoculated plants compared to non-inoculated plants. Expressions of *LOX3* at 108 and 156 hai were significantly reduced for inoculated plants compared to non-inoculated plants of the control treatment (Fig. 14a and c). Expressions of *PR1*, *PAL3*, and *CHI* at 12 hai, *IGL*, *CHS02*, *PR1*, *PAL3*, *LOX3*, *CHI*, and *GLU* at 60 and 156 hai, and *IGL*, *PR1*, *LOX3, CHI*, and *GLU* at 108 hai were significantly lower for inoculated plants compared to non-inoculated plants of the IR stimulus treatment. For IR stimulus treatment, *LOX3* expression was significantly reduced for inoculated plants compared to non-inoculated plants at 108 and 156 hai (Fig. 14b and d).

Comparing IR stimulus and control treatments for non-inoculated and inoculated plants

For non-inoculated plants, expressions of *CHS02*, *PAL3*, *CHI*, and *GLU* at 12 hai, *CHS02*, *PAL3*, and *GLU* at 60 hai as well as *CHS02*, *PR1*, *PAL3*, and *GLU* at 108 hai were significantly reduced for IR stimulus treatment compared to the control treatment (Fig. 14a-b). For inoculated plants, expressions of *PR1* and *PAL3* at 12 hai, *IGL*, *PAL3*, and *GLU* at 60 hai, *IGL* and *CHI* at 108 hai as well as *IGL*, *CHS02*, *PAL3*, and *GLU* at 156 hai were significantly reduced for IR stimulus treatment compared to the control treatment (Fig. 14c-d). Expressions of *LOX3* at 12 and 60 hai and *Bm* from 60 to 156 hai were significantly reduced for IR stimulus treatment compared to the control treatment (Fig. 14c-d).

3.13. PCA analysis

According to the cluster analysis with complete linkage and Pearson distance, three clusters were generated: inoculated plants from control treatment, inoculated plants from IR stimulus treatment, and non-inoculated plants from control and IR stimulus treatments (Fig. 15). One principal component (PC) explained most of data variation (PC1 = 51.1% and PC2 = 45.8%) (Fig. 13). The PC1 indicated negative scores for C_i, glucose, MDA, H_2O_2, $O_2^{\bullet-}$, CAT, *IGL*, *CHS02*, *PR1*, *PAL3*, *LOX3*, *CHI*, and *GLU* while positive scores were obtained for Zn, N, *A*, g_s, *E*, F_v/F_m, Y(II), Y(NPQ), Y(NO), ETR, Chl *a*+*b*, carotenoids, fructose, sucrose, starch, SOD, APX, and GR. The PC2 was characterized by negative scores for Zn, N, F_v/F_m, Y(II), Y(NPQ), Chl *a*+*b*, carotenoids, glucose, fructose, sucrose, starch, $O_2^{\bullet-}$, SOD, AOX, CAT, GR, *IGL*, *CHS02*, *PR1*, *PAL3*, *LOX3*, *CHI*, and *GLU* while positive scores were obtained for *A*, g_s, C_i, *E*, Y(NO), ETR, MDA, and H_2O_2 (Fig. 15).

4. Discussion

The use of IR stimuli represents a sustainable alternative to complement the currently recommended control methods for destructive diseases affecting profitable crops such as maize (Reglinski *et al*., 2023). In the present study, MLB symptoms and fungal colonization on leaf tissues were reduced for IR stimulus-sprayed plants. The potential of the IR stimulus to trigger maize defense reactions against *B. maydis* was clearly confirmed at the physiological, biochemical, and molecular levels. Interestingly, the IR stimulus negatively affected the mycelial growth of *B. maydis* as well as conidia germination *in vitro*. Some IR stimuli such as different formulations of phosphites, oxalic acid, saccharin, and a copper-polyphenolic compound were capable to exert an antimicrobial effect against different pathogens mainly through the rupture of hyphae cell wall that caused great electrolyte leakage (Fagundes-Nacarath *et al*., 2018b; Novaes *et al*., 2019; Chaves *et al*., 2021; Mejri *et al*., 2021; Rodrigues *et al*., 2023).

In the present, IR stimulus-sprayed plants infected by *B. maydis* displayed higher Zn foliar concentration in contrast to the non-infected ones. The reduced foliar symptoms of MLB for IR stimulus-sprayed plants can be accounted to higher Zn concentration. The Zn is a catalytic and structural protein cofactor of certain enzymes such as superoxide dismutase and alcohol dehydrogenase, in addition to its key structural functions in the protein domains of metallothionein that act as antioxidants against reactive oxygen species (ROS) produced due to pathogen infection

(Bastakoti, 2023; Dimkpa and Elmer, 2023). The Zn finger proteins (Znf), which contain one or more Zn ions to stabilize their structure, are involved in the regulation of plant defense reactions against pathogen infection (Han *et al.*, 2021). A meta-analysis study to understand the role of Znf in proteins of resistance (R), gene found 70 proteins related to the resistance of various crops against different diseases and among them, 37% contained Znf domains (Gupta *et al*., 2012). The Zn increased resistance and inhibited the mycelial growth of *Curvularia lunata*, *Alternaria grandis* and *Fusarium solani* on maize, potato and wheat, respectively (Choudhary *et al*., 2019; Khoshgoftarmanesh *et al*., 2010; Machado *et al*., 2018).

The limitations imposed by infection of pathogens of different lifestyles on photosynthesis are associated with lower synthesis and translocation of photoasimilates as well as altered transpiration on stomata (Horbach *et al*., 2011; Dias *et al*., 2020). Changes in host metabolism can be monitored by the chlorophyll fluorescence kinetics linked with the outcome of the gas exchange parameters measurements (Rolfe and Scholes, 2010). Particularly in maize, leaf infection by *B. maydis* seriously compromised photosynthesis as illustrated by changes in leaf gas exchange (lower *A*, gs, and *E* values) and Chl *a* fluorescence [lower F_v/F_m, Y(II), Y(NO), and ETR values) parameters associated with great reduction in the pool of photosynthetic pigments (Altaf *et al.*, 2016). In the present study, the harmful effect caused by *B. maydis* infection on photosynthesis of maize plants was alleviated by the IR stimulus. Higher *A*, g_s and *E* values obtained for diseased leaves of IR stimulus-sprayed plants indicated reflected their better physiological status due to the preservation of stomatal function and reduction in biochemical and dysfunctional limitations. Considering the photosynthetic apparatus, diseased leaves of IR stimulus-sprayed plants displayed smooth alterations in the photochemical performance of photosynthesis based on the great values obtained for F_v/F_m, Y(II), and Y(NPQ). In barley leaves infected by *Blumeria graminis* f. sp. *hordei*, the relationship between ETR values and relative CO_2 assimilation rates was intrinsically linear (Swarbrick *et al*., 2006). In the present study, there was a balance between ETR and *A* indicating the occurrence of the flow of electrons and the rate of CO_2 assimilation during the photosynthetic process on infected leaves of IR stimulus-sprayed. According to Klughammer and Schreiber (2008), Y(NO) indicates the fraction of energy that is dissipated through unregulated extinction processes (e.g., heat and fluorescence) due to closed reaction centers in the PSII at saturated light intensity. Interestingly, the Y(NO) values were lower for infected and IR stimulus-sprayed plants compared to infected and water-sprayed plants. This finding may reflect in less

photodamage on leaf tissues due to the decrease in the amount of energy dissipated through the non-extinction of energy regulated at the PSII level as reported by Rolfe and Scholes (2010). Similar findings were found for common bean plants sprayed with oxalic acid and infected by *Sclerotinia sclerotiorum* (Fagundes-Nacarath *et al*., 2018b) and soybean plants sprayed with phosphite combined with free amino acids and infected by *Phakopsora pachyrhizi* (Picanço *et al*., 2022). The reduction in MLS symptoms in the leaves of IR stimulus-sprayed plants was associated with higher concentration of photosynthetic pigments (Chl *a+b* and carotenoids) indicating greater preservation of their photosynthetic apparatus and an efficient use of light energy for carbon fixation. Different IR stimuli attenuated the stress imposed by infection of fungal pathogens on the photosynthetic capacity of their hosts due to greater pool of chlorophylls and carotenoids (Fagundes-Nacarath *et al*., 2018a; Dias *et al*., 2020; Silva *et al*., 2022; Rodrigues *et al*., 2023).

The response of plants against pathogen infection occurs through the activation of different sets of defense reactions that demand an abundant and constant supply of energy derived mainly from the carbohydrate metabolism (Rojas *et al*., 2014). In general, infected and water-sprayed plants showed reduced pools of sugars and starch compared to infected and IR stimulus-sprayed plants. Down-regulation of genes encoding for photosynthetic proteins associated with PSI and PSII reaction centers, ATP synthase, RuBisCo activase, and phosphoribulose kinase contributed to lower the foliar concentrations of sugars and starch in pathogen-challenged plants (Bilgin *et al*., 2010). The reduction in the foliar pool of sucrose was greater in comparison to hexose, fructose, and glucose for tomato plants infected by *Botrytis cinerea* due to negative expression of photosynthetic-related genes and impaired photosynthesis (Berger *et al*., 2004). Along with carbon depletion due to reduced photosynthesis, fungal pathogens (*Botryosphaeria dothidea* and *Valsa sordida*) causing canker symptoms affected the distribution of carbohydrates in the stem of poplar plants (Li *et al*., 2019). Foliar concentrations of glucose, fructose (at 108 hai), and sucrose (at 108 and 156 hai) for infected and IR stimulus-sprayed plants were kept higher compared to infected and water-sprayed plants. The starch concentration, the main reserve of carbon in plant tissues, in infected leaves of IR stimulus-sprayed plants was higher. In various host-fungal pathogens interactions, the concentrations of soluble sugars and starch provide the carbon skeletons to act as signals for the functioning of different metabolic pathways responsible for the synthesis of diverse defense-related metabolites (Lecompte *et al*., 2013; Kanwar and Jha, 2019). Higher sugars concentration at the infection sites of *Magnaporthe oryzae* in rice leaves played an important role

in the constitutive and induced chemical defense (Sun *et al*., 2014). An increase in the concentration of soluble sugars seemed to be a determining factor in the defense response of tomato plants sprayed with a phosphite combined with free amino acids against septoria leaf spot (Silva *et al*., 2022). Taken together, these findings suggest a possible increase in the flux of carbon in IR stimulus-sprayed plants for an increased resistance against *B. maydis* infection.

The intense cellular damage caused by infection of necrotrophic and hemibiotrophic pathogens in the tissues of their hosts originates an excessive production of ROS and the activation of an enzymatic antioxidant system takes place to reduce lipid peroxidation (Meisrimler *et al*., 2020). In the present study, discrete depositions of H_2O_2 and $O_2^{\bullet-}$ on leaf tissues and their lower concentrations associated with less membrane damage and lipid peroxidation (lower MDA concentration) were noticed for IR stimulus-sprayed plants as a result of reduced MLB symptoms. In general, higher SOD, CAT, and GR activities for IR stimulus-sprayed plants attenuated the excessive production of H_2O_2 and $O_2^{\bullet-}$ and, consequently, lower the pool of MDA during *B. maydis* infection. Interestingly, great SOD activity during the foliar infection by *B. maydis* for IR stimulus-sprayed plants contributed to catalyze the dismutation of H_2O_2 and $O_2^{\bullet-}$. In this scenario, CAT activity played the pivotal role in the eliminating of H_2O_2 rather than APX activity, which seemed to be higher at an advance stage of *B. maydis* infection. Both APX and GR activities did not increase in the leaves of soybean plants sprayed with a copper-polyphenolic compound and infected by *Phakopsora pachyrhizi* possibly linked to the lower production of singlet oxygen and hydroxyl radicals (Rodrigues *et al*., 2023). Plants such as common bean, rice, soybean, tomato, and wheat exposed to different IR stimuli (e.g., picolinic acid, glutamate, phosphites, and a copper-polyphenolic compound) developed a more robust antioxidant machinery that involved great SOD, APX, CAT, and GR activities to interfere with the infection by pathogens of different lifestyles (Aucique-Pérez *et al*., 2019; Dias *et al*., 2020; Fagundes-Nacarath *et al*., 2018a; Silva *et al*., 2022; Rodrigues *et al*., 2023).

Interestingly, most of the genes studied in the present study were up-regulated for IR stimulus-sprayed plants compared to water-sprayed plants indicating the potential of this IR stimulus to elicit maize defense responses in the absence of *B. maydis* infection. Notably, the pattern of gene expression for infected plants was more evident upon their exposition to the IR stimulus. Interestingly, *IGL* (from 60 to 156 hai), *CHS02* (at 156 hai), *PR1* (at 12 hai), *PAL3* (at 12, 60, and 156 hai), *CHI* (at 108 hai), and *GLU* (at 60 and 156 hai) were strongly up-regulated in

maize leaves of IR stimulus-sprayed plants facing *B. maydis* infection highlighting their contribution to increased resistance against MLB. Plants exogenously exposed to different IR stimuli encountered profound changes at the physiological, transcriptional, and metabolic levels to have their defense capacity boosted against pathogen infection (Mauch-Mani *et al*., 2017; Kesel *et al*., 2021). The enzymatic roles of indole-glycerolphosphate lyases (a maize enzyme catalyzing the conversion of indole-3-glycerol phosphate to indole, which is subsequently converted into the benzoxazinoid secondary metabolites (DIBOA [2,4-di-hidroxi-2H-1,4- benzoxazin-3(4H)-ona] and its derivative methoxy DIMBOA [2,4-dihidroxi-7-metoxi-2H-1,4-benzoxazin-3(4H)-ona]) originated from *IGL* expression were similar to those enzymes coded by *Bx1* (benzoxazin 1) (Frey *et al*., 2009; Neal *et al*., 2012). The contribution of benzoxazinoids is not only limited to their biocidal properties, but their role as regulatory signals to activate host defense responses against *B. maydis* and *Exserohilum turcicum* infections in maize (Zhou *et al*., 2018). The importance of flavonoids and isoflavonoids for plant resistance against diseases is well recognized and *CHS02* expression plays a key role in the regulation of their biosynthesis (Dao *et al*., 2011). Soybean plants sprayed with a copper-polyphenolic compound showed up-regulation of *CHIB1* indicating the biosynthesis of flavonoids in response to *P. pachyrhizi* infection (Rodrigues *et al*., 2023). The *PR1* was up-regulated only at 12 hai in infected maize leaves of IR stimulus-sprayed plants. Manghwar *et al*., (2018) reported up-regulation of *PR1* in leaves infected by *Bipolaris sorokiniana* highlighting its role for the increased resistance of maize plants. In tomato leaves sprayed with a phosphite combined with free amino acids and infected by *S. lycopersici*, the *PR1b1* was up-regulated (Silva *et al*., 2022).

For IR stimulus-sprayed plants, the phenylpropanoid pathway was important for their increased resistance against MLB considering the up-regulation of *PAL3* at 12, 60, and 156 hai. The PAL converts the aromatic amino acid phenylalanine to *trans*-cinnamic acid from which a plethora of phenolics, flavonoids, and phytoalexins are originated along with lignin production (Hyun *et al*., 2011). Maize resistance against *B. maydis* infection was dependent on higher PAL activity (Schauffler *et al*., 2022). In the present study, up-regulations of *CHI* and *GLU* at 108 and 156 hai, respectively, for infected and IR stimulus-sprayed plants was linked to their increased resistance against MLB. In maize plants, expression of classes I and II of chitinase genes belonging to the PR-4 family contributed to their resistance against *Fusarium moniliforme* infection (Bravo *et al*., 2003). Expression of *Chit2* in maize calluses affected the colonization by *Fusarium*

graminearum (Dowd *et al*., 2018). Maize genotypes resistant to *Fusarium verticillioides* infection exhibited great *β*-1,3-glucanase activity (Zhang *et al*., 2023). The resistance of wheat plants against *Fusarium graminearum* infection was linked to great expressions of *TaPR3* and *TaGlu2* that encode for chitinase and *β*-1,3-glucanase, respectively (Gunupuru *et al*., 2019). In the present study, lower *LOX3* expression occurred for infected and water-sprayed plants at 12 and 60 hai. In plant tissues infected by pathogens, especially the necrotrophic ones, the lipoxygenases catalyze the oxidation of polyunsaturated fatty acids released by ROS-induced lipid peroxidation to produce oxylipins that will be enzymatically metabolized into traumatin and jasmonates (Shi *et al*., 2020). Interestingly, down-regulation of *LOX3* for infected and IR stimulus-sprayed plants may be attributed to the lower production of MDA and ROS in the smaller foliar lesions caused by *B. maydis* infection.

In conclusion, the zinc-polyphenolic compound showed potential to increase maize resistance against MLB considering collectively the physiological, biochemical, and molecular evidences reported in the present study. Based on the PCA analysis, infected leaves of maize plants responded differently to water and IR stimulus treatments. For IR stimulus-sprayed plants, in particular, a set of well-portrayed mechanisms such as a more preserved photosynthetic apparatus, expression of genes involved in the host defense reactions, and a more robust antioxidant metabolism was of extreme relevance to impair the infection process of *B. maydis*. It is tempting to assume that using this IR stimulus, combined with well-known control strategies, could become a promising alternative for MLB management in field conditions from the perspective of a more sustainable agriculture.

5. References

Aucique-Pérez, C.E. *et al*. Picolinic acid spray stimulates the antioxidative metabolism and minimizes impairments on photosynthesis on wheat leaves infected by *Pyricularia oryzae*. **Physiol Plant**, v. 167, p. 628-644, 2019.

Altaf, M. *et al*. Study on the response of different maize cultivars to various inoculum levels of *Bipolaris maydis* (Y. Nisik & C. Miyake) shoemaker under field conditions. **J Entomol Zool Stud**, v. 4, p. 533-537, 2016.

Bastakoti, S. Role of zinc in management of plant diseases: A review. **Cogent Food Agric**, v. 9, p. 1080, 2023.

Bataglia, O. *et al*. Métodos de análise química de plantas. Instituto Agronômico de Campinas, Campinas. 48 p, 1983.

Berger, S. *et al*. Complex regulation of gene expression, photosynthesis and sugar levels by pathogen infection in tomato. **Physiol Plant**, v. 122, p. 419-428, 2004.

Bilgin, D.D. *et al*. Biotic stress globally downregulates photosynthesis genes. **Plant Cell Environ**, v. 33, p. 1597-1613, 2010.

Bravo, J.M. *et al*. Fungus- and wound-induced accumulation of mRNA containing a class II chitinase of the pathogenesis-related protein 4 (PR-4) family of maize. **Plant Mol Biol**, v. 52, p. 745-759, 2003.

Cabot, C. *et al*. A role for zinc in plant defense against pathogens and herbivores. **Front Plant Sci**, v. 10, p. 1171, 2019.

Chaves, J.A.A. *et al*. Physiological and biochemical responses of tomato plants to white mold affected by manganese phosphite. **J Phytopathol**, v. 169, p. 149-167, 2021.

Choudhary, R.C. *et al*. Zinc encapsulated chitosan nanoparticle to promote maize crop yield. **Int J Biol Macromol**, v. 127, p. 126-135, 2019.

Dai, Y. *et al*. Sensitivity of *Cochliobolus heterostrophus* to three demethylation inhibitor fungicides, propiconazole, diniconazole and prochloraz, and their efficacy against southern corn leaf blight in Fujian province, China. **Eur J Plant Pathol**, v. 152, p. 447-459, 2018.

Dao, T.T.H., Linthorst, H.J.M., Verpoorte, R. Chalcone synthase and its functions in plant resistance. **Phytochem Rev**, v. 10, p. 397-412, 2011.

Dimkpa, C.O., Elmer, W.H. Zinc and plant disease. In: Datnoff LE, Elmer WH, and Rodrigues FA (Eds.). Mineral and Plant Nutrition. The American Phytopathological Society, St. Paul, p. 265-296, 2023.

Kesel, J. *et al*. The induced resistance lexicon: do's and don'ts. **Trends Plant Sci**, v. 26, p. 685-691, 2021.

Debona, D. *et al*. Biochemical changes in the leaves of wheat plants infected by *Pyricularia oryzae*. **Phytopathology**, v. 102, p. 1121-1129, 2012.

Dias, C.S. *et al*. Effect of glutamate on *Pyricularia oryzae* infection of rice monitored by changes in photosynthetic parameters and antioxidant metabolism. **Physiol Plant**, v. 169, p. 179-193, 2020.

Dowd, P.F. *et al*. Identification of a maize (*Zea mays*) chitinase allele sequence suitable for a role in ear rot fungal resistance. **Agri Gene**, v. 7, p. 15-22, 2018.

Fagundes-Nacarath, I.R.F. *et al*. Phosphites attenuate *Sclerotinia sclerotiorum*-induced physiological impairments in common bean. **Acta Physiol Plant**, v. 40, p. 1-14, 2018a.

Fagundes-Nacarath, I.R.F., Debona, D., Rodrigues, F.A. Oxalic acid-mediated biochemical and physiological changes in the common bean-*Sclerotinia sclerotiorum* interaction. **Plant Physiol Biochem**, v. 129, p. 109-121, 2018b.

Fernie, A.R. The contribution of plastidial phosphoglucomutase to the control of starch synthesis within the potato tuber. **Planta**, v. 213, p. 418-426, 2001.

Frey, M. *et al*. Benzoxazinoid biosynthesis, a model for evolution of secondary metabolic pathways in plants. **Phytochemistry**, v. 70, p. 1645-1651, 2009.

Gunupuru, L.R. *et al*. A plant biostimulant made from the marine brown algae *Ascophyllum nodosum* and chitosan reduce Fusarium head blight and mycotoxin contamination in wheat. **PLoS One**, v. 14, p. 1-19, 2019.

Gupta, S.K. *et al*. Comparative analysis of zinc finger proteins involved in plant disease resistance. **PLoS One**, v. 7, p. 1-15, 2012.

Han, G. *et al*. The roles of CCCH zinc-finger proteins in plant abiotic stress tolerance. **Int J Mol Sci**, v. 22, p. 8327, 2021.

Han, X. *et al*. Effects of phosphite as a plant biostimulant on metabolism and stress response for better plant performance in *Solanum tuberosum*. **Ecotoxicol Environ Saf**, v. 210, p. 111873, 2021.

Heath, R.L., Packer, L. Photoperoxidation in isolated chloroplasts. **Arch Biochem Biophys**, v. 125, p. 189-198, 1968.

Hoagland, D., Arnon, D. The water-culture method for growing plants without soil. Agricultural Experiment Station, Berkeley: California, 1950.

Jaidka, M., Bathla, S., Kaur, R. Improved technologies for higher maize production. In: Hossain A (Ed). Maize - Production and Use. IntechOpen, p. 55-65, 2020.

Hyun, M.W. *et al*. Fungal and plant phenylalanine ammonia-lyase. **Mycobiology**, v. 39, p. 257-265, 2011.

Huang, W. *et al*. Biosynthesis and regulation of salicylic acid and N-Hydroxypipecolic acid in plant immunity. **Mol Plant**, v. 13, p. 31-41, 2020.

Kang, J. *et al*. Simple detection of *Cochliobolus* fungal pathogens in maize. **Plant Pathol J**, v. 34, p. 327-334, 2018.

Kanwar, P., Jha, G. Alterations in plant sugar metabolism: signatory of pathogen attack. **Planta**, v. 249, p. 305-318, 2019.

Kim, Y.H. *et al*. Regulation of jasmonic acid biosynthesis by silicon application during physical injury to *Oryza sativa* L. **J Plant Res**, v. 127, p. 525-532, 2014.

Khoshgoftarmanesh, A.H. *et al*. Zinc nutrition effect on the tolerance of wheat genotypes to *Fusarium* root-rot disease in a solution culture experiment. **Soil Sci Plant Nutr**, v. 56, p. 234-243, 2010.

Klughammer, C., Schreiber, U. Complementary PS II quantum yields calculated from simple fluorescence parameters measured by PAM fluorometry and the saturation pulse method. **PAM Appl Notes**, v. 1, p. 27-35, 2008.

Kumar, C. *et al*. *In vitro* evaluation of fungicides, botanicals and bio-agents against the maydis leaf light disease of maize caused by *Helminthosporium maydis*. **Pharma Innov**, v. 10, p. 399-406, 2021.

Lang, C.A. Simple microdetermination of Kjeldahl nitrogen in biological materials. **Anal Chem**, v. 30, p. 1692-1692, 1958.

Latef, A.H. *et al*. Extracts from yeast and carrot roots enhance maize performance under seawater-induced salt stress by altering physio-biochemical characteristics of stressed plants. **J Plant Growth Regul**, v. 38, p. 966-979, 2019.

Lecompte, F., Abro, M.A., Nicot, P.C. Can plant sugars mediate the effect of nitrogen fertilization on lettuce susceptibility to two necrotrophic pathogens: *Botrytis cinerea* and *Sclerotinia sclerotiorum*? **Plant Soil**, v. 369, p. 387-401, 2013.

Li, P. *et al*. Fungal canker pathogens trigger carbon starvation by inhibiting carbon metabolism in poplar stems. **Sci Rep**, v. 9, p. 1-14, 2019.

Livak, K.J., Schmittgen, T.D. Analysis of relative gene expression data using real-time quantitative PCR and the $2^{-\Delta\Delta CT}$ method. **Methods**, v. 25, p. 402-408, 2001.

Machado, P.P. *et al*. Could the supply of boron and zinc improve resistance of potato to early blight? **Potato Res**, v. 61, p. 169-182, 2018.

Manghwar, H. *et al*. Expression analysis of defense related genes in wheat and maize against *Bipolaris sorokiniana*. **Physiol Mol Plant Pathol**, v. 103, p. 36-46, 2018.

Marçal, D.M.S. *et al*. Elevated [CO_2] benefits coffee growth and photosynthetic performance regardless of light availability. **Plant Physiol Biochem**, v. 158, p. 524-535, 2021.

Mauch-Mani, B. *et al*. Defense priming: An adaptive part of induced resistance. **Annu Rev Plant Biol**, v. 68, p. 485-512, 2017.

Medeiros, D.B. *et al*. Impaired malate and fumarate accumulation due to the mutation of the tonoplast dicarboxylate transporter has little effects on stomatal behavior. **Plant Physiol**, v. 175, p. 1068-1081, 2017.

Meisrimle, C.N. *et al*. Interior design: how plant pathogens optimize their living conditions. **New Phytol**, v. 229, p. 2514-2524, 2020.

Mejri, S. *et al*. Saccharin provides protection and activates defense mechanisms in wheat against the hemibiotrophic pathogen *Zymoseptoria tritici*. **Plant Dis**, v. 105, p. 780-786, 2021.

Meshram, S. *et al*. Comparative transcriptome analysis of fungal pathogen *Bipolaris maydis* to understand pathogenicity behavior on resistant and susceptible non-CMS maize genotypes. **Front Microbiol**, v. 13, p. 837056, 2022.

Neal, A.L. *et al*. Benzoxazinoids in root exudates of maize attract *Pseudomonas putida* to the rhizosphere. **PLoS One**, v. 7, p. 1-14, 2012.

Novaes, M.I.C. *et al*. Physiological and biochemical responses of soybean to white mold affected by manganese phosphite and fluazinam. **Acta Physiol Plant**, v. 41, p. 186, 2019.

Picanço, B.B.M., Silva, B.N., Rodrigues, F.A. Potentiation of soybean resistance against *Phakopsora pachyrhizi* infection using phosphite combined with free amino acids. **Plant Pathol**, v. 71, p. 1496-1510, 2022.

Pieterse, C. *et al*. Induced systemic resistance by beneficial microbes. **Annu Rev Phytopathol**, v. 52, p. 347-375, 2014.

Raiesi, T., Golmohammadi, M. Changes in nutrient concentrations and biochemical characteristics of Mexican lime (*Citrus aurantifolia*) infected by phytoplasma. **J Gen Plant Pathol**, v. 86, p. 486-493, 2020.

Ranum, P. *et al*. Global maize production, utilization, and consumption. **Ann N Y Acad Sci**, v. 1312, p. 105-112, 2014.

Reglinski, T. *et al*. The practical role of induced resistance for crop protection. **Phytopathology**, v. 113, p. 719-731, 2023.

Rojas, C.M. *et al*. Regulation of primary plant metabolism during plant-pathogen interactions and its contribution to plant defense. **Front Plant Sci**, v. 5, p. 1-12, 2014.

Rolfe, S.A., Scholes, J.D. Chlorophyll fluorescence imaging of plant-pathogen interactions. **Protoplasma**, v. 247, p. 163-175, 2010.

Rodrigues, F.C. *et al*. A copper-polyphenolic compound as an alternative for the control of Asian soybean rust. **Trop Plant Pathol**, v. 48, p. 69-483, 2023.

Schauffler, G.P., Anjos, J., Piero, R.M. Defense mechanisms involved in the resistance of maize cultivars to *Bipolaris maydis.* **Eur J Plant Pathol**, v. 163, p. 269-277, 2022.

Shi, Y. *et al*. Legume lipoxygenase: Strategies for application in food industry. **Legum Sci**, v. 2, p. 1-15, 2020.

Shine, M.B. *et al*. Signaling mechanisms underlying systemic acquired resistance to microbial pathogens. **Plant Sci**, v. 279, p. 81-86, 2019.

Silva, B.N. *et al*. Physiological and biochemical insights into induced resistance on tomato against septoria leaf spot by a phosphite combined with free amino acids. **Physiol Mol Plant Pathol**, v. 120, p. 101854, 2022.

Silveira, P.R. *et al*. Biochemical and physiological changes in maize plants supplied with silicon and infected by *Exserohilum turcicum.* **J Phytopathol**, v. 169, p. 393-408, 2021.

Sun, L. *et al*. Sugar homeostasis mediated by cell wall invertase GRAIN INCOMPLETE FILLING 1 (GIF1) plays a role in pre-existing and induced defence in rice. **Mol Plant Pathol**, v. 15, p. 161-173, 2014.

Swarbrick, P.J., Schulze-Lefert, P., Scholes, J.D. Metabolic consequences of susceptibility and resistance (race-specific and broad-spectrum) in barley leaves challenged with powdery mildew. **Plant Cell Environ**, v. 29, p. 1061-1076, 2006.

Tanwar, A. Role of Zinc-Based Nanoparticles in the Management of Plant Diseases. In: Ingle AP (Ed.). Nanotechnology in Plant Growth Promotion and Protection: Recent Advances and Impacts. John Wiley & Sons Ltd. p. 239-258, 2021.

Vaghela, B. *et al*. Plant chitinases and their role in plant defense: A comprehensive review. **Enzyme Microb Technol**, v. 159, p. 110055, 2022.

Van Oosten, M.J., Pepe, O., De Pascale, S. The role of biostimulants and bioeffectors as alleviators of abiotic stress in crop plants. **Chem Biol Technol Agric**, v. 4, p. 1-12, 2017.

Yang, J. *et al*. The crosstalks between jasmonic acid and other plant hormone signaling highlight the involvement of jasmonic acid as a core component in plant response to biotic and abiotic stresses. **Front Plant Sci**, v. 10, p. 1-19, 2019.

Zhang, L. *et al*. Integrative transcriptome and proteome analysis reveals maize responses to *Fusarium verticillioides* infection inside the stalks. **Mol Plant Pathol**, v. 24, p. 693-710, 2023.

7. Tables and Figures

Table 1. Genes, and their primer sequences, analyzed in the leaves of maize plants non-inoculated or inoculated with *Bipolaris maydis* and sprayed with water (control) or with induced resistance (IR) stimulus by using real-time quantitative reverse transcription PCR. Abbreviations: indole-3-glycerol phosphate lyase (*IGL*), chalcone synthase (*CHS02*), pathogenesis-related protein 1 (*PR1*), phenylalanine ammonia-lyase 3 (*PAL3*), linoleate 9S-lipoxygenase 3 (*LOX3*), endochitinase (*CHI*), endo-1,3(4)-*β*-D-glucanase (*GLU*), nonribosomal peptide synthetase from *B. maydis* (*Bm*), and cytosolic glyceraldehyde-3-phosphate dehydrogenase (*GAPDH*).

Genes	GenBank Id.	Primer sense 5'-3'	Primer antisense 5'-3'
IGL	NM_001301469.1	GCCTCATAGTTCCCGACCTC	GAATCCTCGTGAAGCTCGTG
CHS02	NM_001155550.1	TCACCGACCTCAAGGAGAAGTT	TGTACCGCTTCCGGATCATC
PR1	U82200.1	CCTACGGCGAGAACCTCTT	TCGTAGTACTGCTTCTCGGACA
PAL3	XM_020537583.3	AAGGTGTTCGTCGGCATC	TCCCACTCCTTGAGGCACT
LOX3	NM_001112045.1	CGCCAACTCCTGGGTCTAC	TCTGGCTTGGCAGGTACG
CHI	NM_001165432.1	GGTGCGAACGTGGCTAAT	CCGGGTGTAGAAGTTCTTGC
GLU	NM_001316316.1	CAGACCGGTCCATCCACGG	AGTACCCTGCCTTTGCAACCT
Bm	MN783607	TCTCGACAAGCAAATCAAAC	AGATGATTGCAGTGGTGTTG
GAPDH	NM_001111943.1	AAGCCGGTCACCGTCTTT	CATCTTTGCTTGGGGCAGA

Table 2. Analysis of variance for the effects of induced resistance (IR) stimulus, plant inoculation (PI), sampling time (ST), and the interactions IR × PI, IR × ST, PI × ST, and IR × PI × ST on conidia germination (CG), foliar concentrations of zinc (Zn) and nitrogen (K), severity of maize leaf blight (Sev), leaf gas exchange parameters [rate of net CO_2 assimilation (*A*), stomatal conductance to water vapor (g_s), internal CO_2 concentration (C_i), and transpiration rate (*E*)], chlorophyll *a* fluorescence parameters [maximum PSII quantum efficiency (F_v/F_m), photochemical yield (Y(II)), yield for dissipation by down-regulation (Y(NPQ), yield for non-regulated dissipation (Y(NO), and electron transport rate (ETR)], concentrations of photosynthetic pigments [chlorophyll *a*+*b* (Chl *a*+*b*) and carotenoids (Car)], carbohydrates (glucose, fructose, sucrose, and starch), metabolites [malondialdehyde (MDA), hydrogen peroxide (H_2O_2), and superoxide anion radical ($O_2^{\bullet-}$)], activities of antioxidative enzymes [superoxide dismutase (SOD), ascorbate peroxidase (APX), catalase (CAT), and glutathione reductase (GR)], and gene expression [indole-3-glycerol phosphate lyase (*IGL*), chalcone synthase (*CHS02*), pathogenesis-related protein 1 (*PR1*), phenylalanine ammonia-lyase 3 (*PAL3*), linoleate 9S-lipoxygenase3 (*LOX3*), endochitinase (*CHI*), endo-1,3(4)-*β*-D-glucanase (*GLU*), and nonribosomal peptide synthetase from *Bipolaris maydis* (*Bm*)].

Variables/ Parameters	*F* values						
	IR	PI	ST	IR × PI	IR × ST	PI × ST	IR × PI × ST
CG	**257.11**	-	-	-	-	-	-
Zn	**538.14**	**15.23**	-	**13.67**	-	-	-
N	**5.5**	0.21	-	0.04	-	-	-
Sev	**356.82**	-	-	-	-	-	-
A	**23.68**	**195.83**	**53.64**	**16.92**	2.69	**24.10**	0.96
g_s	**12.91**	**104.08**	**27.75**	**7.07**	1.35	**19.15**	1.52
C_i	**25.35**	0.64	**11.30**	**39.58**	**3.07**	**5.24**	**3.66**
E	**6.31**	**135.58**	**59.30**	**19.46**	1.16	**17.20**	1.25
F_v/F_m	**29.34**	**49.06**	**5.96**	**19.26**	**5.53**	**3.12**	**3.82**
Y(II)	**38.12**	2.21	**4.05**	**32.68**	**4.93**	**5.16**	2.31
Y(NPQ)	0.66	**12.34**	**22.18**	**6.83**	**3.00**	0.59	0.81
Y(NO)	**14.48**	**18.81**	**8.03**	**15.86**	2.19	2.77	2.67
ETR	**21.59**	**128.81**	**19.25**	**10.70**	0.54	**17.61**	1.66
Chl *a*+*b*	**11.43**	**27.98**	**19.02**	**12.56**	0.66	2.23	1.73
Car	**31.09**	**45.87**	**20.88**	**23.84**	**4.62**	**10.19**	2.55
Glucose	1.76	**7.28**	**3.15**	1.12	0.36	2.26	0.48
Fructose	2.97	2.08	2.17	1.78	1.36	0.06	0.40
Sucrose	**8.32**	**26.16**	**4.07**	3.91	1.50	1.72	1.63
Starch	**18.03**	2.03	**4.74**	**9.52**	1.75	**5.64**	2.72
MDA	**10.19**	**73.67**	**3.82**	**11.56**	0.75	**14.27**	1.22
H_2O_2	**6.26**	**51.65**	**20.69**	**6.71**	**2.98**	**6.54**	1.35
$O_2^{\bullet-}$	**16.55**	**83.57**	1.06	**15.60**	1.69	**11.39**	1.80
SOD	**25.94**	2.05	**97.98**	**6.12**	1.22	**3.28**	0.95
APX	3.83	**103.23**	**15.93**	0.06	**4.29**	**16.25**	0.67
CAT	**21.09**	**44.83**	**30.02**	**11.79**	2.72	**21.81**	0.29

GR	1.66	0.09	**4.41**	0.03	**3.91**	**38.09**	**3.52**
IGL	**605.22**	**346.10**	**552.93**	**521.24**	**226.65**	**318.52**	**547.09**
CHS02	**455.89**	**416.65**	**243.43**	1.84	**73.54**	**441.98**	**269.13**
PR1	**15.23**	**1640.19**	**485.40**	**4.10**	**9.35**	**281.32**	**12.79**
PAL	**248.36**	**272.56**	**178.72**	**640.09**	**125.68**	**251.93**	**248.84**
LOX3	**703.29**	**1575.64**	**1086.47**	**706.18**	**363.10**	**458.14**	**382.61**
CHI	**880.89**	**7865.54**	**2222.63**	**553.67**	**704.37**	**2026.00**	**757.34**
GLU	**856.29**	**2431.59**	**200.44**	**259.86**	**209.98**	**238.50**	**353.30**
Bm	**1347.40**	-	**521.55**	-	**223.10**	-	-

*Bold values are significant ($P \leq 0.05$)

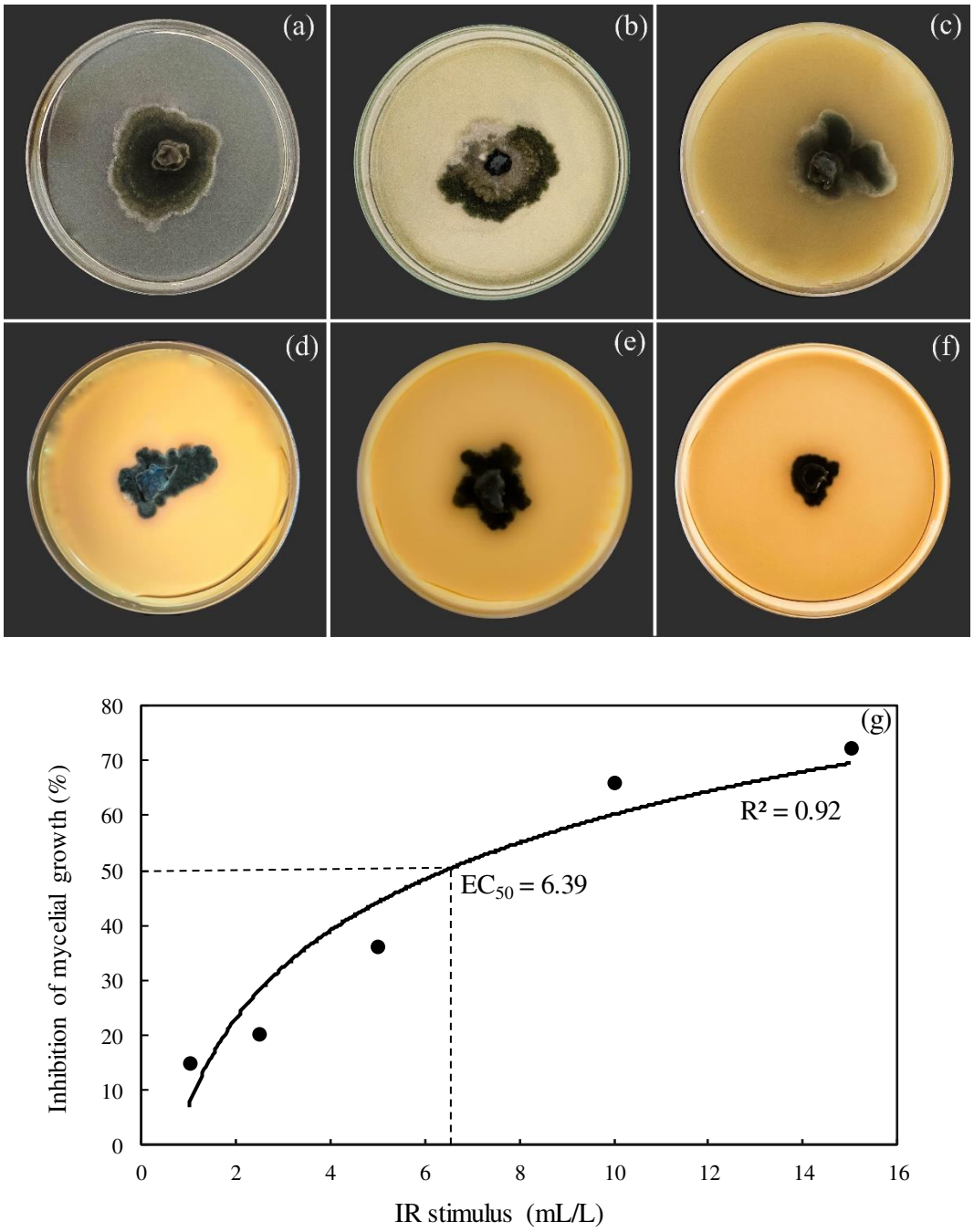

Figure 1. Mycelial growth of *Bipolaris maydis* in Petri dishes containing potato-dextrose-agar amended with 0 (a), 1 (b), 2.5 (c), 5 (d), 10 (e), and 15 (f) mL of induced resistance (IR) stimulus per liter. Effective concentration (EC_{50}) of IR stimulus inhibiting the mycelial growth of *B. maydis* in 50% (g).

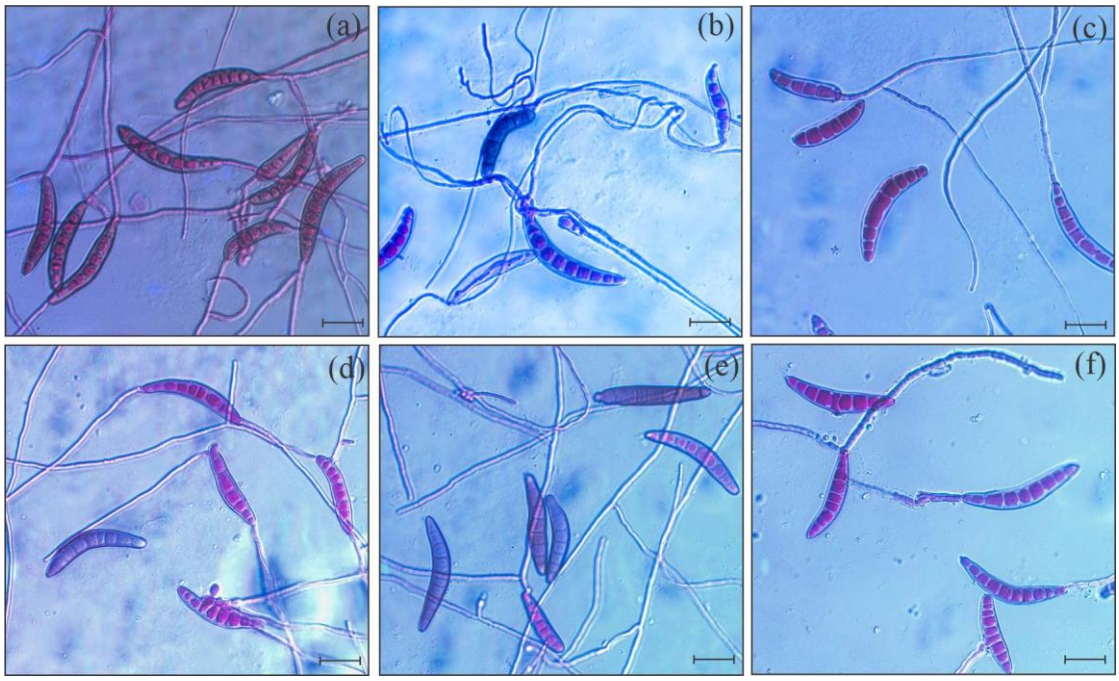

Figure 2. Visual aspect of conidia germination from *Bipolaris maydis* previously exposed to 0 (a), 1 (b), 2.5 (c), 5 (d), 10 (e), and 15 (f) mL of induced resistance (IR) stimulus per liter. Scale bars = 10 μm.

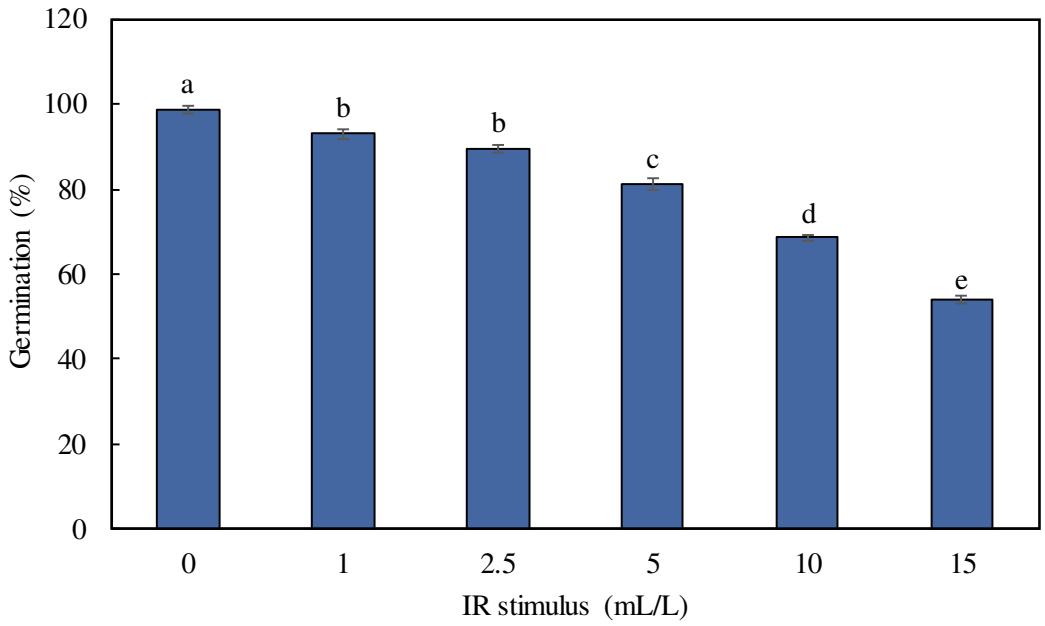

Figure 3. Conidia germination of *Bipolaris maydis* (a) previously exposed to 0, 1, 2.5, 5, 10, and 15 mL of induced resistance (IR) stimulus per liter. Means followed by different letters are significantly different according to Tukey´s test ($P \leq 0.05$). Bars represent the standard error of the means.

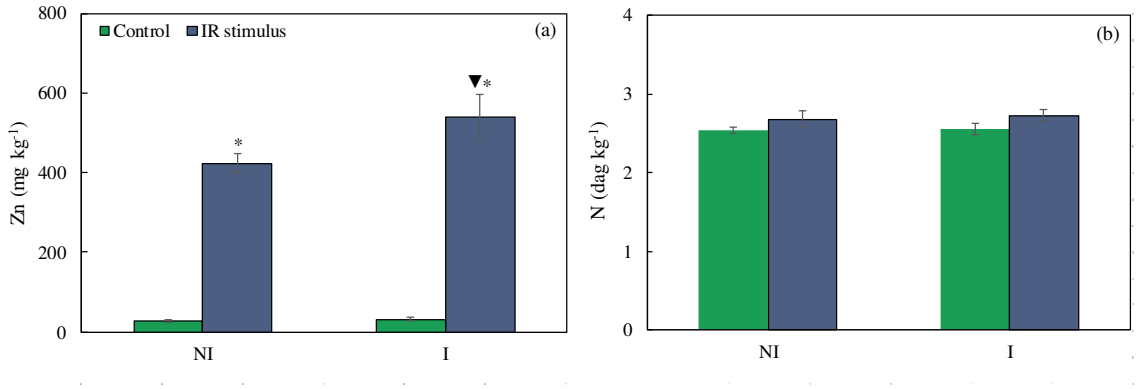

Figure 4. Foliar concentrations of zinc (Zn) (a) and nitrogen (N) (b) for maize plants non-inoculated or inoculated with *Bipolaris maydis* and sprayed with water (control) or with induced resistance (IR) stimulus. Means for NI and I treatments followed by an inverted triangle (▼) and for control and IR stimulus treatments followed by an asterisk (*), at each evaluation time, are significantly different according to *F* test ($P \leq 0.05$). Bars represent the standard error of the means.

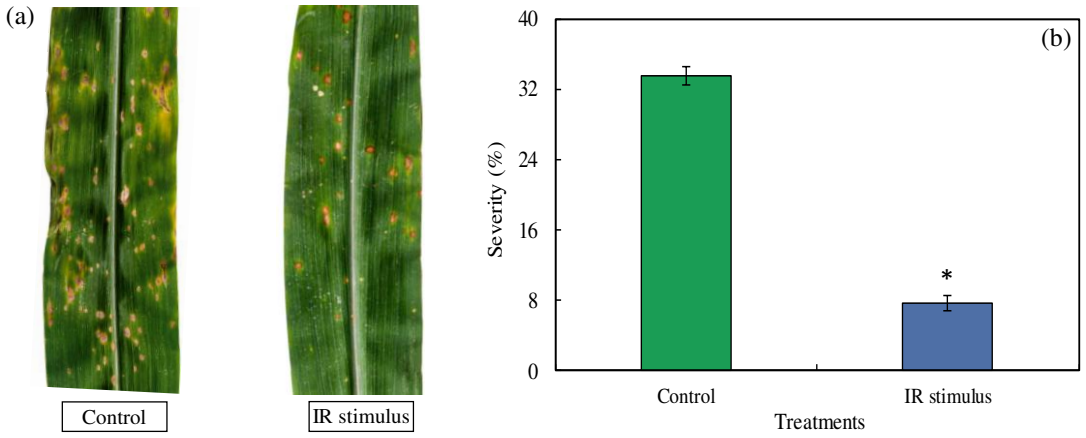

Figure 5. Symptoms of maize leaf blight (a and b) and disease severity (c) for maize plants non-inoculated or inoculated with *Bipolaris maydis* and sprayed with water (control) or with induced resistance (IR) stimulus. Means from control and IR stimulus treatments (graph c) followed by an asterisk (*) are significantly different ($P \leq 0.05$) according to F test. Bars represent the standard error of the means. Disease symptoms and severity are representative of plants at 7 days after inoculation with *B. maydis*.

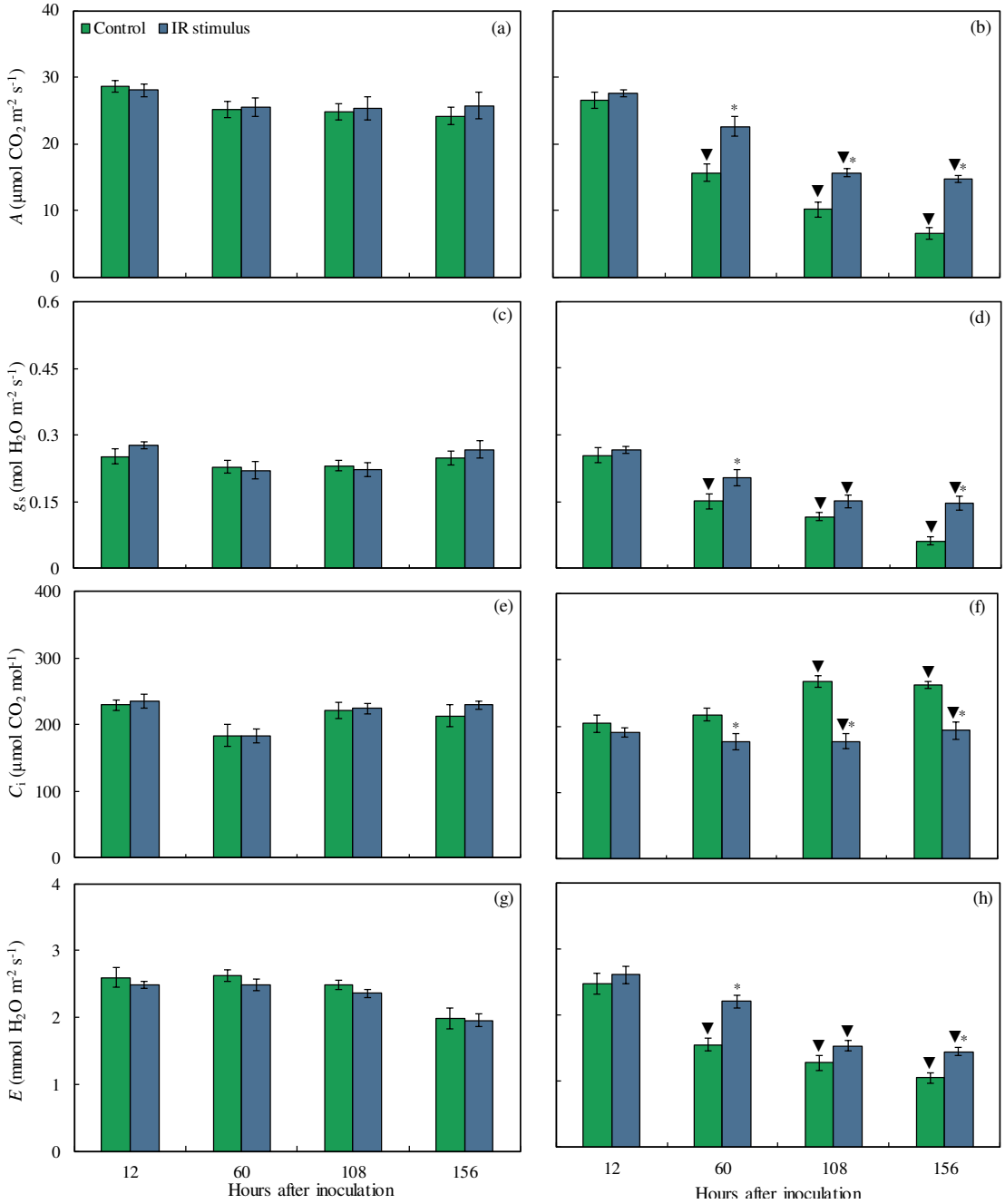

Figure 6. Leaf gas exchange parameters: net carbon assimilation rate (*A*) (a and b), stomatal conductance to water vapor (g_s) (c and d), internal CO_2 concentration (C_i) (e and f), and transpiration rate (*E*) (g and h) determined on the leaves of maize plants non-inoculated (NI) (a, c, e, and g) or inoculated (I) (b, d, f, and h) with *Bipolaris maydis* and sprayed with water (control) or with induced resistance (IR) stimulus. Means for NI and I treatments followed by an inverted triangle (▼) and for control and IR stimulus treatments followed by an asterisk (*), at each evaluation time, are significantly different ($P \leq 0.05$) according to *F* test. Bars represent the standard error of the means.

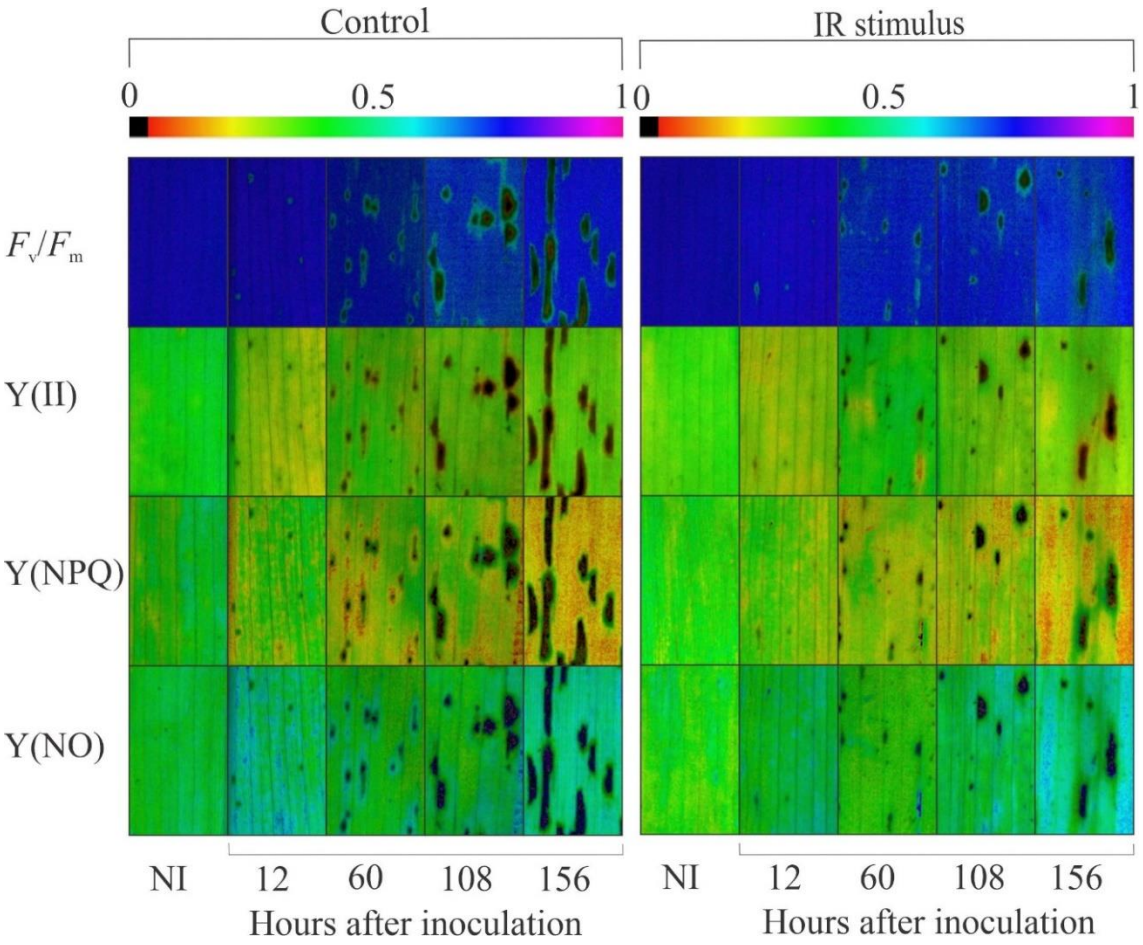

Figure 7. Images of chlorophyll *a* fluorescence parameters maximum PSII quantum efficiency (F_v/F_m), photochemical yield [Y(II)], yield for dissipation by down-regulation [Y(NPQ)], and yield for non-regulated dissipation [Y(NO)] for leaves of maize plants non-inoculated or inoculated with *Bipolaris maydis* and sprayed with water (control) or with induced resistance (IR) stimulus.

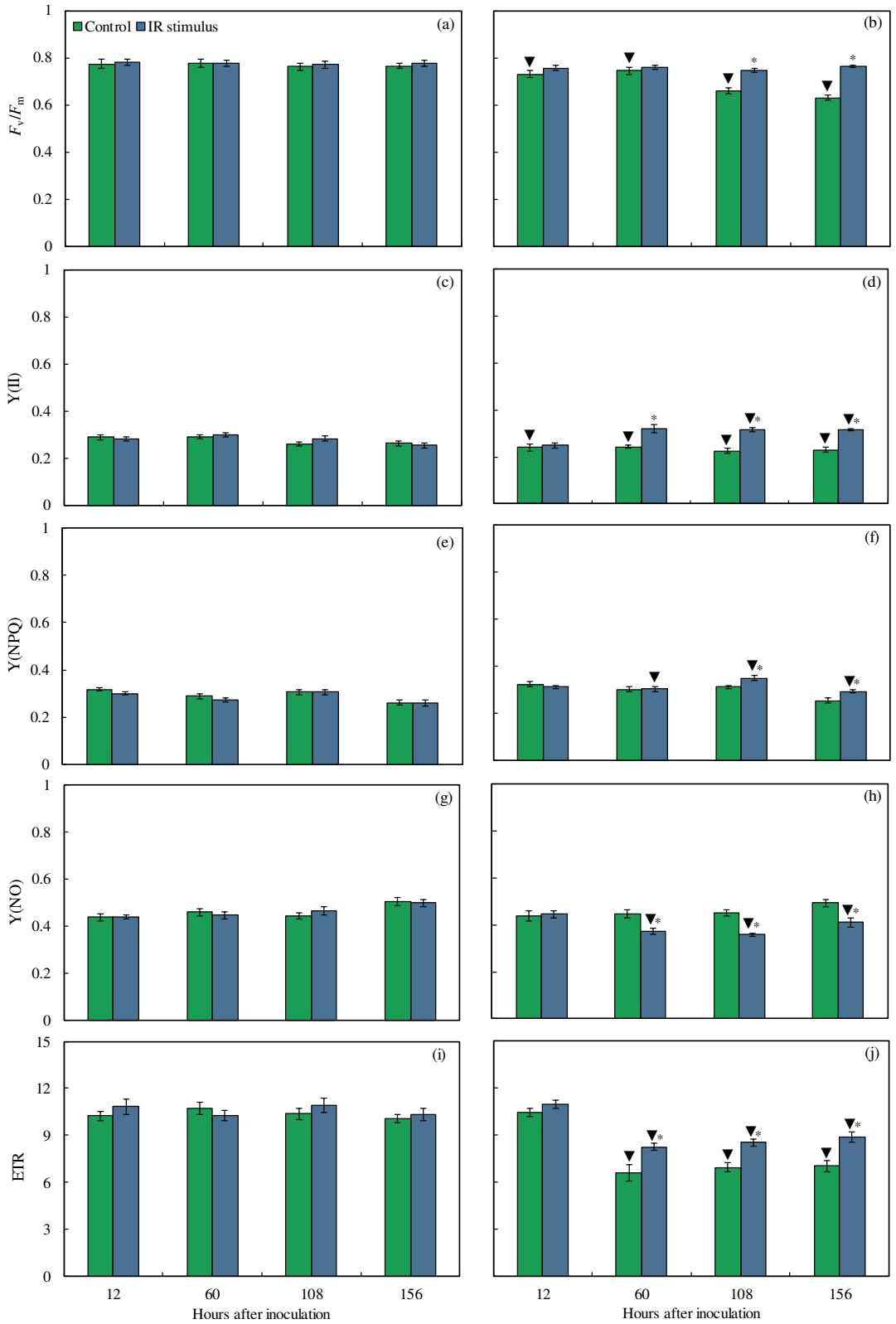

Figure 8. Quantification of chlorophyll *a* fluorescence parameters maximum PSII quantum efficiency (F_v/F_m) (a and b), photochemical yield [Y(II)] (c and d), yield for dissipation by down-regulation [Y(NPQ)] (e and f), yield for non-regulated dissipation [Y(NO)] (g and h), and electron

transport rate (ETR) (i and j) on leaves of maize plants non-inoculated (NI) (a, c, e, g, and i) or inoculated (I) (b, d, f, h, and j) with *Bipolaris maydis* and sprayed with water (control) or with induced resistance (IR) stimulus. Means for NI and I treatments followed by an inverted triangle (▼) and for control and IR stimulus treatments followed by an asterisk (*), at each evaluation time, are significantly different ($P \leq 0.05$) according to F test. Bars represent the standard error of the means.

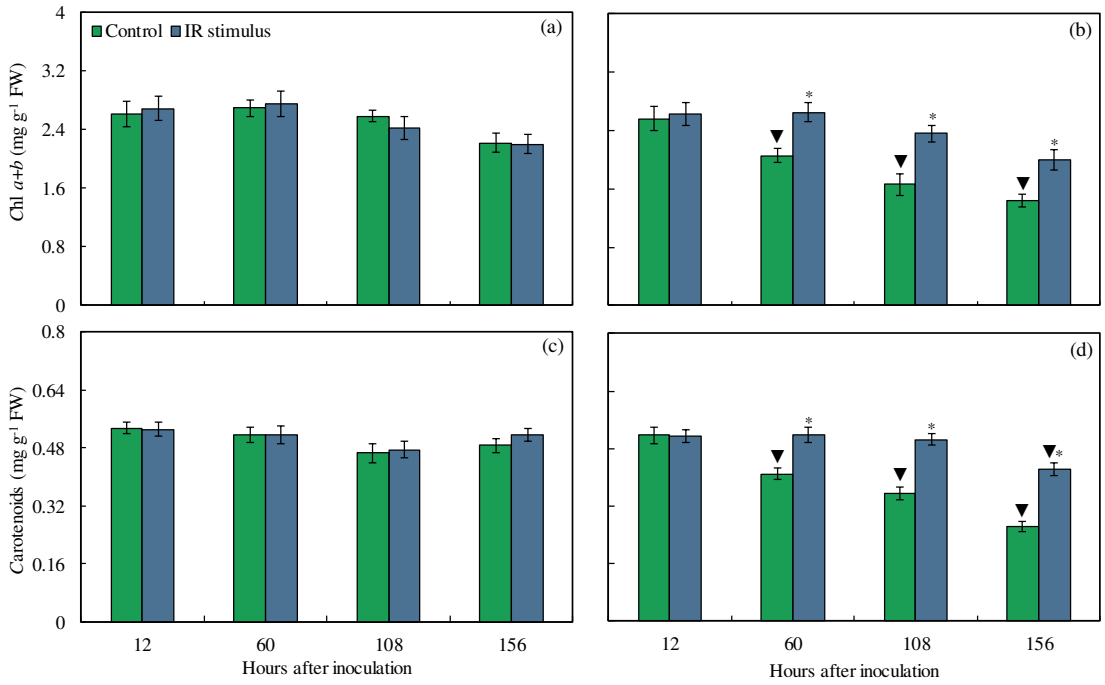

Figure 9. Concentrations of chlorophyll *a+b* (Chl *a+b*) (a and b) and carotenoids (c and d) determined on leaves of maize plants non-inoculated (NI) (a and c) or inoculated (I) (b and d) with *Bipolaris maydis* and sprayed with water (control) or with induced resistance (IR) stimulus. Means for NI and I treatments followed by an inverted triangle (▼) and for control and IR stimulus treatments followed by an asterisk (*), at each evaluation time, are significantly different ($P \leq 0.05$) according to *F* test. Bars represent the standard error of the means.

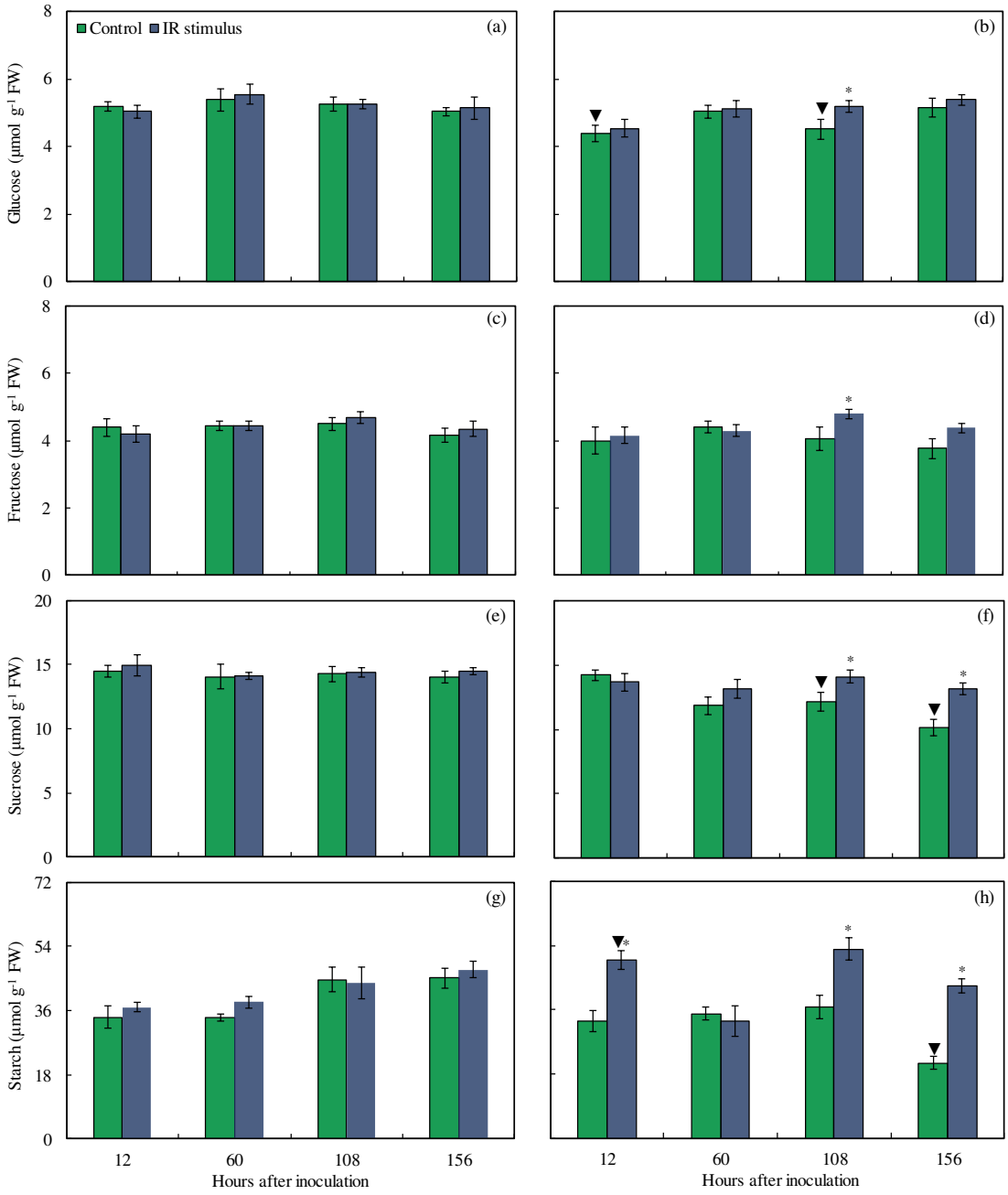

Figure 10. Concentrations of glucose (a and b), fructose (c and d), sucrose (e and f), and starch (g and h) determined on leaves of maize plants non-inoculated (NI) (a, c, e, and g) or inoculated (I) (b, d, f, and h) with *Bipolaris maydis* and sprayed with water (control) or with induced resistance (IR) stimulus. Means for NI and I treatments followed by an inverted triangle (▼) and for control and IR stimulus treatments followed by an asterisk (*), at each evaluation time, are significantly different ($P \leq 0.05$) according to F test. Bars represent the standard error of the means. FW = fresh weight.

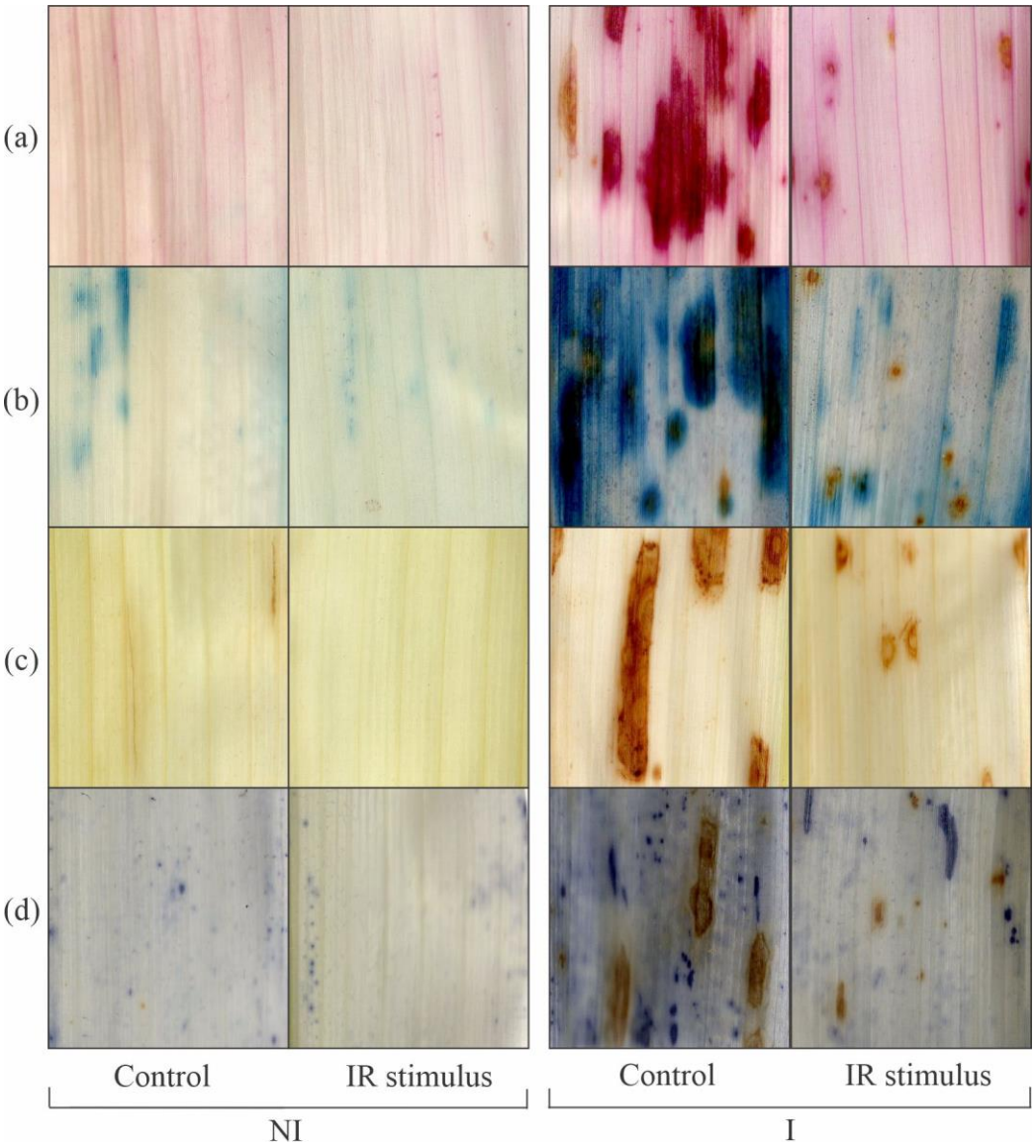

Figure 11. Histochemical detection of lipid peroxidation (a), membrane damage (b), hydrogen peroxide (c), and superoxide anion radical (d) on leaves of maize plants non-inoculated or at 156 hours after inoculation (hai) with *Bipolaris maydis* that were previously sprayed with water (control) or with induced resistance (IR) stimulus.

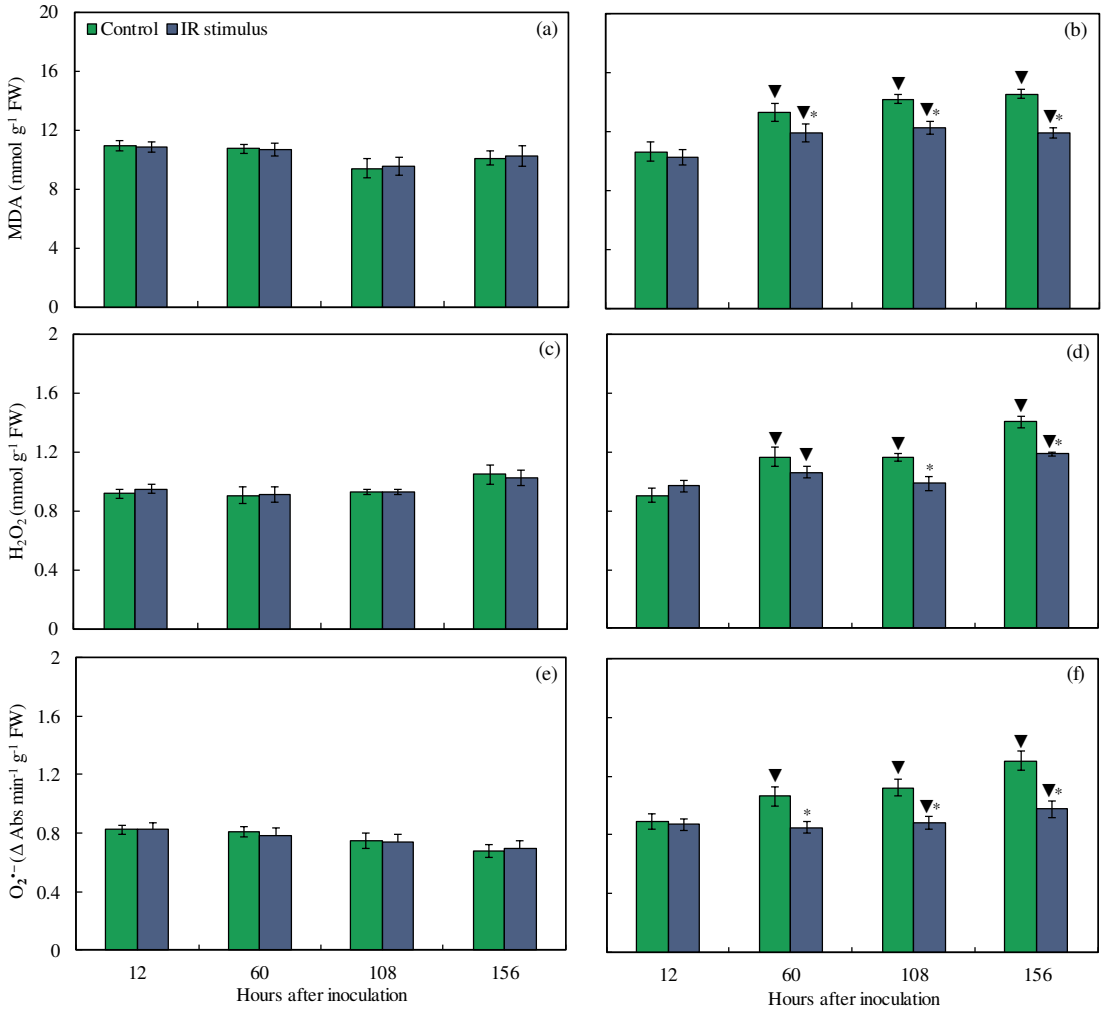

Figure 12. Concentrations of malondialdehyde (MDA) (a and b), hydrogen peroxide (H_2O_2) (c and d), and superoxide anion radical ($O_2^{\bullet-}$) (e and f) determined on leaves of maize plants non-inoculated (NI) (a, c, and e) or inoculated (I) (b, d, and f) with *Bipolaris maydis* and sprayed with water (control) or with induced resistance (IR) stimulus. Means for NI and I treatments followed by an inverted triangle (▼) and for control and IR stimulus treatments followed by an asterisk (*), at each evaluation time, are significantly different ($P \leq 0.05$) according to *F* test. Bars represent the standard error of the means. FW = fresh weight.

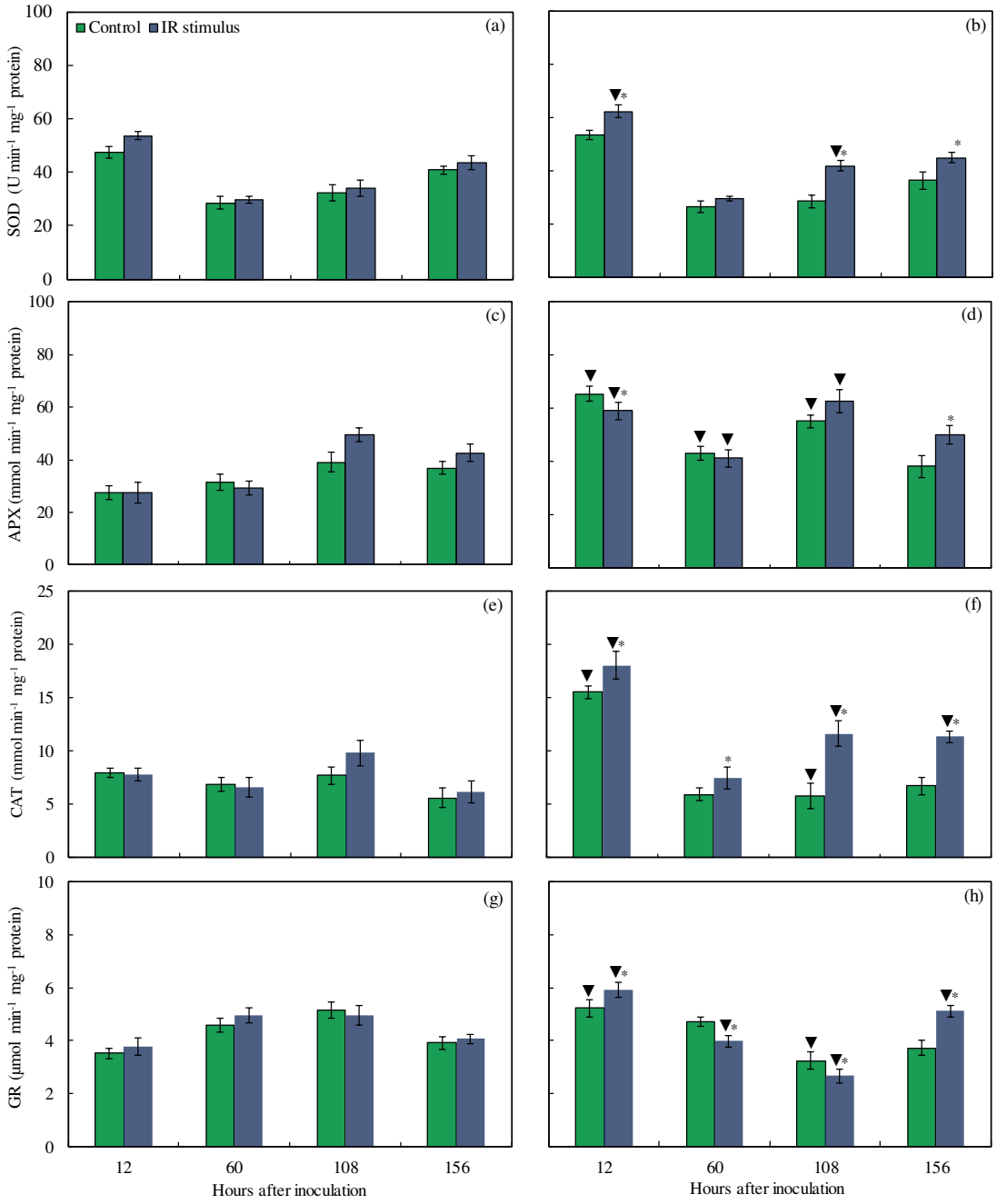

Figure 13. Activities of superoxide dismutase (SOD) (a and b), ascorbate peroxidase (APX) (c and d), catalase (CAT) (e and f), and glutathione reductase (GR) (g and h) determined on leaves of maize plants non-inoculated (NI) (a, c, e, and g) or inoculated (I) (b, d, f, and h) with *Bipolaris maydis* and sprayed with water (control) or with induced resistance (IR) stimulus. Means for NI and I treatments followed by an inverted triangle (▼) and for control and IR stimulus treatments followed by an asterisk (*), at each evaluation time, are significantly different ($P \leq 0.05$) according to *F* test. Bars represent the standard error of the means.

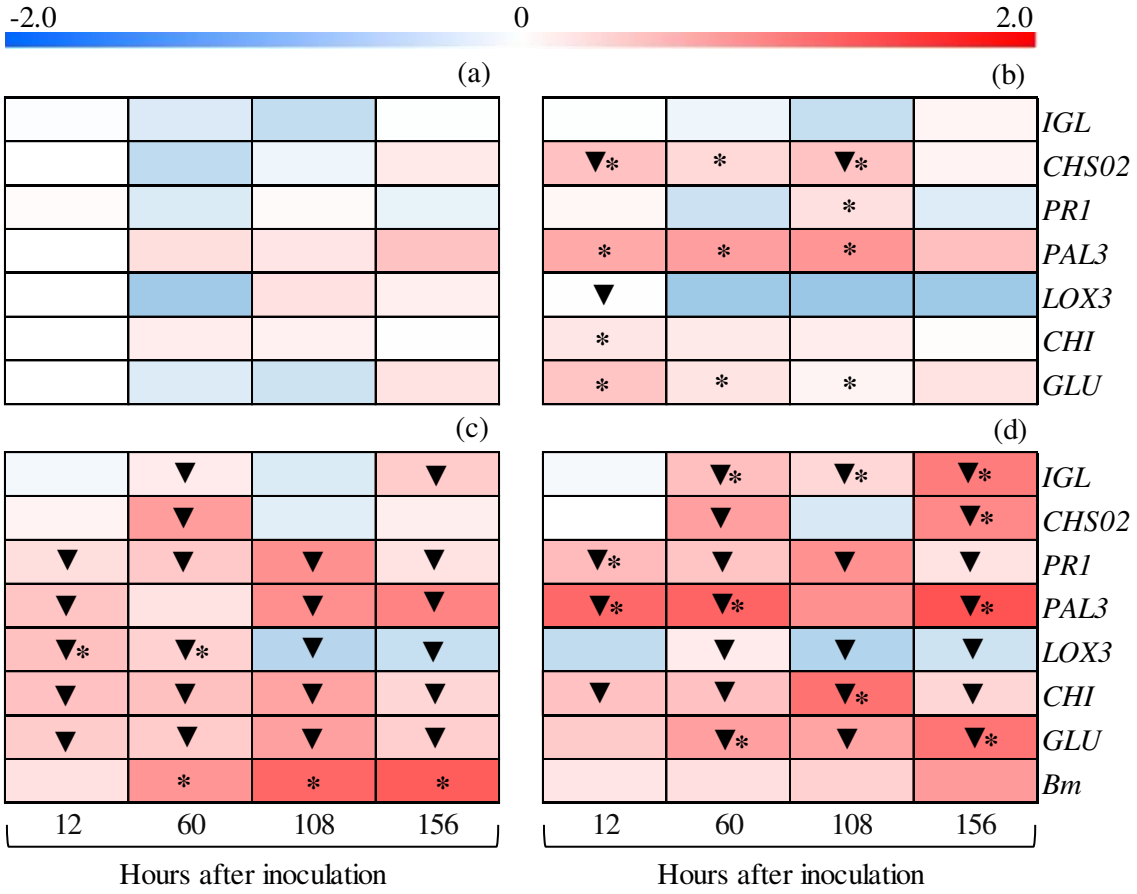

Figure 14. Expression profile of genes for leaves of maize plants non-inoculated (NI) (a and b) or inoculated (I) (c and d) with *Bipolaris maydis* and sprayed with water (control) (a and c) or with induced resistance (IR) stimulus (b and d). Color cells represent the relative transcript levels ranging from blue (-2) to red (2). Amplification of *GAPDH* from maize plants was the internal control for data normalization. Fold changes for expression of each gene were calculated based on the transcript level obtained from leaves of NI plants from the control treatment at 12 hours after inoculation (hai), except for *Bm*. For *Bm*, transcript level obtained from leaves of I plants from the control treatment at 12 hai was used in the calculation. Four biological replications, with three technical replicates each, were used for each leaf sample. Means for NI and I plants followed by an inverted triangle (▼) and for control and IR stimulus treatments followed by an asterisk (*), at each evaluation time, are significantly different ($P \leq 0.05$) according to F test. Abbreviations: indole-3-glycerol phosphate lyase (*IGL*), chalcone synthase (*CHS02*), pathogenesis-related protein 1 (*PR1*), phenylalanine ammonia-lyase 3 (*PAL3*), linoleate 9S-lipoxygenase3 (*LOX3*), endochitinase (*CHI*), endo-1,3(4)-*β*-D-glucanase (*GLU*), nonribosomal peptide synthetase from *B. maydis* (*Bm*), and cytosolic glyceraldehyde-3-phosphate dehydrogenase (*GAPDH*).

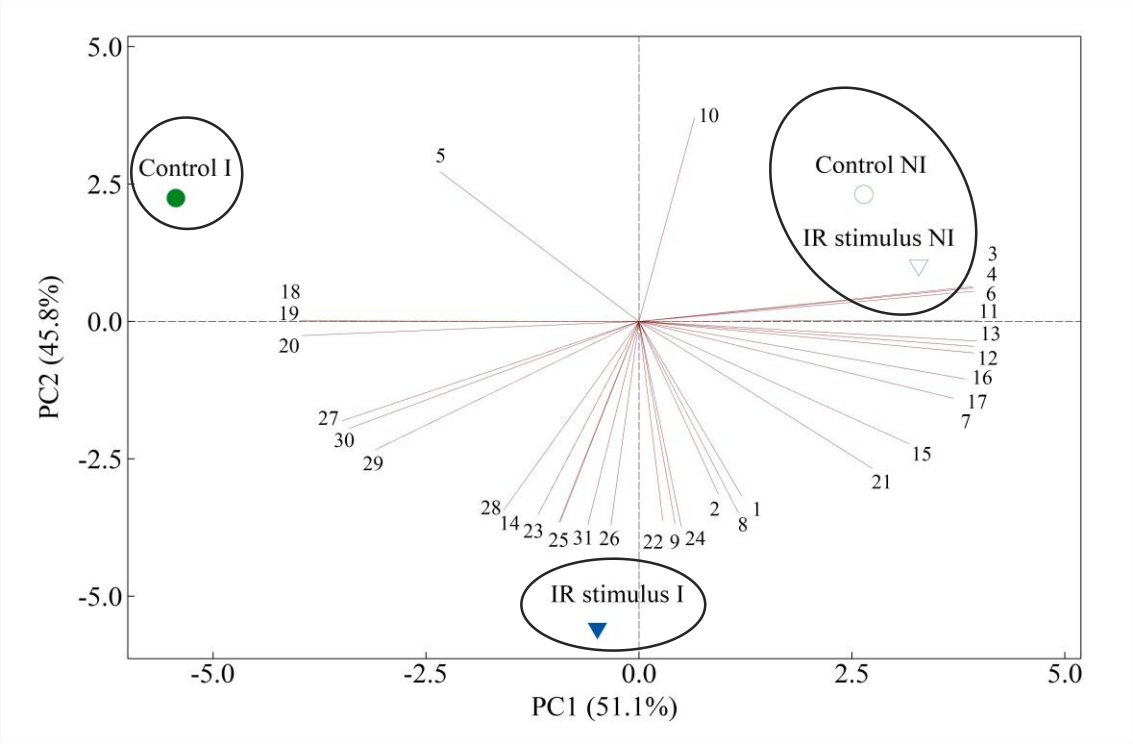

Figure 15. Score and loading plots of principal component analysis (PCA) for variables and parameters determined on leaves of maize plants non-inoculated (NI) (a and b) or inoculated (I) (c and d) with *Bipolaris maydis* and sprayed with water (control) (a and c) or with induced resistance (IR) stimulus. Numbers in the loading plots are as follow: foliar concentrations of Zn and N (1 and 2, respectively), leaf gas exchange (3, 4, 5, and 6, respectively, to *A*, g_s, C_i, and *E*) and chlorophyll *a* fluorescence (7, 8, 9, 10, and 11, respectively, to F_v/F_m, Y(II), Y(NPQ), Y(NO), and ETR) parameters, concentrations of photosynthetic pigments (12 and 13, respectively, to Chl *a+b* and Car), carbohydrates (14, 15, 16, and 17, respectively, to glucose, fructose, sucrose, and starch), and metabolites (18, 19, and 20, respectively, to MDA, H_2O_2, and $O_2^{\bullet-}$), activities of antioxidant enzymes (21, 22, 23, and 24, respectively, to SOD, APX, CAT, and GR), and genes expression (25, 26, 27, 28, 29, 30, and 31, respectively, to *IGL*, *CHS02*, *PR1*, *PAL3*, *LOX3*, *CHI*, and *GLU*). Groups were generated from cluster analysis with complete linkage and Pearson distance. Data from variables and parameters used in the PCA analysis were obtained from NI and I plants at 156 hours after inoculation.

Chapter 2

Physiological and Biochemical Aspects of Silicon-Mediated Resistance of Maize Plants against Maydis Leaf Blight

ABSTRACT

Maize leaf blight (MLB), caused by the fungus *Bipolaris maydis*, has potential to cause considerable yield losses in maize production. The hypothesis that maize plants with higher foliar silicon (Si) concentration can be more resistant against MLB was investigated in this study. This goal was achieved through an in-depth analysis of the photosynthetic apparatus (parameters of leaf gas exchange and chlorophyll (Chl) *a* fluorescence and pool of photosynthetic pigments) and changes in activities of defense-related enzymes and those involved in the antioxidative metabolism in leaves of maize plants non-supplied (0 mM) or supplied (2 mM) with Si and non-challenged or challenged with *B. maydis*. The +Si plants showed reduced MLB symptoms (smaller lesions and lower disease severity) due to higher foliar Si concentration and less production of malondialdehyde, hydrogen peroxide, and radical anion superoxide compared to -Si plants. Higher values for leaf gas exchange (rate of net CO_2 assimilation, stomatal conductance to water vapor, and transpiration rate) and chlorophyll *a* fluorescence (variable-to-maximum Chl *a* fluorescence ratio, photochemical yield, and yield for dissipation by down-regulation) parameters along with preserved pool of chlorophyll *a*+*b* and carotenoids were noticed for infected +Si plants compared to infected -Si plants. Activities of defense (chitinase, β-1,3-glucanase, phenylalanine ammonia-lyase, polyphenoloxidase, peroxidase, and lipoxygenase) and antioxidative (ascorbate peroxidase, catalase, superoxide dismutase, and glutathione reductase) enzymes were higher for infected +Si plants compared to infected -Si plants. Collectively, this study highlights the importance of using Si to boost the resistance of maize plants against MLB considering the more operative defense reactions and the robustness of the antioxidative metabolism along with the preservation of the photosynthetic apparatus.

Keywords: Antioxidative metabolism. Host defense responses. Photosynthesis. Plant nutrition. Reactive oxygen species.

RESUMO

A mancha-foliar-de-Bipolaris (MFB), causada pelo fungo *Bipolaris maydis*, tem grande potencial para causar perdas consideráveis no rendimento e produção do milho. A hipótese de que as plantas de milho com maior concentração foliar de silício (Si) podem ser mais resistentes à MFB foi investigada neste estudo. Esse objetivo foi alcançado por meio de uma análise aprofundada do aparato fotossintético (parâmetros de trocas gasosas foliares, fluorescência da clorofila (Chl) a e *pool* de pigmentos fotossintéticos) e mudanças nas atividades de enzimas relacionadas à defesa e aquelas envolvidas no metabolismo antioxidante em folhas de plantas de milho não supridas (0 mM) ou supridas (2 mM) com Si e não desafiadas ou desafiadas com *B. maydis*. As plantas +Si apresentaram sintomas reduzidos de MFB (lesões menores e menor gravidade da doença) devido à maior concentração foliar de Si e à menor produção de malondialdeído, peróxido de hidrogênio e ânion radical superóxido em comparação com as plantas -Si. Foram observados valores mais altos para os parâmetros de trocas gasosas foliares (taxa de assimilação líquida de CO_2, condutância estomática ao vapor de água e taxa de transpiração) e fluorescência da clorofila *a* (taxa de fluorescência da Chl *a* variável a máxima, rendimento fotoquímico e rendimento da dissipação não-regulada), juntamente com o *pool* preservado de clorofila *a*+*b* e carotenoides para plantas infectadas +Si em comparação com plantas infectadas -Si. As atividades das enzimas de defesa (quitinase, β-1,3-glucanase, fenilalanina amônia-liase, polifenoloxidase, peroxidase e lipoxigenase) e antioxidantes (ascorbato peroxidase, catalase, superóxido dismutase e glutationa redutase) foram maiores nas plantas infectadas +Si em comparação com as plantas infectadas -Si. Em conjunto, este estudo destaca a importância do uso do Si para aumentar a resistência das plantas de milho contra a MFB, considerando as reações de defesa mais operantes e a robustez do metabolismo antioxidante, juntamente com a preservação do aparato fotossintético.

Palavras-chave: Metabolismo antioxidante. Respostas de defesa do hospedeiro. Fotossíntese. Nutrição mineral. Espécies reativas de oxigênio.

1. Introduction

Maydis leaf blight (MLB), caused by the fungus *Bipolaris maydis* (Y. Nisik. & Miyake) Shoemaker, is the most important and widespread foliar disease of maize and represents a potential threat to global maize production (Dai *et al*., 2020; Manamgoda *et al*., 2014). During the fungal infection process, the germ tubes formed from a germinated conidium penetrate the leaves through stomata or directly through the cuticular walls with the aid of hydrolytic enzymes (Wheeler, 1977). The major MLB symptoms are rectangular to elliptical necrotic lesions of brown to tan colors that develop on both abaxial and adaxial leaf surfaces (Smith *et al*., 1970). Yield losses caused by MLB are greatly associated with the damage to the photosynthetic apparatus due to an extensive leaf area with larger necrotic lesions surrounded by intense chlorosis, reduced plant growth, and poor allocation of assimilates from leaves to the developing grains (Dai *et al*., 2020). The management of MLB has been achieved using resistant maize genotypes considering that available commercial hybrids exhibit low basal level of resistance to this disease (Meshram *et al*., 2022). Foliar sprays of different fungicides and crop rotation are key strategies used for MLB control (Dai *et al*., 2018; Kumar *et al*., 2021). The disease epidemic rate can be slowed by keeping adequate levels of macro and micronutrients in the plant tissues during the different plant growth stages (Tripathi *et al*., 2022). Silicon (Si) provides numerous beneficial effects for plants facing different types of abiotic and biotic stresses after being absorbed from the soil solution in the form of monosilicic acid (H_4SiO_4) and transported to shoots (Debona *et al*., 2023). The passive mechanism of Si uptake by plants occurs via mass flow (Ma and Yamaji, 2006). Particularly in maize, plants are able to actively uptake and accumulate high amounts of Si on leaves due to the expression of *ZmLsi1* and *ZmLsi2* genes (Mitani *et al*., 2009). The proteins allow that the H_4SiO_4 pass through the root cells to shoots via transpiratory flow and the discharge into the xylem vessels occurs through the expression of *ZmLsi6* (Mitani *et al*., 2009). The effect of Si on plant-pathogen interactions has centered around two main mechanisms known as physical and or biochemical/molecular (Debona *et al*., 2017, 2023). The physical role of Si is due to the accumulation of this element below the cuticle of epidermal cells to act as a stronger physical barrier (polymerized H_4SiO_4) that may prevent or delay the penetration of some pathogens (Debona *et al*., 2017, 2023). The biochemical resistance mediated by Si is associated with the potentiation of defense-related enzymes (e.g., chitinases, β-1,3-glucanase, phenylalanine ammonia-lyase, polyphenoloxidase, and peroxidase) and metabolites (e.g., dopamine, phenolics compounds, flavonoids, phytoalexin, and lignin), and a

more robust antioxidative metabolism (Debona *et al*., 2017, 2023; Rodrigues and Datnoff, 2015). Physiological processes enhanced by Si are related to the improved photosynthetic performance of stressed plants by pathogen infection along with regulation of their carbohydrate metabolism (Debona *et al*., 2017, 2023). Notably, maize plants supplied with Si showed more operative photosynthetic machinery and more efficient antioxidant metabolism during infection by *Exserohilum turcicum* and *Stenocarpella macrospora* (Hawerroth *et al*., 2019; Silveira *et al*., 2021).

Taking into consideration the mechanistic basis behind the potentiation of resistance of different profitable crops against diseases mediated by Si as well as the lack of information on the physiological and biochemical process taking place in the maize-*B. maydis* interaction, the present study hypothesized that Si could allow maize plants to respond against fungal infection more efficiently. This strategy could be linked to earlier and stronger defense reactions as well as better photosynthetic performance in combination with the well-coordinated and efficient regulation of carbohydrate metabolism and changes in antioxidant metabolism to minimize the damage caused by *B. maydis* on Si-supplied plants.

2. Material and methods

2.1. Plant growth and Si supply

Seeds of the maize hybrid B2433PWU (Brevant, São Paulo, Brazil), susceptible to *B. maydis*, were sown in plastic pots containing 2 kg of Tropstrato® (mixture of pine bark, peat, and expanded vermiculite; Vida Verde, São Paulo, Brazil) substrate. The concentration of Si in the substrate was 4.6 mg kg^{-1}. A total of 1.63 g of calcium phosphate was added to each pot to provide phosphorus to plants before sowing. After the emergence of seedlings (≈ five days), only two plants were kept per pot. Plants were fertilized with the nutrient solution (100 mL per pot twice a week) proposed by Hoagland and Arnon (1950), with a few modifications, as follow: 2.6 mM KCl, 0.6 mM K_2SO_4, 1.2 mM $MgSO_4$, 1.0 mM CH_4N_2O, 1.2 mM NH_4NO_3, 0.0002 mM $(NH_4)_6Mo_7O_{24}$, 0.03 mM H_3BO_4, 0.04 mM $ZnSO_4$, 0.01 mM $CuSO_4$, 0.03 mM $MnCl_2$, 0.015 mM $FeSO_4$, and 0.015 mM ethylenediaminetetraacetic acid disodium (EDTA). Deionized water was used to prepare the nutrient solution. Potassium silicate (PS) (FertiSil®, PQ Corporation, São Paulo, Brazil; 13% K_2O and 26.59% SiO_2) was used as the Si source. The two plants per pot received 200 mL of a PS

solution (0.34 mL PS/L; 2 mM Si, pH 6.5 ± 0.2 by adding either an HCl or NaOH solution at 0.5 M) prepared with deionized water daily for 30 days. For the control treatment, plants in each pot received 200 mL of a KCl solution (1.19 mL KCl/L; 1.53 mM K, pH 6.5 ± 0.2 adjusted as mentioned above) daily for 30 days. The K concentration between plants receiving either PS or KCl was kept the same (1.53 mM K). Plants were kept in the greenhouse (temperature of 28 ± 5°C, relative humidity of 80 ± 5%, and natural photosynthetically active radiation (PAR) of 900 ± 15 μmol photons m^{-2} s^{-1} measured at midday).

2.2. Inoculum production and plant inoculation

Stripes of filter paper containing fungal mycelia of the monosporic isolate of *B. maydis* UFV-DPF-*Bm*12 were transferred to Petri dishes containing potato-dextrose-agar. The dishes were incubated in a growth chamber (25°C and 12 h light/12 h dark photoperiod) for 15 days. Conidia produced in each dish were collected using sterile water containing 0.01% Tween 20 and 0.5% gelatin (w/v). The conidial suspension was calibrated to 1×10^3 conidia/mL using a hemacytometer. Plants at the V6 growth stage (30 days after emergence) were inoculated with a conidial suspension of *B. maydis* using a VL Airbrush atomizer (Paasche Airbrush Co., Chicago, IL, USA). After inoculation, plants were kept inside a mist growth chamber (25°C and relative humidity of 90 ± 5%) for 24 h. After this period, plants were transferred to the greenhouse (28 ± 2°C, relative humidity of 80 ± 5%, and natural PAR of 900 ± 15 μmol photons m^{-2} s^{-1} measured at midday) until the end of the experiments.

2.3. Evaluation of MLB severity

The fifth expanded leaf, from base to top, of each plant per replication of each treatment was collected at 156 hours after inoculation (hai), scanned at 600 dpi resolution, and the images were processed using the QUANT software (Fagundes-Nacarath *et al.*, 2018) to estimate the values of severity.

2.4. Determination of foliar Si and K concentrations

At the end of the experiment (156 hai), the fifth and sixth leaves, from base to top, of each plant per replication of each treatment were collected, washed in deionized water, dried for 72 h at 65°C, and ground in a ball mill (TECNAL TE 350, Piracicaba, SP, Brazil) for 2 min. The Si

concentration was determined by the colorimetry method with hydrochloric acid, oxalic acid, and ammonium molybdate in a spectrophotometer at 410 nm (Korndörfer *et al*., 2004). The K concentration was determined by digestion in nitric perchloric acid solution followed by optical emission spectrophotometer with inductively coupled plasma reading (ICP-OES) (DV8300, PerkinElmer) (Mesquita *et al*., 2019).

2.5. Detection of Si and K on leaves using the X-ray microanalysis

The energy dispersive X-ray spectroscopy (EDS) using a scanning electron microscope (LEO 1430VP; Carl Zeiss, Germany) with an attached X-ray detector system (Tracor TN5502, Middleton, WI) was used to determine the insoluble composition and relative levels of Si and K in the adaxial surface of infected leaves from -Si and +Si plants at 156 hai. Leaf samples were carefully placed in envelopes inside a desiccator with silica gel for 15 days. After complete dehydration, a total of four leaf fragments ($\approx 1 \times 1$ cm^2) containing MLS lesions were mounted onto one aluminum stub (two stubs per treatment) and coated with a thin film of evaporated carbon (Quorum Q150 T, England, UK). The EDS microanalysis of all samples was performed at the magnification of 200 × with an accelerating voltage of 20 kV and a working distance of 10 mm. The distribution patterns of Si and K were based on secondary electron images, X-ray emission spectra, and corresponding X-ray elemental maps according to the methods of Goldstein *et al*., (2003) and Williams *et al*., (2002). A total of six images were obtained from the fragments of each treatment.

2.6. Determination of leaf gas exchange parameters

The net carbon assimilation rate (A), stomatal conductance to water vapor (g_s), internal CO_2 concentration (C_i), and transpiration rate (E) were measured on the fifth leaf, from base to top, of each plant per replication of each treatment at 12, 60, 108, and 156 hai from 09:00 to 12:00 h using a portable open-system infrared gas analyzer (LI-6400, LI-COR Inc., Lincoln, NE, USA). These parameters were also evaluated on the same leaves of non-inoculated plants at the evaluation times mentioned above. All measurements were carried out under the following conditions: leaf temperature controlled at 25°C, chamber CO_2 concentration of 420 ppm, PAR of 1200 µmol m^{-2} s^{-1}, and the amount of blue light set with 10% of PAR to optimize stomatal aperture (Marçal *et al*., 2021).

2.7. Imaging and quantification of Chl *a* fluorescence parameters

The Imaging-PAM fluorometer and the Imaging Win software MAXI version (Heinz Walz GmbH) were used to obtain the images and parameters of Chl *a* fluorescence using the fifth leaf, from base to top, of each plant per replication of each treatment at 12, 60, 108, and 156 hai and also from non-inoculated plants at these same evaluation times. The methodology described by Fagundes-Nacarath *et al*., (2018) was used to determine the parameters variable-to-maximum chlorophyll *a* fluorescence ratio (F_v/F_m), photochemical yield [Y(II)], yield for dissipation by down-regulation [Y(NPQ)], yield for non-regulated dissipation [Y(NO)], and electron transport rate (ETR).

2.8. Determination of photosynthetic pigments concentration

The concentrations of Chl *a*, Chl *b*, and carotenoids were determined using methanol as the solvent. Leaf tissue (50 mg) obtained from the leaves used to determine the parameters of Chl *a* fluorescence was ground in liquid nitrogen using a vibration ball mill (Retsch, Haan, Germany) and the fine powder was homogenized in 700 µL of methanol. The supernatant was used for quantify concentrations of Chl *a*, Chl *b*, and carotenoids at 470, 653, and 666 nm, respectively, using a saturated solution of methanol as a blank (Wellburn, 1994).

2.9. Biochemical assays

The fifth leaf, from base to top, of each plant per replication of each treatment was collected at 12, 60, 108, and 156 hai. Leaves from non-inoculated plants were sampled at these same evaluation times. Leaf samples were kept in liquid nitrogen during sampling and stored at -80°C until further analysis.

2.10. Determining sugars and starch concentrations: leaf tissue (50 mg) was ground into a fine powder as described above and mixed with 700 µL of methanol at 80°C for 20 min to extract sugars and starch according to Medeiros *et al*., (2017). Glucose, fructose, and sucrose were determined in the soluble phase of the methanolic solution while starch was determined in the pellet following the methodology proposed by Fernie (2001).

2.11. Determining malondialdehyde (MDA) concentration: leaf tissue (100 mg) was ground as described above and homogenized in 2 mL of 0.1% (w/v) trichloroacetic acid solution and the homogenate was centrifuged at 12,000 *g* for 15 min at 4°C. After centrifugation, 250 µL of the supernatant was added to 750 µL of thiobarbituric acid solution and homogenized in a thermomixer for 30 min at 95°C. The samples were centrifuged at 9,000 *g* for 10 min and the absorbances were obtained at 600 and 532 nm (Heath and Packer, 1968).

2.12. Determining H_2O_2 and $O_2^{\bullet-}$ concentrations: leaf tissue (100 mg) was ground as described above and homogenized in 1 mL of a mixture containing 50 mM potassium phosphate buffer (pH 6.5) and 1 mM hydroxylamine. The homogenate was centrifuged at 10,000 *g* for 15 min at 4°C. The supernatant was used to determine H_2O_2 concentration following the procedures of Dias *et al*., (2020). Leaf tissue (100 mg) was ground as described above and the fine powder was homogenized in 1 mL of a solution containing 100 mM potassium phosphate buffer (pH 7.2) and 1 mM sodium diethyldithiocarbamate. The homogenate was centrifuged at 22,000 *g* for 20 min at 4°C and the supernatant was used to determine $O_2^{\bullet-}$ concentration according to Chaves *et al*., (2021).

2.13. Determining defense-related enzymes activities: leaf tissue (100 mg) was ground as described above and homogenized in 1 mL of a solution containing 50 mM potassium phosphate buffer (pH 6.8), 0.1 mM EDTA, 1 mM phenylmethylsulfonyl fluoride (PMSF), and 0.5% (w/v) polyvinylpyrrolidone (PVP). The homogenate was centrifuged at 13,000 *g* for 15 min at 4°C and the supernatant was used to determine chitinase (CHI; EC 3.2.1.14), *β*-1,3-glucanase (GLU; EC 3.2.1.39), phenylalanine ammonia-lyase (PAL; EC 4.3.1.24), polyphenoloxidase (PPO; EC 1.10.3.1), peroxidase (POX; EC 1.11.1.7), and lipoxygenase (LOX; EC 1.13.11.12) activities following the procedures described by Fortunato et al. (2014).

2.14. Determining total soluble phenolics (TSP) and lignin thioglycolic acid (LTGA) derivatives: leaf tissue (100 mg) was ground as described above and homogenized in 1 mL of 80% (v/v) methanol solution. The extract was homogenized in a thermomix at 25°C for 12 h and the mixture was centrifuged at 13,000 *g* for 30 min. The methanolic extract was used to determine the

TSP concentration and the pellet was kept at 20°C to determine the concentration of LTGA derivatives according to Fortunato *et al*., (2015).

2.15. Determining antioxidant enzyme activities: leaf tissue (100 mg) was ground as described above and the fine powder was homogenized with 1 mL solution containing 100 mM potassium phosphate buffer (pH 7.8), 0.1 mM EDTA, 1 mM PMSF, and 0.5% (w/v) PVP. The homogenate was centrifuged at 13,000 *g* for 15 min at 4°C and the supernatant was used to determine the activities of ascorbate peroxidase (APX) (EC 1.11.1.11), catalase (CAT) (EC 1.11.1.6), superoxide dismutase (SOD) (EC 1.15.1.1), and glutathione reductase (GR) (EC 1.8.1.7) following the procedure of Debona (2012).

2.16. Experimental design and data analysis

A 2 × 2 factorial experiment, consisting of plants non-supplied (-Si) or supplied with Si (+Si) and non-inoculated or inoculated with *B. maydis*, was arranged in a completely randomized design with four replications per evaluation time to assess disease severity as well to determine the foliar concentrations of Si and K. Another 2 × 2 factorial experiment with the same factors mentioned above and six replications was carried out to evaluate the parameters of leaf gas exchange and Chl a fluorescence as well to quantify the foliar concentration of pigments. Leaf samples for the biochemical assays were obtained from another 2 × 2 factorial experiment with the same factors described above and five replications. Each experimental unit consisted of one plastic pot with two plants. All experiments were repeated once. Data from variables and parameters were checked for normality and homogeneity of variance and subjected to analysis of variance. The treatment means were compared by the *F* test ($P \leq 0.05$). Data from all variables and parameters obtained from the four treatments at 156 hai were used for principal component analysis (PCA). The Minitab Statistical software was used for the statistical analysis mentioned above (Minitab, Inc., 2021).

3. Results

3.1. Analysis of variance

The factor Si rates (Si) was significant for severity, *A*, F_v/F_m, Y(II), ETR, MDA, $O_2^{\bullet-}$, PAL, and LTGA derivatives and the factor plant inoculation (PI) and the Si × PI interaction were significant for most of the variables and parameters evaluated (Table 1).

3.2. Foliar Si and K concentrations and X-ray microanalysis

Foliar Si concentration significantly increased by 70 and 72% for non-inoculated +Si plants and inoculated +Si plants, respectively, compared to their counterparts (Fig. 1a). There was no significant difference between -Si and +Si plants regardless of plant inoculation with *B. maydis* for foliar K concentration (Fig. 1b). There was a differential pattern of Si deposition on the adaxial surface of leaves from -Si and +Si plants at 156 hai based on X-ray microanalysis (Fig. 2). The levels of Si deposition in the infected leaves of +Si plants was 90% higher (8.35 wt %) compared to -Si plants (0.81 wt %) (Fig. 2a and b). The K deposition was similar between the adaxial surface of leaves of -Si and +Si plants (Fig. 2c and d).

3.3. Symptoms of MLB and severity

In the leaves of -Si plants, disease symptoms (number and size of the necrotic and elliptical lesions, lesions coalescence, and chlorosis) were remarkably more expressive in contrast to the leaves of +Si plants (Fig. 3a-b). The severity of MLB was significantly reduced by 47% for +Si plants compared to -Si plants (Fig. 3c).

3.4. Leaf gas exchange parameters

For non-inoculated plants, *A*, g_s, C_i, and *E* were not affected by Si treatments regardless of the evaluation time (Fig. 4a, c, e, and g). For inoculated -Si plants, *A* (15, 21, and 35% at 12, 108, and 156 hai, respectively), g_s (23, 57, and 37% at 12, 108, and 156 hai, respectively), and *E* (17, 44, and 19% at 12, 108, and 156 hai, respectively) were significantly lower while g_s, C_i, and *E* (39, 29, and 23% at 60 hai, respectively) were significantly higher compared to inoculated +Si plants (Fig. 4b, d, f, and h). The *A* (15-58% from 12 to 156 hai), g_s (39 and 51% at 108 and 156 hai, respectively), and *E* (10, 29, and 23% at 12, 108, and 156 hai, respectively) were significantly

lower for inoculated -Si plants compared to non-inoculated -Si plants (Fig. 4a-d and g-h). Significant and lower values for *A* (17 and 39% at 60 and 156 hai, respectively) and g_s (30% at 156 hai) occurred for inoculated +Si plants compared to non-inoculated +Si plants (Fig. 4a-d).

3.5. Imaging and quantification of Chl a fluorescence parameters

Remarkable changes in the images for F_v/F_m, Y(II), Y(NPQ), and Y(NO), based on the darker areas, were noticed in the leaves of -Si plants compared to the leaves of +Si plants from 12 to 156 hai indicating damage to the photosynthetic apparatus (Fig. 5). For non-inoculated plants, F_v/F_m, Y(II), Y(NPQ), Y(NO), and ETR parameters were not affected by -Si and +Si treatments regardless of the evaluation time (Fig. 6a, c, e, and g). For inoculated +Si plants, F_v/F_m (6, 14, and 10% at 60, 108, and 156 hai, respectively), Y(II) (24 and 26% at 108 and 156 hai, respectively), Y(NO) (15% at 60 hai), and ETR (27 and 26% at 108 and 156 hai, respectively) were significantly higher while Y(NO) (15% at 156 hai) was significantly lower compared to inoculated -Si plants (Fig. 6b, d, f, h, and j). For -Si plants, F_v/F_m (8-16% from 60 to 156 hai), Y(II) (24% at 108 hai), Y(NO) (22% at 60 hai), and ETR (29% at 108 hai) were significantly lower while Y(NPQ) (33 and 35% at 60 and 156 hai, respectively) was significantly higher for inoculated plants compared to non-inoculated plants (Fig. 6). For +Si plants, F_v/F_m was significantly lower by 8% and Y(NPQ) was significantly higher by 34% at 156 hai for inoculated plants compared to non-inoculated plants (Fig. 6a-b, e-f).

3.6. Photosynthetic pigments

Concentrations of Chl *a*+*b* and carotenoids for non-inoculated plants were not affected by Si treatments regardless of the evaluation time (Fig. 7a and c). Concentrations of Chl *a*+*b* and carotenoids (34 and 47% at 156 hai, respectively) were significantly higher for inoculated +Si plants compared to inoculated -Si plants (Fig. 7b and d). For -Si plants, concentrations of Chl *a*+*b* (23 and 44% at 108 and 156 hai, respectively) and carotenoids (23 and 29% at 108 and 156 hai, respectively) were significantly lower for inoculated plants compared to non-inoculated plants (Fig. 7a, b, c, and d). For +Si plants, concentrations of Chl *a*+*b* (22 and 23% at 108 and 156 hai, respectively) and carotenoids (25 and 15% at 108 and 156 hai, respectively) were significantly lower for inoculated plants compared to non-inoculated plants (Fig. 7a, b, c, and d).

3.7. Carbohydrates

Concentrations of glucose, fructose, sucrose, and starch for non-inoculated plants were not affected by Si treatments regardless of the evaluation time (Fig. 8a, c, e, and g). For inoculated +Si plants, glucose (38 and 39% at 108 and 156 hai, respectively), fructose (125% at 156 hai), sucrose (27 and 54% at 108 and 156 hai, respectively), and starch (23-34% from 60 to 156 hai) concentrations were significantly higher while fructose concentration (33 and 24% at 60 and 108 hai, respectively) was significantly lower compared to inoculated -Si plants (Fig. 8b, d, f, and h). For -Si plants, concentrations of glucose (70% at 156 hai) and sucrose (38 and 60% at 108 and 156 hai, respectively) were significantly lower while starch concentration (67 and 58% at 12 and 60 hai, respectively) was significantly higher for inoculated plants compared to non-inoculated plants (Fig. 8a-b, e-h). For +Si plants, concentrations of glucose (53% at 156 hai) and sucrose (20% at 108 hai) were significantly lower while the concentration of starch (79, 59, 29, and 28% at 12, 60, 108, and 156 hai, respectively) was significantly higher for inoculated plants compared to non-inoculated plants (Fig. 8a-b and e-h).

3.8. Concentrations of MDA, H_2O_2, and $O_2^{\bullet-}$

Concentrations of MDA, H_2O_2, and $O_2^{\bullet-}$ for non-inoculated plants were not affected by Si treatments regardless of the evaluation time (Fig. 9a, c, and e). For inoculated plants, MDA (18, 27, and 28% at 60, 108, and 156 hai, respectively), H_2O_2 (15, 15, and 24% at 60, 108, and 156 hai, respectively), and $O_2^{\bullet-}$ (62, 33, and 29% at 60, 108, and 156 hai, respectively) concentrations were significantly lower for +Si plants compared to inoculated -Si plants (Fig. 9b, d, and f). For -Si plants, MDA (8, 44, and 34% at 12, 108, and 156 hai, respectively), H_2O_2 (25% at 156 hai), and $O_2^{\bullet-}$ (47-68% from 12 to 156 hai) were significantly higher for inoculated plants compared to non-inoculated plants (Fig. 9). For +Si plants, $O_2^{\bullet-}$ was significantly higher by 40 and 53% at 108 and 156 hai, respectively, for inoculated plants compared to non-inoculated plants (Fig. 9e and f).

3.9. Activities of defense enzymes

Activities of CHI, GLU, PAL, PPO, POX, and LOX activities for non-inoculated plants were not affected by Si treatments regardless of the evaluation time (Fig. 10a, c, e, g, i, and k). The CHI (24 and 38% at 12 and 108 hai, respectively), GLU (20% at 108 hai), PAL (15-38% from 12 to 108 hai), PPO (15% at 108 hai), and POX (17-21% from 12 to 108 hai) activities were

significantly higher for inoculated +Si plants compared to inoculated -Si plants (Fig. 10b, d, f, g, h, and j). The CHI, PAL, PPO, and POX activities were significantly lower at 156 hai for inoculated +Si plants compared to inoculated -Si plants (Fig. 10b, f, h, and j). The GLU (24% at 12 hai) and LOX (26 and 20% at 60 and 156 hai, respectively) activities were significantly lower for inoculated +Si plants compared to inoculated -Si plants (Fig. 10d and l). The GLU (69% at 108 hai), PAL (49% at 156 hai), PPO (44, 51, and 20% at 60, 108, and 156 hai, respectively), POX (31 and 28% at 108 and 156 hai, respectively), and LOX (38, 46, and 51% at 12, 60, and 108 hai, respectively) activities were significantly higher for inoculated -Si plants compared to non-inoculated -Si plants (Fig. 10c-l). The activities of CHI (31 and 25% at 12 and 108 hai, respectively), GLU (76% at 108 hai), PAL (17 and 54% at 12 and 108 hai, respectively), PPO (29 and 62% at 60 and 108 hai, respectively), POX (30, 33, and 43% at 12, 60, and 108 hai, respectively), and LOX (37 and 53% at 12 and 108 hai, respectively) were significantly higher for inoculated +Si plants compared to non-inoculated +Si plants (Fig. 10a-l).

3.10. Concentrations of TSP and LTGA derivatives

For non-inoculated plants, TSP and LTGA derivatives concentrations were not affected by Si treatments regardless of the evaluation time (Fig. 11a and c). For inoculated plants, the concentrations of TSP (16 and 11% at 108 and 156 hai) and LTGA derivatives were significantly higher (33, 25, 33, and 37% at 12, 60, 108, and 156 hai, respectively) for inoculated +Si plants compared to inoculated -Si plants (Fig. 11b and d). The TSP concentration was significantly higher (13 and 23% at 60 and 156 hai, respectively) while the LTGA derivatives concentration was significantly lower (33, 45, and 57% at 12, 108, and 156 hai, respectively) for inoculated -Si plants compared to non-inoculated -Si plants (Fig. 12a-d). The concentrations of TSP (27% at 156 hai) and LTGA derivatives (28% at 60 hai) were significantly higher for inoculated +Si plants compared to non-inoculated +Si plants (Fig. 11a-d).

3.11. Antioxidant enzymes

Antioxidant enzyme activities for non-inoculated plants were not affected by Si treatments regardless of the evaluation time (Fig. 12a, c, e, and g). For inoculated plants, SOD (22 and 28% at 12 and 60 hai, respectively), APX (26% at 12 hai), CAT (21-35% from 12 to 108 hai), and GR (28-49% from 12 to 108 hai) activities were significantly higher for +Si plants compared to -Si

plants (Fig. 12b, d, f, and h). There were significant increases in SOD (28% at 156 hai), APX (24-37% from 60 to 156 hai), and GR (55% at 156 hai) activities for inoculated -Si plants compared to inoculated +Si plants (Fig. 12b, d, and h). Activities of SOD (30 and 44% at 108 and 156 hai, respectively), APX (38, 45, and 58% at 60, 108, and 156 hai, respectively), CAT (40, 44, and 42% at 60, 108, and 156 hai, respectively), and GR (50% at 156 hai) were significantly higher for inoculated -Si plants compared to non-inoculated -Si plants (Fig. 12a-h). Activities of SOD (29% at 108 hai), APX (35 and 37% at 12 and 156 hai, respectively), CAT (48, 58, and 30% at 60, 108, and 156 hai, respectively), and GR (32% at 108 hai) were significantly higher for inoculated +Si plants compared to non-inoculated +Si plants (Fig. 12a-h).

3.12. PCA analysis

Three clusters were generated (NI plants for -Si and +Si treatments, I plants for -Si treatment, and I plants for +Si treatment) based on the cluster analysis with complete linkage and Pearson distance. One principal component (PC) explained most of the variation in the data analyzed (PC1 = 75.1% and PC2 = 21.6%) (Fig. 13). The PC1 showed negative scores for A, g_s, E, F_v/F_m, Y(II), ETR, Chl a+b, carotenoids, glucose, fructose, sucrose, and LTGA derivatives and positive scores for other variables and parameters evaluated. The PC2 was characterized by negative scores for E, sucrose, Y(II), ETR, fructose, starch, C_i, Y(NPQ), LTGA derivatives, glucose, $O_2^{\bullet-}$, APX, CAT, and PAL, and positive scores for other variables and parameters evaluated (Fig. 13).

4. Discussion

It is well known that Si plays a key role in plant resistance against an array of pathogens infecting a diversity of profitable crops (Debona *et al*., 2023). In this study, new pieces of evidence at the physiological and biochemical levels clearly explain the reduction of MLB symptoms by Si. A higher foliar Si concentration for +Si plants reduced the progress of MLB as a result of lower cellular oxidative damage (lower concentrations of MDA, H_2O_2, and $O_2^{\bullet-}$). Different reports highlighted that the intensity of innumerable diseases in gramineous plants such as rice, sugarcane, wheat, and maize were negatively correlated with higher foliar Si concentration when this element was supplied to plants through the roots (Debona *et al*., 2017, 2023; Hawerroth *et al*., 2019). In maize, the uptake and translocation of Si from the roots to the shoots is governed by the presence

of the transporters *ZmLsi1* and *ZmLsi6*, which operates in the active Si uptake mechanism besides a passive mechanism that occurs through the transpiratory flux of water (Debona *et al*., 2017; Mitani *et al*., 2009).

Photosynthesis is the physiological process mostly affected in plants infected by pathogens of different lifestyles that negatively affect the photosynthetic machinery and its functionality reducing, therefore, the efficiency of light capture, energy production, and the synthesis of photoassimilates that could be used by the plant to mount defense reactions (Berger *et al*., 2007). The photosynthetic parameters such as leaf gas exchange and chlorophyll *a* fluorescence are good physiological indicators that provide quantitative information on the extent and nature of the impact imposed by the pathogen on host physiological processes (Scholes and Rolfe, 2009; Kumudini *et al*., 2018). In the present study, Si supply reduced the negative effect of *B. maydis* infection on the photosynthetic capacity of maize plants as indicated by the higher values of A, g_s, and E. In contrast, there was a significant effect of Si on C_i only at 108 hai for infected leaves. In general, +Si infected plants showed a proportional increase in A and g_s simultaneously with unchanged values for C_i at 156 hai indicating that increases in A values during the infection process of *B. maydis* in the leaves of +Si plants were not strongly associated with limitations in CO_2 influx into the stomata for photosynthesis. Thus, changes in A were probably not caused by the obtained values for g_s considering the concomitant increases in the values of these parameters throughout the *B. maydis* infection process without strongly changes in C_i. Therefore, the effect of Si to mitigate the decreases in A should be explained by alleviating the dysfunctions that may take place at the level of biochemical reactions in the chloroplasts that involves CO_2 fixation for a better photosynthetic performance of maize plants. Similar reports have shown the positive effect of Si on keeping a better photosynthetic performance by monitoring the changes in the leaf gas exchange parameters in the following interactions rice-*Pyricularia oryzae* and *Monographella albescens* (Domiciano *et al*., 2015; Tatagiba *et al*., 2016) as well as wheat-*P. oryzae* (Aucique-Pérez *et al*., 2014). The impairment of A in maize plants may also have been associated with the release of hydrolytic enzymes and non-host selective toxins by *B. maydis* into the leaf tissues that can lower CO_2 assimilation due to the destruction of stomata, damage the photosynthetic apparatus, and degradation of photosynthetic pigments (Tsuge *et al*., 2013). However, these dysfunctions were attenuated by Si due to the formation of a thick silica layer below the cuticle that acted as a physical barrier that inhibited or delayed *B. maydis* penetration and its growth over the leaf surface as shown

by the X-rays microanalysis contributing, therefore, to the preservation of the photosynthetic apparatus (Debona *et al*., 2023).

In addition to the impact on the biochemical function of CO_2 fixation, changes in the photochemical capacity of photosynthesis were more prominent at later stages of *B. maydis* infection for -Si plants. Based on the imaging of Chl *a* fluorescence parameters, early damage of fungal infection against photosynthesis can be visualized in a non-invasively way before the symptoms are noticed (Scholes and Rolfe, 2009; Silveira *et al*., 2021; Silva *et al*., 2022). The parameters F_v/F_m and Y(II) represent the capacity of photon energy absorbed by the PSII to be used in photochemical processes and are considered physiological markers to understand the effect of biotic stress-induced photoinhibition and the level of disease impact on photosynthesis (Calatayud *et al*., 2013). In addition, photoinhibition occurring at the PSII level may affect the redox balance of electron transport components for the production of reducing power and consequently the deactivation of RuBisCO (Rochaix, 2011). Interestingly, the infected leaves of +Si plants suffered less photooxidative damage as clearly indicated by the higher values of F_v/F_m, Y(II), and ETR concomitantly without significant changes in Y(NPQ) and Y(NO) values indicating, therefore, that the functionality of the photosynthetic apparatus was preserved. The higher linear electron flow and the Y(II) parameter indicate a key role of the dissipative mechanisms mainly modulated by Si to bring sufficient photochemical energy to be used to support the higher photosynthetic performance of leaves infected with *B. maydis*. The maize and wheat plants supplied with Si and infected by *E. turcicum* and *P. oryzae,* respectively (Domiciano *et al*., 2015; Silveira *et al*., 2021) showed higher values of F_v/F_m, Y(II), and ETR indicating the positive contribution of this element to reduce the dysfunctions at the photochemical level. Plants under stress and supplied with Si displayed greater amount of open PSII reaction centers that resulted in higher excitation energy in the electron flow thus improving the photochemical efficiency of photosynthesis (Rastogi *et al*., 2021). Studies at the transcriptomic level in *Brassica napus* (Etienne *et al*., 2021) and *Cucumis sativus* (Holz *et al*., 2019) showed that Si promoted the differential expression of genes encoding proteins that were involved in photochemical reactions mainly those associated with the light-harvesting complex, PSII, and the electron transport chain resulting in a better integrity of chloroplasts and the photosynthetic apparatus overall.

In addition to the parameters related to Chl *a* fluorescence, the quantification of the pool of photosynthetic pigments is a stronger indicator of the decreased efficiency of the photosynthetic

apparatus of plants infected by hemibiotrophic and necrotrophic pathogens due to the action of hydrolytic enzymes and selective non-host toxins that directly affect chloroplasts and their protein complexes (Aucique-Pérez *et al*., 2020; Silva *et al*., 2022). The loss of functionality of the photosynthetic pigments is one of the main effects caused by *B. maydis* infection in maize leaves (Meshram *et al*., 2022). The reduction of MLB symptoms in the leaves of +Si plants was closely linked to a higher pool of photosynthetic pigments (Chl *a*+*b* and carotenoids) at 156 hai, a later stage on the *B. maydis* infection process, evidencing less damage to the photosynthetic apparatus. Previous studies emphasized that Si plays a crucial role in maintaining the integrity of chloroplasts in the leaves of plants exposed to cellular oxidative stress caused by diseases which will result in the preservation of the photosynthetic pigments pool (Rodrigues and Datnoff, 2015; Tatagiba *et al*., 2016).

Besides photosynthesis, the metabolism of carbohydrates in plants plays a detrimental role during the pathogen infection process (Zaynab *et al*., 2019). The metabolism of soluble sugar represents a very complex physiological process in several host-pathogen interactions considering that the flow of photoassimilates to trigger defense reactions at the pathogen infection sites is greatly demanded by the plants (Zaynab *et al*., 2019; Silva *et al*., 2022). In addition, changes in the levels of photoassimilates may greatly affect the pathogen infection process considering that sugars serve as nutrients and signals during the colonization of host tissues by the pathogens (Kanwar and Jha, 2019). In the present study, down-regulation of photosynthesis may have reduced the pool of sugars and starch in the infected leaves of -Si plants that displayed expressive symptoms of MLB. In general, for infected +Si plants, higher concentrations of glucose and sucrose were found at later stages of fungus infection while starch concentration was kept higher almost during the entire time-course evaluated. These findings clearly indicate a possible effect of Si in enhancing maize resistance against MLB through the modulation of carbohydrate metabolism rather than favoring fungal infection. In rice, Si conferred resistance to brown spot by regulating the expression of photosynthetic genes (e.g. RuBisCO production) and those related to nitrate and nitrite reductases as well as nitrate transporter (Van Bockhaven *et al*., 2015). Rice plants supplied with Si showed increased sucrose concentration in response to *B. oryzae* infection (Dallagnol *et al*., 2013). The expression of Calvin cycle-related genes such as those coding for fructose-1,6-bisphophate aldolase, phosphate isomerase, sedoheptulose-1,7-bisphosphatase, glyceraldehyde-3-phosphate dehydrogenase, fructose-1,6-bisphosphatase, and RuBisCO was repressed in cucumber plants

infected with *Fusarium oxysporum* (Sun *et al*., 2022). However, the expression of the above-mentioned genes increased and improved the pool of soluble sugars and the resistance of cucumber against Fusarium wilt for Si-supplied plants. Interestingly, fructose concentration for infected +Si plants decreased at earlier times of *B. maydis* infection and increased later on. Similar results for fructose accumulation were found for wheat plants supplied with Si and infected with *P. oryzae* indicating a possible use of fructose to favor fungal infection (Peixoto *et al*., 2019). Considering these findings related to the regulatory role of Si on physiological attributes conferring increased resistance of maize against MLB, the pattern of both sugar metabolism and photosynthetic capacity can be used as benchmark markers for the positive effect of Si on maize-*B. maydis* interaction.

It is well known that the great production of MDA in host tissues infected by pathogens results from an intense lipid peroxidation on cell membrane caused by an excess of H_2O_2 or $O_2^{\bullet-}$ (Mayer *et al*., 2001). In response to this oxidative stress due to pathogen infection, an enzymatic antioxidant system with the action of SOD, APX, CAT, and GR activities take place to keep the generation of reactive oxygen species (ROS) at physiologically accepted levels (Dumanović *et al*., 2021). In the present study, MDA concentration was lower for infected leaves of +Si plants from 60 to 156 hai and was linked to reduced production of H_2O_2 or $O_2^{\bullet-}$. In addition, SOD, APX, CAT, and GR activities were greatest at 12 hai with subsequent increase in SOD activity up to 60 hai and CAT and GR activities up to 108 hai. The literature is rich in reports showing that Si can stimulate the enzymatic antioxidant metabolism of pathogen-challenged plants by restricting the oxidative stress caused by an excess of ROS associated with less lipid peroxidation in the infected cells (Rodrigues and Datnoff, 2015; Debona *et al*., 2017, 2023; Song *et al*., 2016; Silveira *et al*., 2021; Sun *et al*., 2022). In the present study, APX activity was higher for infected -Si plants in contrast to infected +Si plants from 60 to 156 hai possibly due to the higher availability of H_2O_2 that needed to be detoxified. The greater concentration of H_2O_2 accompanied by $O_2^{\bullet-}$ may be an indirect indication of the oxidative stress (e.g., action of several hydrolytic enzymes and non-host selective toxins) generated by the colonization of maize leaves of -Si plants by *B. maydis*. Both CAT and APX act in the elimination of H_2O_2, however, it has been suggested that moderate concentrations of H_2O_2 are eliminated mainly by APX with the aid of various reductants such as ascorbate and glutathione (Mittler *et al*., 2022).

Biochemically, the enhancement of the resistance of crops challenged by pathogens by Si is associated with the joint action of defense-related enzymes and the production of phenolic

compounds (Debona *et al*., 2017, 2023; Islam *et al*., 2020). The defense proteins CHI and GLU, which catalyze the hydrolysis of key fungal cell wall components (chitin and β-1,3-glucan, respectively), are important for the resistance of several plant species infected by fungal pathogens of different lifestyles (Sundaresha *et al*., 2010). In the present study, CHI activity was highest at 12 hai while GLU was highest only at 108 hai for infected +Si plants. The results of the present study are corroborated by the findings of Fortunato *et al*., (2014) who found higher CHI and GLU activities in the roots of banana plants supplied with Si. Products of secondary metabolism such as phenolic compounds, lignin, phytoalexins, and flavonoids are dependent on the initial activity of PAL through the phenylpropanoid pathway (Dixon and Paiva, 1995). The PPO and POX play key roles in the oxidation of polyphenols to quinones which are highly toxic against several and in the lignification of cell walls with a caution participation of H_2O_2 (Thipyapong *et al*., 2004). In the present study, PAL and POX activities followed the same increasing trend from 12 to 108 hai, but PPO activity was higher only at 108 hai for infected +Si plants. The Si-mediated resistance in perennial ryegrass against *Magnaporthe oryzae* infection was associated with higher activities of PAL, POX, and PPO (Rahman *et al*., 2015). Increased LOX activity is known to occur in response to the oxidation of fatty acids released by ROS-induced lipid peroxidation that leads to the biosynthesis of jasmonic acid considered to be a signaling molecule for induced systemic resistance against pathogen attack (Viswanath *et al*., 2020). In the present study, lower LOX activity was evidenced for infected -Si plants at 60 and 156 hai. The low LOX activity may be related to lower levels of lipid peroxidation and ROS accumulation during the infection of leaves from +Si plants by *B. maydis* (Kim *et al*., 2014).

For +Si plants, the production of LTGA derivatives increased throughout the *B. maydis* infection process while higher TSP concentration occurred only at later stages of fungal infection. It is known that plants supplied with Si display an increased concentration of phenolics and lignin due to a potentiation of the phenylpropanoid pathway to efficiently counteract the infection process of pathogens of different lifestyles (Debona *et al*., 2017, 2023; Ahanger *et al*., 2020). For example, in maize leaves and banana roots infected with *S. macrospora* and *F. oxysporum* f. sp. *cubense*, respectively, Si potentiated the phenylpropanoid pathway by increasing the production of phenolic compounds and lignin and significantly reducing the damage caused by these pathogens on host tissues (Fortunato *et al*., 2014; Hawerroth *et al*., 2019). The PAL and POX are pivotal enzymes in the biosynthesis of phenolic compounds and lignin (Dixon and Paiva, 1995; Thipyapong *et al*.,

2004) and their higher activities as evidenced in the present study may have greatly contributed to the strengthening of the cell wall in the leaves of +Si plants that may impair the colonization process of *B. maydis*. On top of that, greater production of carbohydrates may have also contributed as respiratory substrates to be used in the formation of energy-rich compounds (e.g., ATP) as well as intermediate compounds that could be linked to the increased resistance of leaves of +Si plants to MLB.

Taken together, the results of the present study integrate physiological and biochemical pieces of evidence for the beneficial role played by Si in enhancing the resistance of leaves of maize against MLB. Based on the PCA analysis, the isolation of the cluster inoculated +Si plants from the other two clusters (NI plants from -Si and +Si treatments as well as I -Si plants) highlights the peculiar effect of this element on the outcome of variables and parameters investigated in the present study. In this regard, plants supplied with Si had a more preserved photosynthetic apparatus, a more robust antioxidative metabolism, greater response of defense-related enzymes, and regulation of carbohydrate metabolism that worked all together in favor of the increased resistance of leaves from +Si plants infected by *B. maydis*.

5. References

Ahanger, M.A., Bhat, J.A., Siddiqui, M.H., Rinklebe, J., Ahmad, P. Integration of silicon and secondary metabolites in plants: A significant association in stress tolerance. **J Exp Bot**, v. 71, p. 6758-6774, 2020.

Aucique-Pérez, C.E., Rios, V.S., Neto, L.B.C., Rios, J.A., Martins, S.C.V., Rodrigues, F.A. Photosynthetic changes in wheat cultivars with contrasting levels of resistance to blast. **J Phytopathol**, v. 168, p. 721-729, 2020.

Aucique-Pérez, C.E., Rodrigues, F.A., Moreira, W., Damatta, F.M. Leaf gas exchange and chlorophyll *a* fluorescence in wheat plants supplied with silicon and infected with *Pyricularia oryzae*. **Phytopathology**, v. 104, p. 143-149, 2014.

Berger, S., Sinha, A.K., Roitsch, T. Plant physiology meets phytopathology : plant primary metabolism and plant – pathogen interactions. **J. Exp. Bot**, v. 58, p. 4019–4026, 2007.

Calatayud, Á. *et al.* Use of chlorophyll fluorescence imaging as diagnostic technique to predict compatibility in melon graft. **Sci Hortic,** v. 149, p. 13-18, 2013.

Chaves J.A. *et al.* Physiological and biochemical responses of tomato plants to white mold affected by manganese phosphite. **J Phytopathol,** v. 169, p. 149-167, 2021.

Dai Y. *et al.* Sensitivity of *Cochliobolus heterostrophus* to three demethylation inhibitor fungicides, propiconazole, diniconazole and prochloraz, and their efficacy against southern corn leaf blight in Fujian province, China. **Eur J Plant Pathol,** v. 152, p. 447-459, 2018.

Dai Y. *et al.* Characterization of natural isolates of *Bipolaris maydis* associated with mating types, genetic diversity, and pathogenicity in Fujian Province, China. **Plant Dis**, v. 104, p. 323-329, 2020.

Dallagnol LJ. Photosynthesis and sugar concentration are impaired by the defective active silicon uptake in rice plants infected with *Bipolaris oryzae*. **Plant Pathol**, v. 62, p. 120-129, 2013.

Debona, D., Rodrigues, F.A., Datnoff, L.E. Silicon's role in abiotic and biotic plant stresses. **Annu Rev Phytopathol**, v. 55, p. 85-107, 2017.

Debona, D., Datnoff, L.E., Rodrigues, F.A. Silicon and plant disease. In: Datnoff LE, Elmer WH, and Rodrigues FA (Eds.). Mineral and Plant Nutrition. The American Phytopathological Society, St. Paul, p. 381-424, 2023.

Dias CS, *et al.* Effect of glutamate on *Pyricularia oryzae* infection of rice monitored by changes in photosynthetic parameters and antioxidant metabolism. **Physiol Plant**, v. 169, p. 179-193, 2020.

Dixon, R.A., Paiva, N.L. Stress-induced phenylpropanoid metabolism. **Plant Cell**, v. 7, p. 1085-1097, 1995.

Domiciano G.P. *et al.* Alterations in gas exchange and oxidative metabolism in rice leaves infected by *Pyricularia oryzae* are attenuated by silicon. **Phytopathology**, v. 105, p. 738-747, 2015.

Dumanović, J. *et al.* The significance of reactive oxygen species and antioxidant defense system in plants: A concise overview. **Front Plant Sci**, v. 11, 2021.

Etienne P. *et al.* Root silicon treatment modulates the shoot transcriptome in *Brassica napus* L. and in particular upregulates genes related to ribosomes and photosynthesis. **Silicon**, v. 13, p. 4047-4055, 2021.

Fagundes-Nacarath, I.R.F., Debona, D., Rodrigues, F.A. Oxalic acid-mediated biochemical and physiological changes in the common bean-*Sclerotinia sclerotiorum* interaction. **Plant Physiol Biochem**, v. 129, p. 109-121, 2018.

Fernie, A.R. The contribution of plastidial phosphoglucomutase to the control of starch synthesis within the potato tuber. **Planta**, v. 213, p. 418-426, 2001.

Fortunato, A.A., da Silva, W.L., Rodrigues, F.A. Phenylpropanoid pathway is potentiated by silicon in the roots of banana plants during the infection process of *Fusarium oxysporum* f. sp. *cubense*. **Phytopathology**, v. 104, p. 597-603, 2014.

Hawerroth, C. *et al.* Silicon-mediated maize resistance to macrospora leaf spot. **Trop Plant Pathol**, v. 44, p.192-196, 2019.

Heath, R.L., Packer, L. Photoperoxidation in isolated chloroplasts. **Arch Biochem Biophys**, v. 125, p. 189-198, 1968.

Hoagland, D., Arnon, D. The water-culture method for growing plants without soil. Agricultural Experiment Station., Berkeley: California, 1950

Holz, S. *et al.* Initial studies on cucumber transcriptome analysis under silicon treatment. **Silicon**, v. 11, p. 2365-2369, 2019.

Islam, W. *et al.* Silicon-mediated plant defense against pathogens and insect pests. **Pestic Biochem Physiol**, v. 168, p. 104641, 2020.

Kanwar, P., Jha, G. Alterations in plant sugar metabolism: signatory of pathogen attack. **Planta**, v. 249, p. 305-318, 2019.

Kim, Y.H. *et al.* Regulation of jasmonic acid biosynthesis by silicon application during physical injury to *Oryza sativa* L. **J Plant Res**, v. 127, p. 525-532, 2014.

Korndörfer, G.H., Pereira, H.S., Nola, A. Análise de silício: solo, planta e fertilizante. Universidade Federal de Uberlândia, Uberlândia.

Kumar, B. *et al.* Maydis leaf blight of maize: Update on status, sustainable management and genetic architecture of its resistance. **Physiol Mol Plant Pathol**, v. 121, p. 101889, 2022.

Kumar C. *et al. In vitro* evaluation of fungicides, botanicals and bio-agents against the maydis leaf light disease of maize caused by *Helminthosporium maydis*. **Pharma Innov**, v. 10, p. 399-406, 2021.

Kumudini, B.S. *et al.* Primary plant metabolism during plant-pathogen interactions and its role in defense. In: Ahmad P, Ahanger MA, Singh VP, Tripathi DK, Alam P, Alyemeni MN (Eds). Plant Metabolites and Regulation Under Environmental Stress. Elsevier Inc. pp. 215-229, 2018.

Ma, J.F., Yamaji, N. Silicon uptake and accumulation in higher plants. **Trends Plant Sci**, v. 11, p. 392-397, 2006.

Manamgoda, D.S., *et al.* The genus *Bipolaris*. **Stud Mycol,** v. 79, p. 221-288, 2014.

Marçal, D.M.S., *et al.* Elevated [CO_2] benefits coffee growth and photosynthetic performance regardless of light availability. **Plant Physiol Biochem**, v. 158, p. 524-535, 2021.

Mayer, A.M., Staples, R.C., Gil-ad, N.L. Mechanisms of survival of necrotrophic fungal plant pathogens in hosts expressing the hypersensitive response. **Phytochemistry**, v. 58, p. 33-41, 2001.

Medeiros, D.B. *et al.* Impaired malate and fumarate accumulation due to the mutation of the tonoplast dicarboxylate transporter has little effects on stomatal behavior. **Plant Physiol,** v. 175, p. 1068-1081, 2017.

Meshram, S., *et al.* Comparative transcriptome analysis of fungal pathogen *Bipolaris maydis* to understand pathogenicity behavior on resistant and susceptible non-CMS maize genotypes. **Front Microbiol**, v. 13, p. 837056, 2022.

Mesquita, G.L. *et al.* Foliar application of manganese increases sugarcane resistance to orange rust. **Plant Pathol**, v. 68, p. 1296-1307, 2019.

Mitani, N., Yamaji, N., Ma, J.F. Identification of maize silicon influx transporters. **Plant Cell Physiol**, v. 50, p. 5-12, 2009.

Mittler, R. *et al.* Reactive oxygen species signalling in plant stress responses. **Nat Rev Mol Cell Biol**, v. 23, p. 663-679, 2022.

Peixoto, M.U. *et al.* Silicon alleviates changes in the source-sink relationship of wheat plants infected by *Pyricularia oryzae*. **Phytopathology**, v. 109, p. 1129-1140, 2019.

Rastogi, A. *et al.* Does silicon really matter for the photosynthetic machinery in plants? **Plant Physiol Biochem** 169:40-48, 2021.

Rochaix, J.D. Regulation of photosynthetic electron transport. **Biochim Biophys Acta – Bioenerg,** v. 1807, p. 375-383, 2011.

Rodrigues, F.A., *et al.* Silicon potentiates host defense mechanisms against infection by plant pathogens. In: Rodrigues FA and Datnoff LE (Eds.) Silicon and Plant Diseases. Springer. p. 109-138, 2015.

Scholes, J., Rolfe, S. Chlorophyll fluorescence imaging as tool for understanding the impact of fungal diseases on plant performance: a phenomics perspective. **Funct Plant Biol**, v. 36, p. 880-892, 2009.

Silva, B.N. *et al.* Physiological and biochemical insights into induced resistance on tomato against Septoria leaf spot by a phosphite combined with free amino acids. **Physiol Mol Plant Pathol,** v. 120, p. 101854, 2022.

Silveira, P.R. *et al.* Biochemical and physiological changes in maize plants supplied with silicon and infected by *Exserohilum turcicum*. **J Phytopathol**, v. 169, p. 393-408, 2021.

Smith, D.R, HookerA, L., Lim, S.M. Physiologic races of *Helminthosporium maydis*. **Plant Dis Report**, v. 54, p. 819-22, 1970.

Song, A. *et al.* The role of silicon in enhancing resistance to bacterial blight of hydroponic- and soil-cultured rice. **Sci Rep**, v. 6, p. 1-13, 2016.

Sun, S. *et al.* Silicon enhances plant resistance to Fusarium wilt by promoting antioxidant potential and photosynthetic capacity in cucumber (*Cucumis sativus* L.). **Front Plant Sci**, v. 13, p. 1-16, 2022.

Sundaresha, S. *et al.* Enhanced protection against two major fungal pathogens of groundnut, *Cercospora arachidicola* and *Aspergillus flavus* in transgenic groundnut over-expressing a tobacco β-1-3 glucanase. **Eur J Plant Pathol**, v. 126, p. 497-508, 2010.

Tatagiba, S.D., DaMatta, F.M., Rodrigues, F.A. Silicon partially preserves the photosynthetic performance of rice plants infected by *Monographella albescens*. **Ann Appl Biol**, v. 168, p. 111-121, 2016.

Thipyapong, P., Hunt, M.D., Steffens, J.C. Antisense downregulation of polyphenol oxidase results in enhanced disease susceptibility. **Planta**, v. 220, p. 105-117, 2004.

Tsuge, T. *et al.* Host-selective toxins produced by the plant pathogenic fungus *Alternaria alternata.* **FEMS Microbiol Rev**, v. 37, p. 44-66, 2013.

Van Bockhaven, J. *et al.* Primary metabolism plays a central role in moulding silicon-inducible brown spot resistance in rice. **Mol Plant Pathol**, v. 16, p. 811-824, 2015.

Viswanath, K.K., Varakumar, P, Pamuru, R.R. Plant lipoxygenases and their role in plant physiology. **J Plant Biol**, v. 63, p. 83-95, 2020.

Wellburn, A.R. The spectral determination of chlorophylls *a* and *b*, as well as total carotenoids, using various solvents with spectrophotometers of different resolution. **J Plant Physiol**, v. 144, p. 307-313, 1994.

Wheeler, H. Ultrastructure of penetration by *Helminthosporium maydis*. **Physiol Plant Patho**, v. 11, p. 171-178, 1977.

Zaynab, M., Fatima, M., Sharif, Y. Role of primary metabolites in plant defense against pathogens. **Microb Pathog** 137, p. 103728, 2019.

7. Table and Figures

Table 1. Analysis of variance for the effects of silicon (Si), plant inoculation (PI), and the Si × PI interaction for foliar concentrations of Si and potassium (K), Bipolaris leaf spot severity (Sev), leaf gas exchange parameters [rate of net CO_2 assimilation (A), stomatal conductance to water vapor (g_s), internal CO_2 concentration (C_i), and transpiration rate (E)], chlorophyll *a* fluorescence parameters [variable-to-maximum chlorophyll *a* fluorescence ratio (F_v/F_m), photochemical yield (Y(II)), yield for dissipation by down-regulation (Y(NPQ), yield for non-regulated dissipation (Y(NO), and electron transport rate (ETR)], concentrations of photosynthetic pigments [chlorophyll *a*+*b* (Chl *a*+*b*) and carotenoids (Car)], carbohydrates (glucose, fructose, sucrose, and starch), malondialdehyde (MDA), hydrogen peroxide (H_2O_2), and superoxide anion radical ($O_2^{\bullet-}$), total soluble phenolics (TSP) and lignin-thioglycolic acid (LTGA) derivatives as well as activities of defense [chitinase (CHI), β-1,3-glucanase (GLU), phenylalanine ammonia-lyase (PAL), polyphenoloxidase (PPO), peroxidase (POX), and lipoxygenase (LOX)] and antioxidative [superoxide dismutase (SOD), ascorbate peroxidase (APX), catalase (CAT), glutathione reductase (GR)] enzymes.

Variables/ Parameters	*F* values*						
	Si	PI	ST	Si x PI	Si x ST	PI x ST	Si x PI x ST
Si	**545.7**	1.5		0.02			
K	1.9	1.6		0.2			
Sev	**136.3**						
A	**12.8**	**113.7**	**22.7**	**8.5**	0.9	**11.6**	0.2
g_s	**10.6**	0.5	**28.4**	1.7	**5.6**	**17.0**	**5.7**
C_i	0.6	**9.1**	**26.4**	0.3	**8.8**	1.1	**6.4**
E	**5.5**	**4.4**	**11.3**	**5.3**	**7.4**	2.2	**6.2**
F_v/F_m	**30.6**	**89.9**	**3.9**	**23.9**	**6.3**	**20.3**	**9.2**
Y(II)	**13.1**	2.2	**9.3**	1.4	**3.5**	**4.9**	0.5
Y(NPQ)	0.3	**10.2**	**3.4**	0.7	0.6	**4.5**	0.2
Y(NO)	0.2	0.3	**17.6**	0.2	**4.8**	**9.3**	**3.7**
ETR	**19.1**	**7.7**	**11.9**	**6.0**	**5.7**	**7.9**	0.2
Chl *a*+*b*	0.2	**30.4**	**15.6**	1.5	2.3	**3.1**	0.6
Car	0.0	**14.3**	**15.3**	0.6	1.9	**4.5**	0.4
Glucose	**5.5**	**29.8**	**4.3**	0.1	3.0	**20.2**	1.5
Fructose	3.1	**3.5**	**18.5**	1.0	**3.5**	0.6	**3.5**
Sucrose	**5.0**	**17.2**	**4.6**	**7.3**	2.0	**5.2**	1.0
Starch	2.3	**195.5**	**8.2**	0.8	**3.3**	**19.3**	**3.1**
MDA	**16.4**	**20.2**	0.2	**17.3**	**3.1**	**6.0**	0.9
H_2O_2	1.3	3.6	1.4	1.9	2.2	2.0	1.4
$O_2^{\bullet-}$	**85.4**	**298.8**	**85.5**	**83.1**	1.7	**43.9**	1.3
SOD	0.0	**23.4**	**11.5**	0.4	**3.5**	**9.7**	**3.5**
APX	**8.2**	**87.8**	**32.2**	**13.3**	**3.5**	**11.0**	**5.8**
CAT	4.1	**122.5**	**60.8**	2.1	1.8	**18.3**	**3.0**
GR	0.4	0.9	**16.7**	0.5	**19.9**	**15.9**	**18.4**

CHI	2.9	**21.6**	**18.9**	**5.8**	**9.0**	**19.4**	**6.5**
GLU	0.02	**41.1**	**44.6**	0.0	**6.9**	**37.4**	**3.1**
PAL	**7.1**	**65.9**	**5.2**	**4.6**	**5.9**	**11.3**	**8.5**
PPO	3.2	**103.4**	**47.6**	0.0	**4.4**	**44.8**	**3.3**
POX	0.9	**71.2**	**24.6**	1.4	**4.5**	**5.7**	**4.4**
LOX	0.1	**217.2**	**156.3**	2.1	**7.1**	**92.7**	**6.6**
TSP	0.3	**15.5**	**28.2**	2.8	**3.7**	**18.1**	**3.8**
LTGA derivatives	**17.4**	**25.0**	**11.7**	**33.0**	0.9	**11.2**	0.8

*Bold values are significant at $P \leq 0.05$

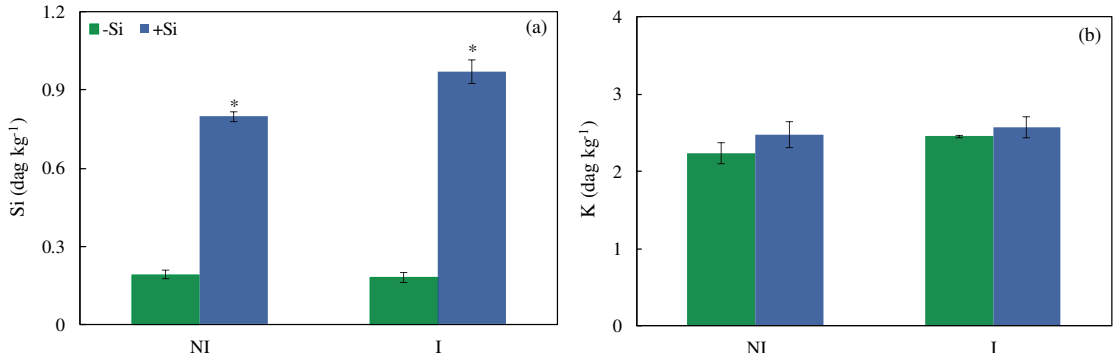

Figure 1. Foliar concentrations of silicon (Si) (a) and potassium (K) (b) for maize plants non-supplied (-Si) or supplied (+Si) with silicon (Si) and non-inoculated (NI) or inoculated (I) with *Bipolaris maydis*. Means for -Si and +Si treatments followed by an asterisk (*) and for NI and I treatments followed by an inverted triangle (▼) are significantly different ($P \leq 0.05$) according to the *F* test. Bars represent the standard error of the means.

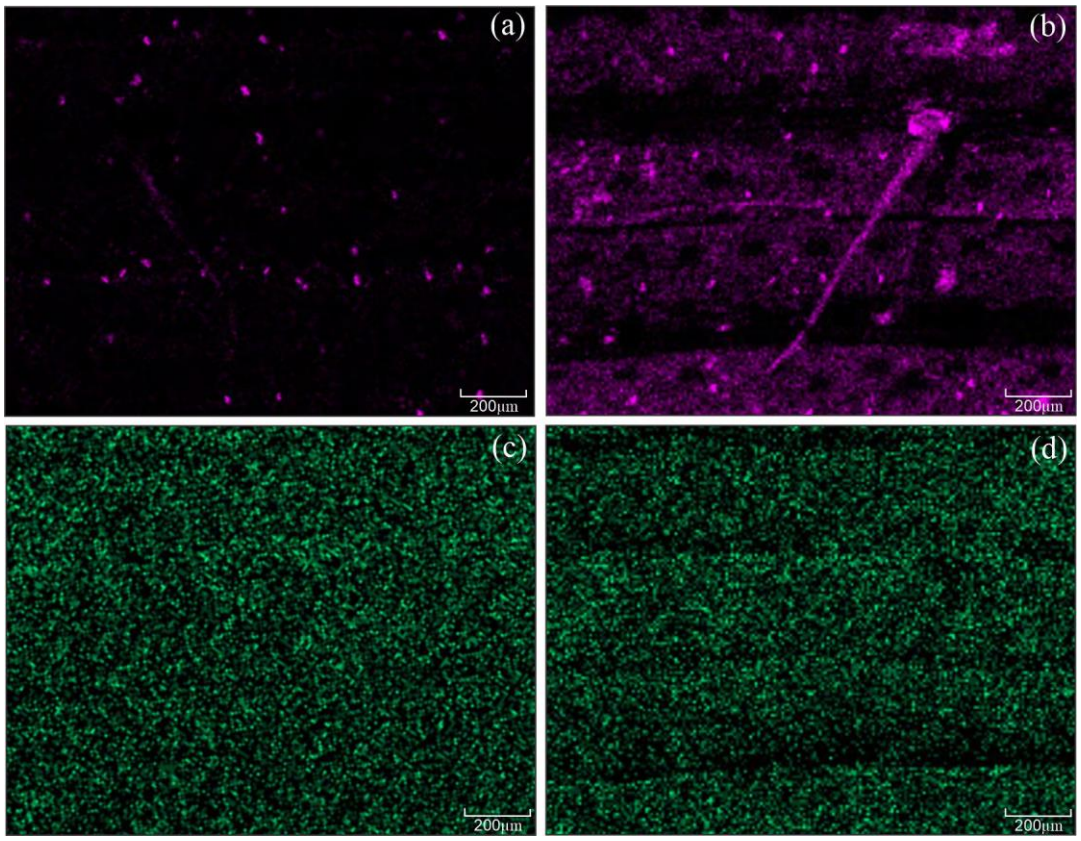

Figure 2. X-ray maps for silicon (Si) (a and b) and potassium (K) (c and d) in the leaves of maize plants non-supplied (-Si) (a and c) or supplied (+Si) (b and d) with silicon (Si) at 156 hours after inoculation with *Bipolaris maydis*. In the X-ray maps, purple (a and b) and green (c and d) fluorescent dots correspond to the accumulation of Si and K, respectively. Black is the absence of Si and K. The intensity of Si and K depositions were obtained based on the X-ray emission spectra of the X-ray maps [Si = 0.81, error (E) = 0.04 (a); Si = 8.35, E = 0.09 (b); K = 5.91, E = 0.09 (c); and K = 4.25, E = 0.07 (d)] compared to other chemical elements such as carbon, oxygen, magnesium, phosphorus, sulfur, and chlorine.

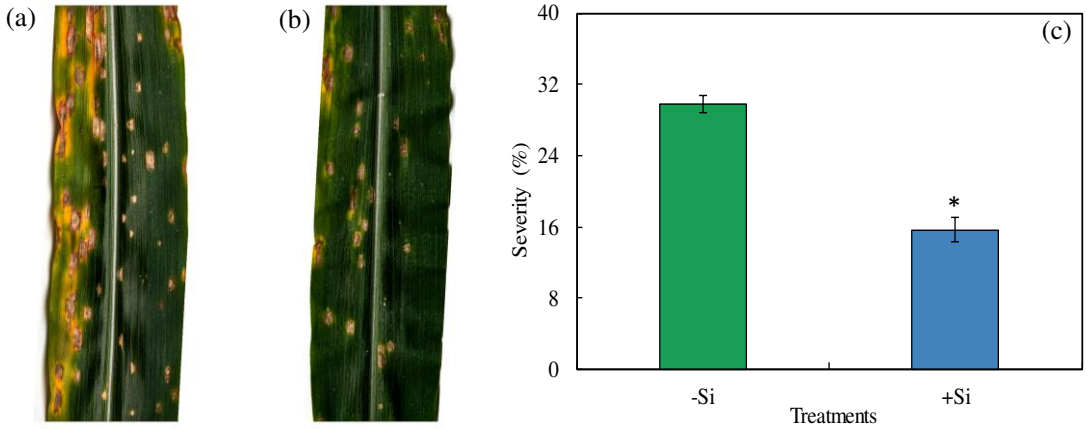

Figure 3. Symptoms of Bipolaris leaf spot (a and b) and severity (c) for maize plants non-supplied (-Si) or supplied (+Si) with silicon (Si). Means for -Si and +Si treatments (graph c) followed by an asterisk (*) are significantly different ($P \leq 0.05$) according to the *F* test. Bars represent the standard error of the means. Imaging of leaves with disease symptoms and the assessment of severity were performed seven days after plant inoculation with *Bipolaris maydis*.

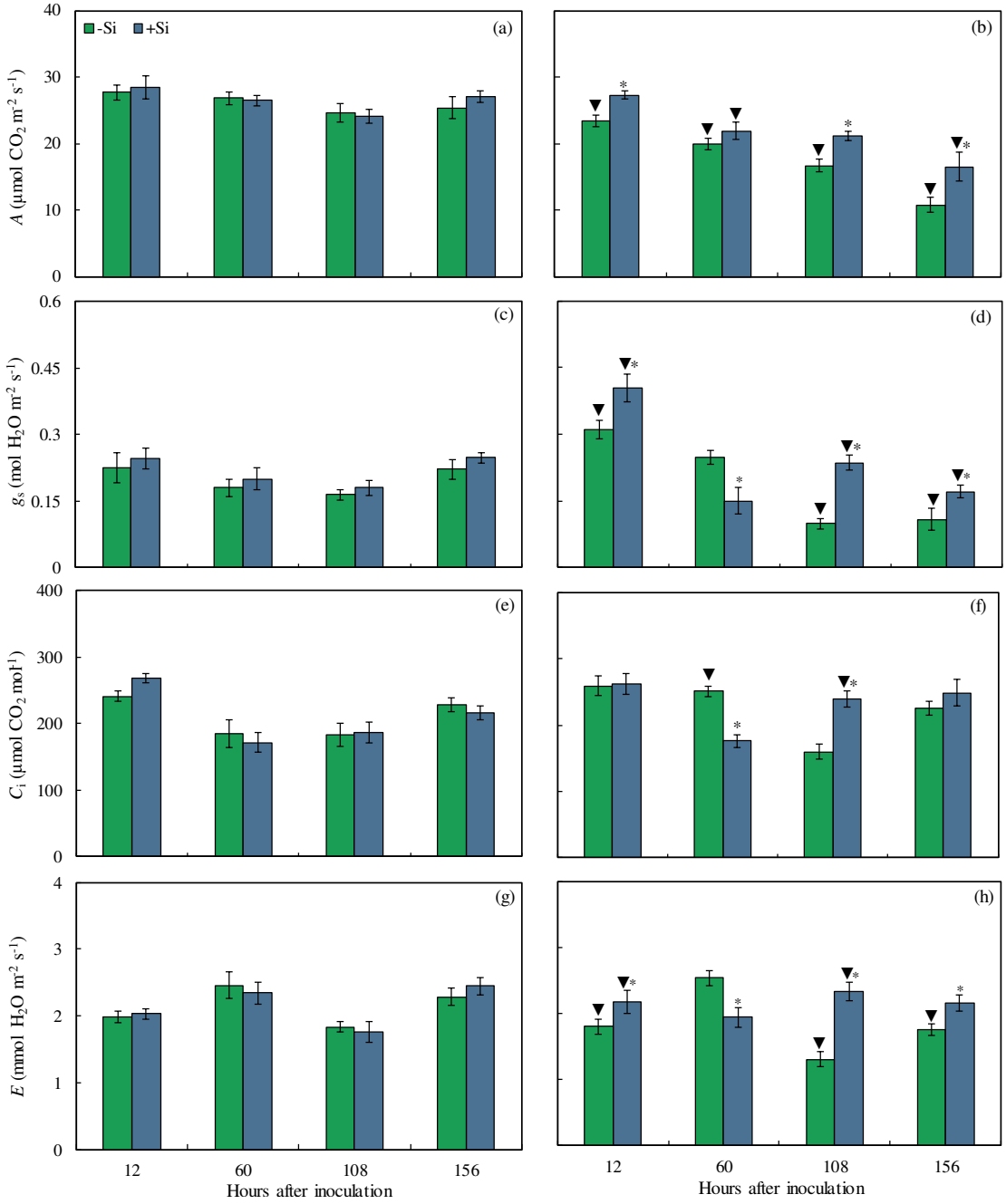

Figure 4. Leaf gas exchange parameters net carbon assimilation rate (*A*) (a and b), stomatal conductance to water vapor (g_s) (c and d), internal CO_2 concentration (C_i) (e and f), and transpiration rate (*E*) (g and h) determined on the leaves of maize plants non-inoculated (NI) (a, c, e, and g) or inoculated (I) (b, d, f, and h) with *Bipolaris maydis* and non-supplied (-Si) or supplied (+Si) with silicon (Si). Means for NI and I plants followed by an inverted triangle (▼) and for -Si and +Si treatments followed by an asterisk (*), at each evaluation time, are significantly different ($P \leq 0.05$) according to the *F* test. Bars represent the standard error of the means.

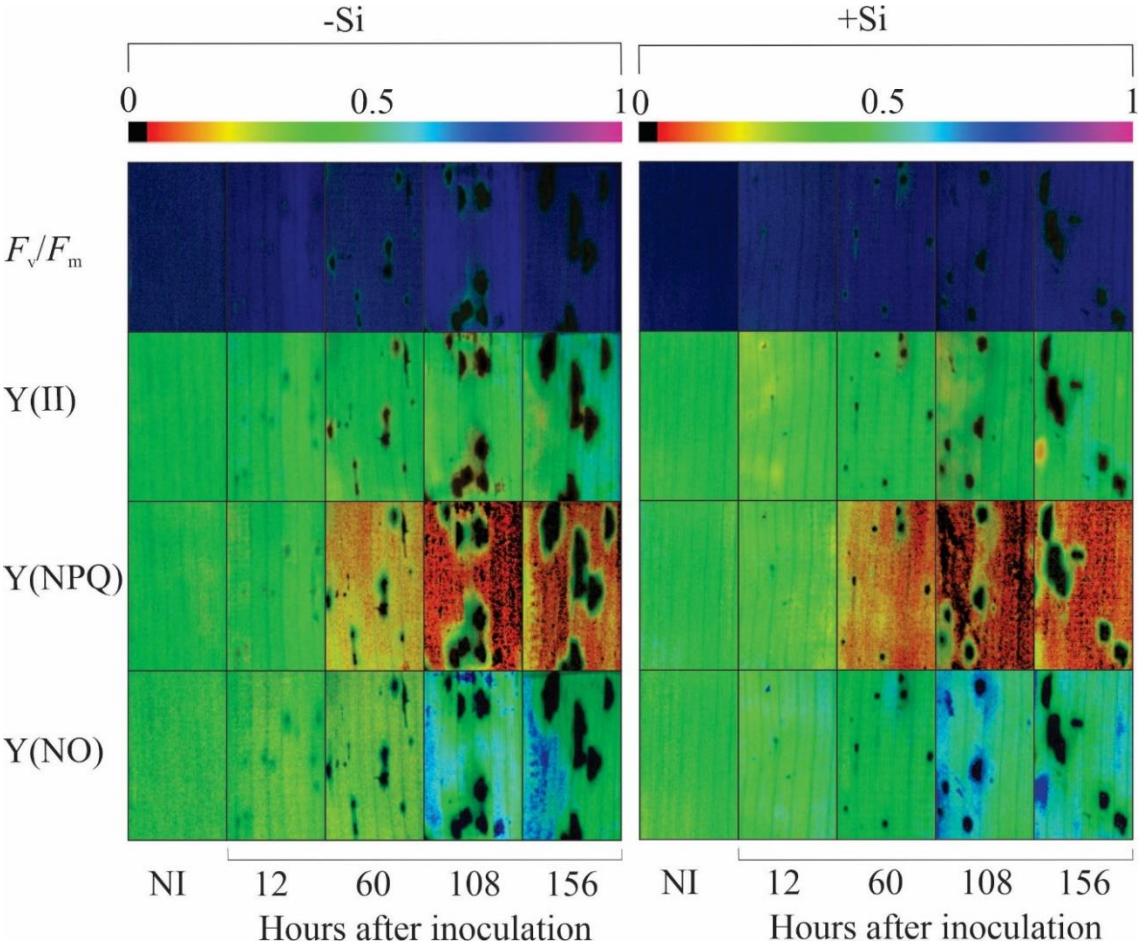

Figure 5. Images of chlorophyll *a* fluorescence parameters variable-to-maximum chlorophyll *a* fluorescence ratio (F_v/F_m), photochemical yield [Y(II)], yield for dissipation by down-regulation [Y(NPQ)], and yield for non-regulated dissipation [Y(NO)] obtained from the leaves of maize plants non-supplied (-Si) or supplied (+Si) with silicon (Si) and non-inoculated (NI) or at different times after inoculation with *Bipolaris maydis.*

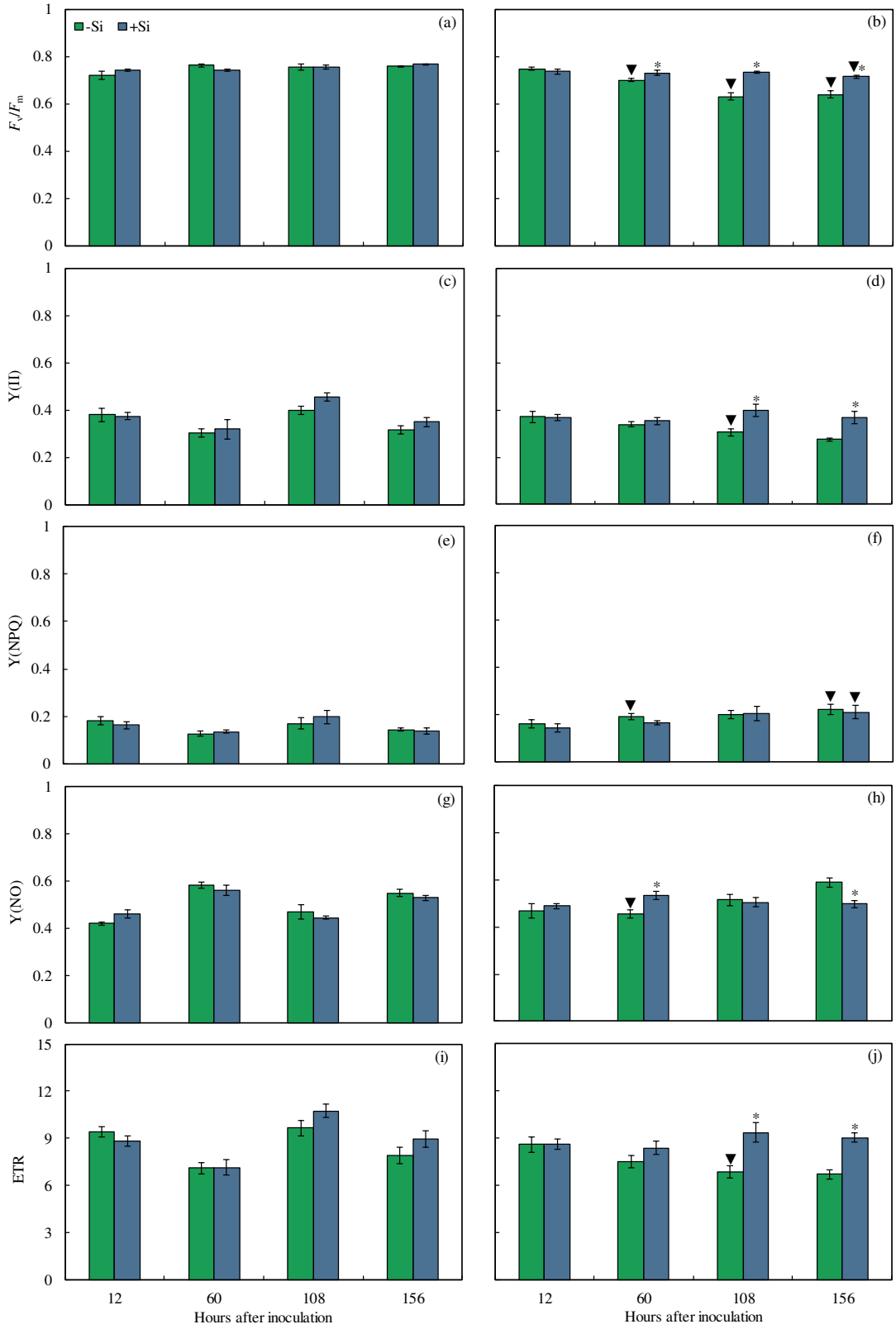

Figure 6. Quantification of chlorophyll *a* fluorescence parameters variable-to-maximum chlorophyll *a* fluorescence ratio (F_v/F_m) (a and b), photochemical yield [Y(II)] (c and d), yield for

dissipation by down-regulation [Y(NPQ)] (e and f), yield for non-regulated dissipation [Y(NO)] (g and h), and electron transport rate (ETR) (i and j) determined on the leaves of maize plants non-inoculated (NI) (a, c, e, g, and i) or inoculated (I) (b, d, f, h, and j) with *Bipolaris maydis* and non-supplied (-Si) or supplied (+Si) with silicon (Si). Means for NI and I plants followed by an inverted triangle (▼) and for -Si and +Si treatments followed by an asterisk (*), at each evaluation time, are significantly different ($P \leq 0.05$) according to the F test. Bars represent the standard error of the means.

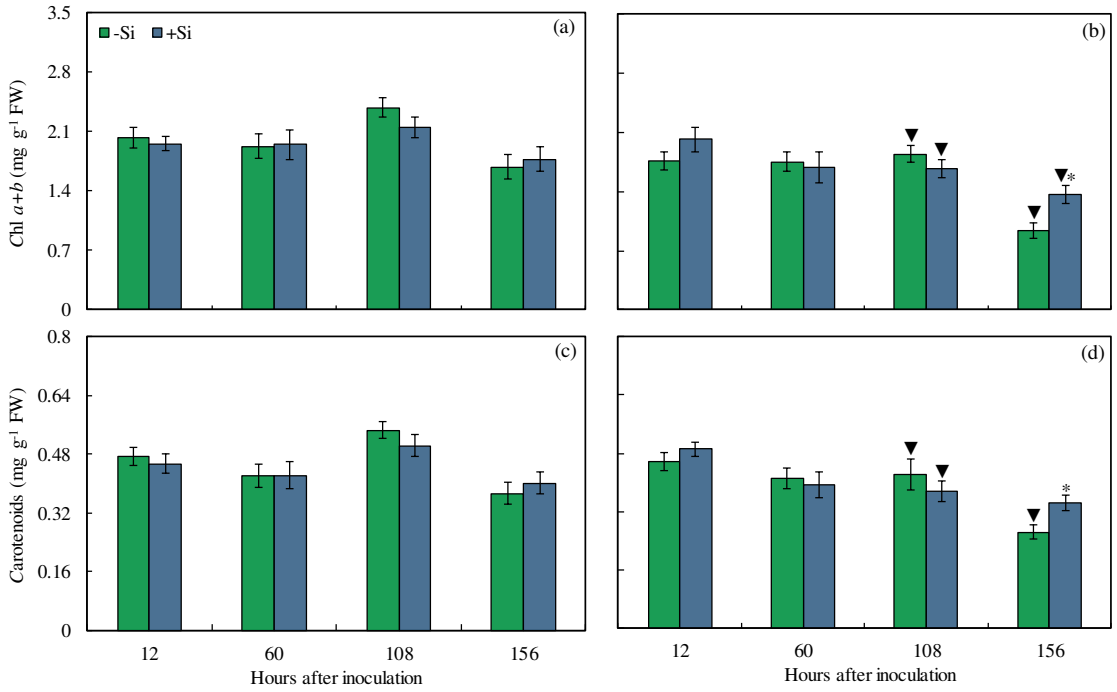

Figure 7. Concentrations of chlorophyll *a*+*b* (Chl *a*+*b*) (a and b) and carotenoids (c and d) determined on the leaves of maize plants non-inoculated (NI) (a and c) or inoculated (I) (b and d) with *Bipolaris maydis* and non-supplied (-Si) or supplied (+Si) with silicon (Si). Means for NI and I plants followed by an inverted triangle (▼) and for -Si and +Si treatments followed by an asterisk (*), at each evaluation time, are significantly different ($P \leq 0.05$) according to the *F* test. Bars represent the standard error of the means. FW = fresh weight.

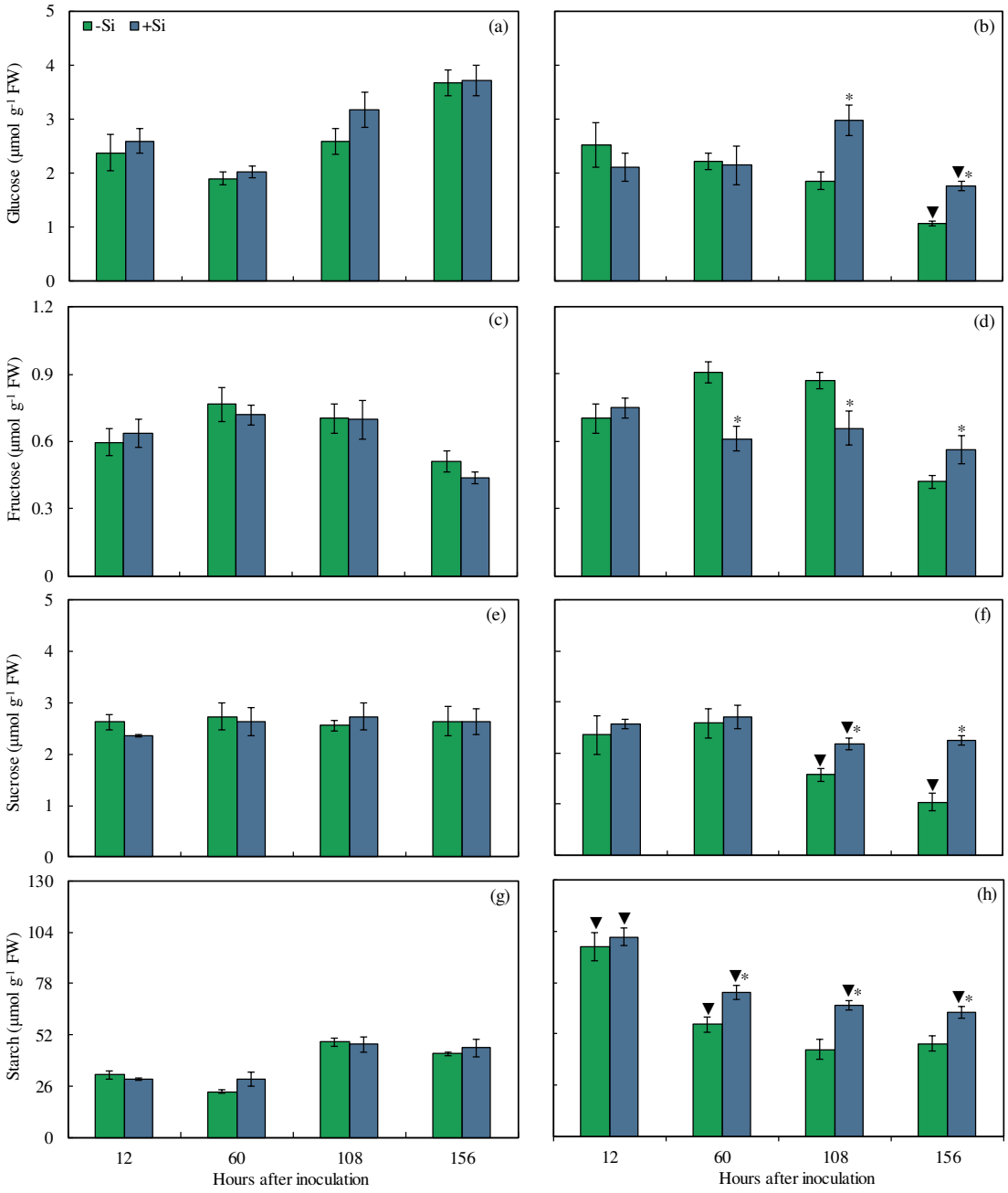

Figure 8. Concentrations of glucose (a and b), fructose (c and d), sucrose (e and f), and starch (g and h) determined on the leaves of maize plants non-inoculated (NI) (a, c, e, and g) or inoculated (I) (b, d, f, and h) with *Bipolaris maydis* and non-supplied (-Si) or supplied (+Si) with silicon (Si). Means for NI and I plants followed by an inverted triangle (▼) and for -Si and +Si treatments followed by an asterisk (*), at each evaluation time, are significantly different ($P \leq 0.05$) according to the *F* test. Bars represent the standard error of the means. FW = fresh weight.

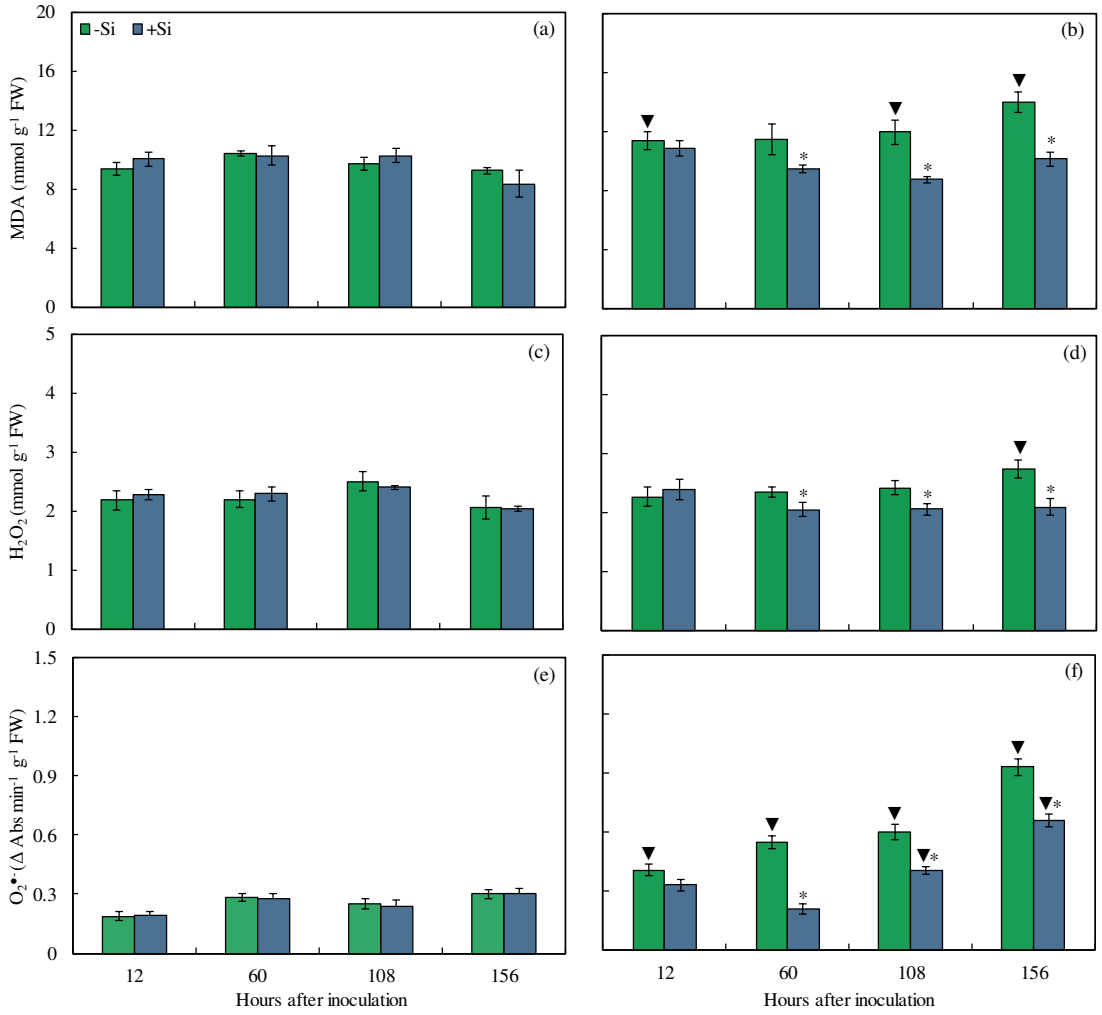

Figure 9. Concentrations of malondialdehyde (MDA) (a and b), hydrogen peroxide (H_2O_2) (c and d), and superoxide anion radical ($O_2^{\bullet-}$) (e and f) determined on the leaves of maize plants non-inoculated (NI) (a, c, and e) or inoculated (I) (b, d, and f) with *Bipolaris maydis* and non-supplied (-Si) or supplied (+Si) with silicon (Si). Means for NI and I plants followed by an inverted triangle (▼) and for -Si and +Si treatments followed by an asterisk (*), at each evaluation time, are significantly different ($P \leq 0.05$) according to the *F* test. Bars represent the standard error of the means. FW = fresh weight.

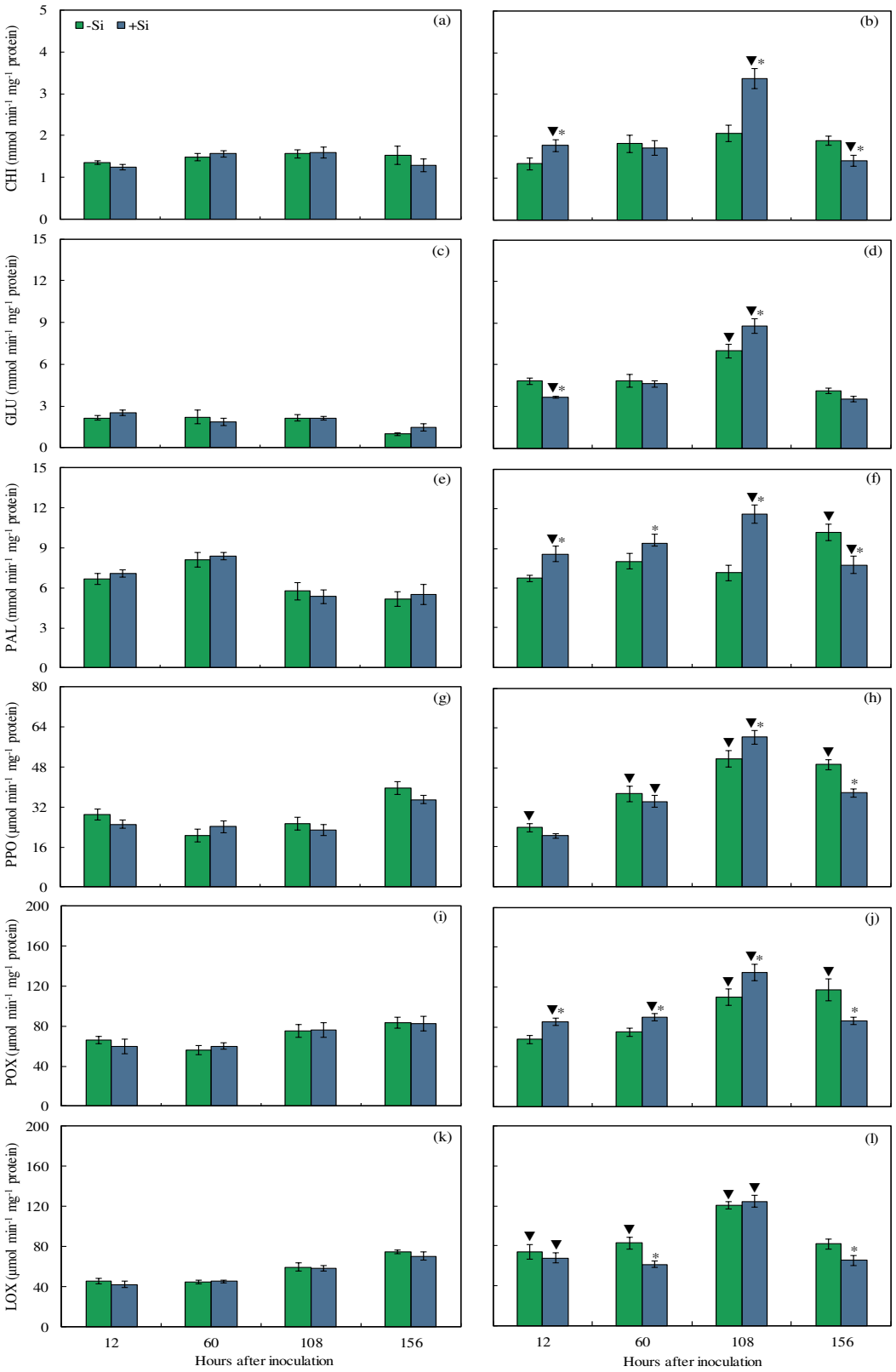

Figure 10. Activities of chitinase (CHI) (a and b), *β*-1,3-glucanase (GLU) (c and d), phenylalanine ammonia-lyase (PAL) (e and f), polyphenoloxidase (PPO) (g and h), peroxidase (POX) (i and j),

and lipoxygenase (LOX) (k and l) determined on the leaves of maize plants non-inoculated (NI) (a, c, e, and g) or inoculated (I) (b, d, f, and h) with *Bipolaris maydis* and non-supplied (-Si) or supplied (+Si) with silicon (Si). Means for NI and I plants followed by an inverted triangle (▼) and for -Si and +Si treatments followed by an asterisk (*), at each evaluation time, are significantly different ($P \leq 0.05$) according to the *F* test. Bars represent the standard error of the means.

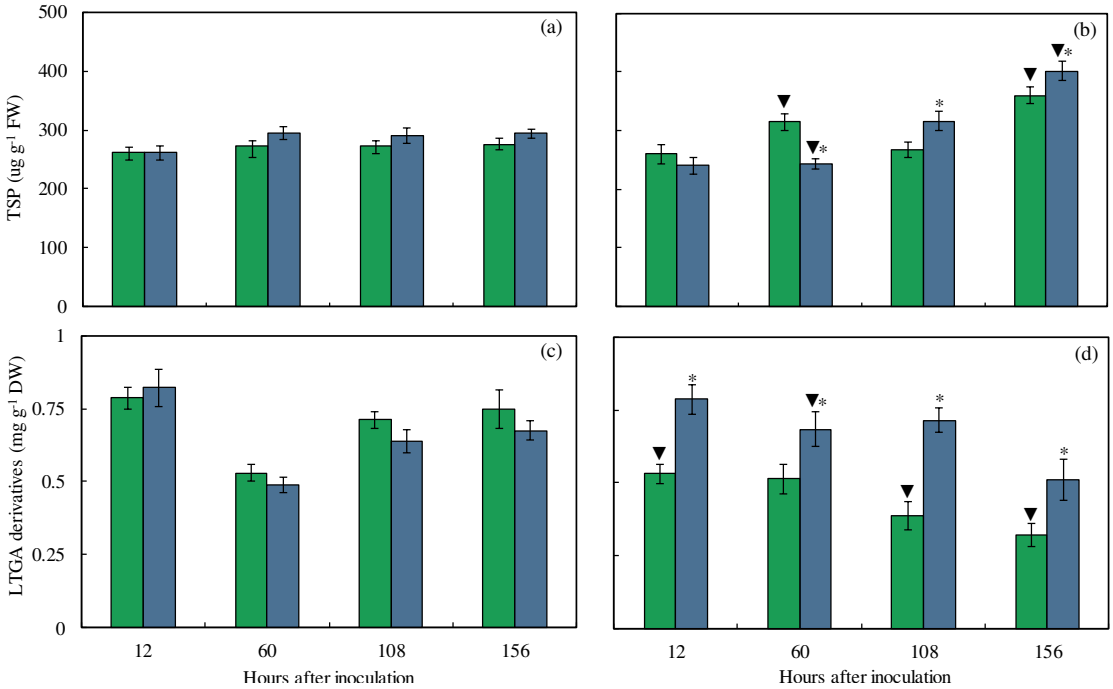

Figure 11. Concentrations of total soluble phenolics (TSP) (a and b) and lignin-thioglycolic acid (LTGA) derivatives (c and d) determined on leaves of the maize plants non-inoculated (NI) (a and c) or inoculated (I) (b and d) with *Bipolaris maydis* and non-supplied (-Si) or supplied (+Si) with silicon (Si). Means for NI and I plants followed by an inverted triangle (▼) and for -Si and +Si treatments followed by an asterisk (*), at each evaluation time, are significantly different ($P \leq 0.05$) according to the *F* test. Bars represent the standard error of the means. FW and DW = fresh weight and dry weight, respectively.

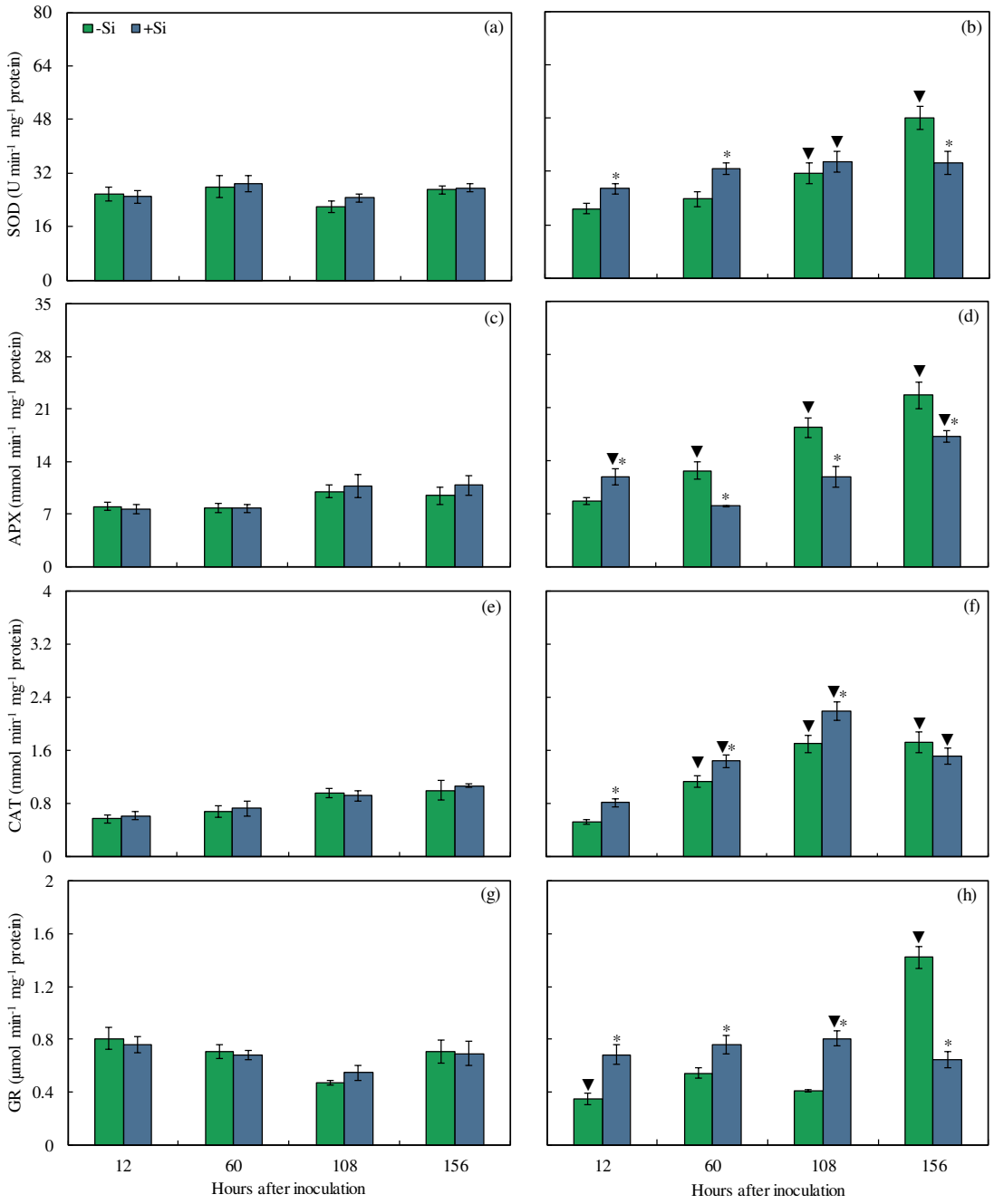

Figure 12. Activities of superoxide dismutase (SOD) (a and b), ascorbate peroxidase (APX) (c and d), catalase (CAT) (e and f), and glutathione reductase (GR) (g and h) determined on the leaves of maize plants non-inoculated (NI) (a, c, e, and g) or inoculated (I) (b, d, f, and h) with *Bipolaris maydis* and non-supplied (-Si) or supplied (+Si) with silicon (Si). Means for NI and I plants followed by an inverted triangle (▼) and for -Si and +Si treatments followed by an asterisk (*), at each evaluation time, are significantly different ($P \leq 0.05$) according to the *F* test. Bars represent the standard error of the means.

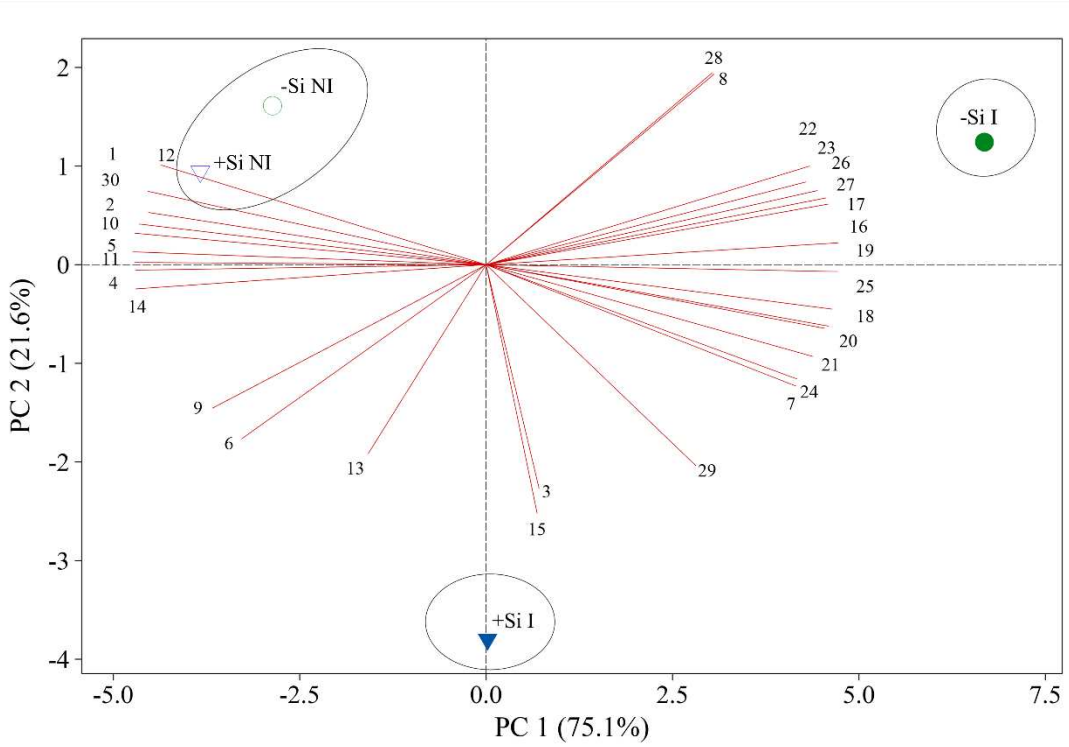

Figure 13. Score and loading plots of principal component analysis (PCA) for variables and parameters determined on the leaves of maize plants non-inoculated (NI) or inoculated (I) with *Bipolaris maydis* and non-supplied (-Si) or supplied (+Si) with silicon (Si). Numbers in the leading plot are as follow: leaf gas exchange (1, 2, 3, and 4, respectively, to A, g_s, C_i, and E) and chlorophyll *a* fluorescence [5, 6, 7, 8, and 9, respectively, to F_v/F_m, Y(II), Y(NPQ), Y(NO), and ETR] parameters, concentrations of photosynthetic pigments (10 and 11, respectively, to Chl *a*+*b* and Car), carbohydrates (12, 13, 14, and 15, respectively, to glucose, fructose, sucrose, and starch), and metabolites (16, 17, 18, 29, and 30, respectively, to MDA, H_2O_2, $O_2^{\bullet-}$, TSP, and LTGA derivatives), activities of antioxidant (19, 20, 21, and 22, respectively, to SOD, APX, CAT, and GR) and defense (23, 24, 25, 26, 27, and 28, respectively, to CHI, GLU, PAL, PPO, POX, and LOX) enzymes. Groups were generated from cluster analysis with complete linkage and Pearson distance. Data from variables and parameters used in the PCA analysis were obtained from NI and I plants at 156 hours after inoculation.